Faculdade de Engenharia da Universidade do Porto

Biological response to surface modified magnesium alloys-based biodegradable implants

Mónica Pereira Garcia

Dissertação submetida para satisfação parcial dos requisitos do

grau de Doutor em Engenharia Biomédica

Porto, 2015

Thesis prepared under the supervision of:

Professora Maria Helena Fernandes (Supervisor)

Faculdade de Medicina Dentária da Universidade do Porto

Maria de Fátima Grilo da Costa Montemor (Co-supervisor)

Instituto Superior Técnico, Universidade de Lisboa

The experimental work described in this thesis was conducted at:

Laboratory for Bone Metabolism and Regeneration,

Faculdade de Medicina Dentária da Universidade do Porto

Base materials, anodised and polymeric-coatings were prepared at Instituto Superior Técnico da Universidade de Lisboa (IST), The Institute of Precision Mechanics (IPM) of the Faculty of Materials Science & Engineering, Warsaw University of Technology and the Materials Engineers Group sp. z o.o. (MEG), a spin-off company of the Faculty of Materials Science & Engineering, Warsaw University of Technology.

The research described in this thesis was performed within the project:
"A new generation of biodegradable implants obtained from magnesium alloys functionalized by means of advanced surface treatment"; European Micro and Nano Technology Network, FP7 - ERAMNT/0002/2009

À minha família

Abstract

In recent years, a new generation of biodegradable metallic materials, magnesium (Mg) alloys, gained more attention for bone tissue applications. Mg alloys present a set of properties suitable for bone tissue regeneration, especially the similar mechanical characteristics. The main limitation for the of Mg alloys for these applications is the fast degradation rate in physiological environment. Many attempts have been proposed in literature to improve the lifetime of Mg implants by controlling its degradation rate, with various results.

The aim of this work was to characterize the cytocompatibility of an innovative surface multifunctionalisation technology for Mg alloys in order to use these materials as biodegradable implants in orthopaedic applications.

A series of surfaces were analysed for their biocompatibility in this work: (i) bare AZ31, AZ61 and RZ5 Mg alloys, (ii) anodised AZ31 and RZ5 Mg alloys, and (iii) polymeric-based coatings applied on bare and anodised Mg AZ31 alloy. Two polymeric coatings were used, namely based on polyether imide (PEI) and polycaprolactone (PCL) as base material; the coatings were used alone and, also, containing different concentrations of nanohydroxyapatite particles (HA).

Direct and indirect assays were used in the cytocompatibility testing. In the direct assay, cells were cultured on the materials' surface, and, in the indirect assay, cells were cultured in the presence of extracts from the Mg-based substrates. In the direct assays, MG-63 osteoblastic cells were used as the cell culture model. In the indirect assays, cell response was assessed for human mesenchymal stem cells, human osteoclastic cells and human endothelial cells. Cell behaviour was analysed for cell viability/proliferation and specific phenotype parameters.

MG-63 cells cultured on the surface of naked Mg alloys showed a decrease in viability/proliferation, especially AZ61 alloy. These results were associated with a higher corrosion rate in AZ61, creating a dynamic surface unsuitable for cell attachment

and proliferation. Comparatively, the anodised alloys showed an increase in viability/proliferation, evidencing a better surface and environment for cell attachment and further growth. Regarding the cell response over the polymeric coatings, firstly, one experiment was performed in which the coating was applied to glass coverslips in order to analyse the biocompatibility of the various coating compositions, without the influence of the Mg alloy. Both coatings presented an improved biological performance compared to the bare and the anodised alloy. Additionally, a better cell response was observed for the polymeric coatings containing HA particles, with a significant increase in viability/proliferation and functional activity. A similar behaviour was found on the coatings applied to Mg alloys, compared to uncoated samples.

In the indirect assays, cell response was evaluated in the presence of extracts from the Mg-based materials AZ31 alloy, anodised AZ31 alloy and anodised AZ31 alloy coated with the polymeric coating PEI containing 2% HA. The extract was added to cultures of human mesenchymal stem cells (HMSC), human peripheral blood mononuclear cells (PBMC) and human umbilical vein endothelial cells (HUVEC). Cell response to the extracts from AZ31 alloy and anodised AZ31 alloy was concentration and cell-dependent. At high concentrations, the extracts were found to be cytotoxic for all tested cells. However, at low concentrations, the extracts elicited positive effects, increasing cell proliferation and functional activity. The extracts from anodised AZ31 alloy coated with PEI containing 2%HA did not cause significant effects on the cell behaviour on the tested concentration range.

To evaluate the contribution of Mg ion in the cellular response, a range of Mg concentrations was tested in osteoblastic, osteoclastic and endothelial cell cultures. The results showed a dose-dependent effect. At high concentrations, Mg ion caused an inhibitory effect in all cell types. In low concentrations no significant effects were observed in osteoblastic and endothelial cells, however in osteoclastic cell cultures, an increase in DNA content and TRAP activity was noticed.

In conclusion, Mg alloys showed promising characteristics for bone tissue applications. Surface treatments of the alloy, by anodisation and polymeric-based coatings, increased the cytocompatibility of the Mg alloys. The multifunctionalization approach of the Mg alloys proposed in this study appears to be a promising strategy to

obtain biologically safe and active biodegradable Mg-based materials for bone tissue applications.

Key words: Magnesium alloys, anodisation, polymeric coatings, cytocompatibility, human mesenchymal stem cells, osteoclastic cells, endothelial cells

Resumo

As ligas de magnésio (Mg), uma nova geração de materiais metálicos biodegradáveis, têm vindo a evidenciar grande interesse para aplicações no tecido ósseo. As ligas de magnésio apresentam um conjunto de propriedades apropriadas para a regeneração do tecido ósseo. A maior limitação das ligas de Mg é a sua rápida taxa de degradação em ambiente fisiológico. Várias técnicas têm sido propostas para melhorar o tempo de vida dos implantes de Mg controlando a sua degradação, com variadas taxas de sucesso.

Este trabalho teve como objectivo a caracterização da citocompatibilidade de uma tecnologia de multifuncionalização de superfície para ligas de Mg, de forma a utilizar estes materiais como implantes biodegradáveis em aplicações ortopédicas.

O trabalho experimental incluiu a avaliação da citocompatibilidade de uma série de superfícies: (i) as ligas base AZ31, AZ61 e RZ5, (ii) as ligas AZ31 e RZ5 anodizadas e (iii) revestimentos poliméricos aplicados na liga base a anodisada AZ31. Foram utilizados dois revestimentos poliméricos, baseados em poliéster imida (PEI) e policaprolactona (PCL) como material base, em que algumas das composições continham diferentes concentrações de partículas de nanohidroxiapatite (HA).

A avaliação da citocompatibilidade incluiu ensaios directos e indirectos. Nos ensaios directos, as células foram cultivadas na superfície dos materiais, e nos ensaios indirectos, as células foram cultivadas na presença de extractos obtidos dos substratos de Mg. Nos testes directos, as culturas de células osteoblásticas MG-63 foram usadas como modelo de estudo. Nos testes indirectos, a resposta celular foi avaliada para células pluripotentes mesenquimais humanas, células osteoclásticas humanas e células endoteliais humanas. O comportamento celular foi avaliado para a viabilidade/proliferação celular e parâmetros fenotípicos específicos.

As células MG-63 cultivadas na superfície das ligas base de Mg apresentaram um decréscimo na viabilidade/proliferação, principalmente a liga AZ61. Estes resultados

foram associados com uma maior taxa de corrosão nesta liga, que origina uma superfície dinâmica inadequada para a adesão e proliferação celular. Comparativamente, as ligas anodizadas exibiram um aumento na viabilidade/proliferação, evidenciando uma melhor superfície e ambiente para a adesão e crescimento celular. Relativamente à resposta celular nos revestimentos poliméricos, inicialmente, o revestimento foi aplicado em lamelas de vidro de forma a analisar a citocompatibilidade de diversas composições, sem a influência da liga de Mg. Os revestimentos poliméricos apresentaram melhor desempenho biológico que a liga base ou anodizada. Em ambos, observou-se uma melhor resposta celular nos revestimentos com partículas de HA na sua composição, com um aumento significativo na viabilidade /proliferação e actividade funcional. Nos revestimentos aplicados na liga de Mg verificou-se um comportamento semelhante, comparando com as amostras base.

Nos ensaios indirectos, a resposta celular foi avaliada na presença de extractos da liga AZ31, liga AZ31 anodizada e liga AZ31 anodizada revestida com PEI contendo 2% de HA. Os extractos foram adicionados a culturas de células estaminais mesenquimais humanas (hMSC), células mononucleares humanas do sangue periférico (PBMC) e células endoteliais humanas da veia umbilical (HUVEC). A resposta celular aos extractos da liga AZ31 e liga anodizada revelou ser dependente da concentração e tipo celular. Em concentrações elevadas, os extractos mostraram ser citotóxicos para todas as células testadas. No entanto, em concentrações baixas, os extractos causaram efeitos positivos, aumentando a proliferação celular e actividade funcional. Os extractos provenientes da liga AZ31 anodizada com revestimento polimérico não causaram efeitos significativos no comportamento celular, na gama de concentrações testada.

De forma a avaliar a contribuição do ião Mg na resposta celular, uma gama de concentrações de Mg foi testada em culturas celulares osteoblásticas, osteoclásticas e endoteliais. Os resultados mostraram um efeito dependente da dose. Concentrações elevadas do ião Mg mostraram ter um efeito inibitório em todas as culturas celulares. Em concentrações mais baixas não foram observados efeitos significativos nas culturas osteoblásticas e endoteliais, no entanto, nas culturas osteoclásticas, observou-se um aumento na concentração do DNA e na actividade da TRAP.

Em conclusão, as ligas de Mg demonstraram possuir características promissoras para aplicações no tecido ósseo. Os tratamentos de superfície das ligas, por anodização

e revestimentos poliméricos, aumentaram a citocompatibilidade das ligas de Mg. Os resultados evidenciam que os revestimentos poliméricos são uma estratégia promissora para a obtenção de implantes de Mg biologicamente seguros e activos para aplicações ortopédicas.

Palavras-chave: ligas de magnésio, anodização, revestimento polimérico, citocompatibilidade, células pluripotentes mesenquimais humanas, células osteoclásticas, células endoteliais

Acknowledgements

The present dissertation could not be done without the contribution of several people and entities to which I want to express my gratitude, specially thanking:

my supervisor, Prof. Maria Helena Raposo Fernandes, from Faculdade de Medicina Dentária, Universidade do Porto, for the constant support, incentive, supervision and knowledge transmitted, essential to the development of this project;

my co-supervior, Prof. Maria de Fátima Grilo da Costa Montemor, from Instituto Superior Técnico, Universidade de Lisboa, for all the support and supervision in the development of this project;

Prof. Fernando Jorge Monteiro, the coordinator of the PhD program in Biomedical Engineering at FEUP, for the support given throughout the PhD program;

all the researchers and students (Liliana, Marta, Angela, José Carlos, Tatiana, Elisabete, Fábio e Suzy), at Laboratory for Bone Metabolism and Regeneration, FMDUP, for the support, especially Pedro Gomes and João Rodrigues, for all the help, tips and advices;

the European Micro and Nano Technology, for the financial support given to the project FP7 - ERAMNT/0002/2009;

all my friends for their friendship, support and incentive during the development and concretization of this thesis,

my family, for their unconditional support and incentive during this period of my life.

Content

List of Figures

List of Tables

List of Abbreviations

Al – Aluminium

ALP – Alkaline phosphatase

BMP-2 – Bone morphogenetic protein 2

C – Carbon

Ca – Calcium

Ca2 – Carbonic anhydrase 2

CAM – Chick chorioallantoic membrane

Catk – Cathepsin K

CD31 - Platelet endothelial cell adhesion molecule

Ce – Cerium

CLSM – Confocal laser scanning microscopy

Col-1 – Collagen type 1

c-src - Proto-oncogene tyrosine-protein kinase

DETA – Diethylenetriamine

DMAc – N,N-dimethylacetamide

DMSO – Dimethylsulphoxide

ECGS – Endothelial cell growth supplement

HA – Nanohydroxyapatite / Nanohidroxiapatite

hMSC – Human mesenchymal stem cells / Células estaminais mesenquimais humanas

HUVECS – Human umbilical vein endothelial cells / Células endoteliais humanas da veia umbilical

JNK - c-Jun N-terminal kinase

K – Potassium

La – Lanthanum

M-CSF – Macrophage colony-stimulating factor

MEK - Mitogen-activated protein/extracellular signal-regulated kinase kinase

Mg – Magnesium / Magnésio

Mn – Manganese

MSC – Mesenchymal stem cells

MTT – 3-(4,5-Dimethylthiazol-2-yl)-2,5,diphenyltetrazolium

Na – Sodium

NFATc - Nuclear factor of Activated T-Cells

NF-kB – Nuclear factor kappa-light-chain-enhancer of activated B cells

OPG – Osteoprotegerin

P – Phosphorus

p38 MAPK – p38 Mitogen-activated protein kinase

PBMC – Human peripheral blood mononuclear cells / Células mononucleares humanas do sangue periférico

PCL – Polycaprolactone / Policaprolactona

PEI – Polyether imide / Poliéster imida

PEO - Plasma electrolytic oxidation

PLLA – Poly-L-lactic acid

PLLC – Poly(lactic-co-glycolic acid)

PVAc – Polyvinyl acetate

RANK – Receptor activator of nuclear factor kappa-B

RANKL – Receptor activator of nuclear factor kappa-B ligand

REE – Rare earth elements

Runx-2 – Runt-related transcriptor factor 2

SEM – Scanning electron microscopy

Si – Silicon

TRAP – Tartrate-resistance acid phosphatase

VE-cadherin – Vascular endothelial cadherin

VWF - Von Willebrand factor

Y - Yttrium

Zn – Zinc

Zr – Zirconium

Chapter 1

Motivation, objectives and structure of the thesis

In recent years, magnesium (Mg) and its alloys have gain attention for biomedical applications owning to a set of characteristics especially suitable for orthopaedics applications. To begin with, it is an important cation in the human body, predominantly present in bone tissue [1,2]. Mg has several important roles in the cells, such as regulation of proliferation, differentiation and apoptosis [3]. The mechanical properties of Mg alloys are similar to bone tissue, compared to available metallic alloys [4]. However, the main characteristic of Mg alloys is the fast degradation in physiological environment [5], which can be used as an advantage. As such, Mg alloys have been suggested for temporary bone implants, in the form of screw or bone plates.

Nowadays, the main limitation of Mg-based metallic implants is controlling the degradation in physiological environment, insuring proper bone tissue regeneration before implant degradation. The fast degradation of Mg alloys can lead to excess of Mg^{2+} and increase risk of failure of the implant before the proper bone tissue regeneration.

Many attempts have been proposed in literature to improve the lifetime of Mg implants, controlling its degradation rate to ensure durability and good bone adhesion. Firstly, alterations in the alloying composition of Mg alloys have been described useful in decreasing corrosion rate [5,6]. Anodisation is a method to increase corrosion resistance by creating a protection coating composed of Ca, P, F, O and H (β-TCP and $CaHPO_4.2H_2O$ on the surface of the material [7]. Other methods describe the use of coatings based on calcium phosphate or hydroxyapatite (HA) [7,8,9] and polymeric coatings [10,11]. However, the barrier properties of these coatings are still poor and corrosion starts too soon, leading to reduction of the implant lifetime.

Therefore, the improvement of the barrier properties and the accurate control of the corrosion rate of Mg alloys are the most important technical challenges to promote the use of innovative bioresorbable Mg implants, a new and growing market.

Within this context, the project “A new generation of biodegradable implants obtained from magnesium alloys functionalized by means of advanced surface treatment” - European Micro and Nano Technology Network, FP7 - ERAMNT/0002/2009, has been conducted by a consortium formed by Instituto

Superior Técnico da Universidade de Lisboa (IST, Coordinator), The Institute of Precision Mechanics (IPM) of the Faculty of Materials Science & Engineering, Warsaw University of Technology, the Materials Engineers Group sp. z o.o. (MEG), a spin-off company of the Faculty of Materials Science & Engineering, Warsaw University of Technology, and Faculdade de Medicina Dentária da Universidade do Porto (FMDUP). IST, IPM and MEG were responsible for the development and characterization of Mg-based substrates, and FMDUP for the cytocompatibility and biocompatibility testing of the developed materials.

The research work presented in this thesis has been performed at FMDUP, and includes the *in vitro* studies conducted during the several stages of the development of the Mg-based materials, providing information needed for the progressive optimization of the substrates with better biological response.

Hence, the main **objective** of this work was to characterize the cytocompatibility of several Mg alloy surface treatments, including anodisation and polymeric-based coatings, in order to use these materials as biodegradable implants in orthopaedic applications. Firstly, the cytocompatibility of three Mg alloys - AZ31, AZ61 and RZ5 - was analysed in order to select the best ones. Subsequently, the porous layer created by plasma electrolytic oxidation (PEO) of the Mg alloy and composed of Ca, P, F, O and Mg, was also assessed for the cell response. At the final stage, two polymeric coatings, based on polyether imide (PEI) and polycaprolactone (PCL), used alone and with different concentrations of nanohydroxyapatite particles (HA), were tested.

Cytocompatibility studies were performed using direct testing assays, i.e. the cells were seeded over the surface of the Mg-based substrates, and also indirect testing assays, in which the cell behaviour was assessed in the presence of extracts from the Mg-based materials. In the direct assays, MG-63 osteoblastic cells were used as the cell culture model. In the indirect assays, cell response was assessed for the behaviour of human mesenchymal stem cells, human osteoclastic cells and human endothelial cells. Cell response was analysed for cell viability/proliferation and specific phenotype parameters.

Following the motivation and the context for the development of this work, the thesis has the following **structure**:

Chapter 2 contains a comprehensive state-of-the-art review on the most important topics discussed along the thesis. It contains information about bone physiology, magnesium biomaterials for bone regeneration, and *in vitro* and *in vivo* studies of magnesium alloys;

Chapter 3 contains a detailed description of the materials and methods used in the experimental work. It describes the cell culture studies of the direct and indirect testing assays, detailing the methodology used in the characterization of the cellular behaviour;

Chapter 4 includes the direct cytocompatibility studies, describing the osteoblastic cell behaviour over the Mg-based substrates, using MG-63 cells as the culture model;

Chapter 5 describes the indirect cytocompatibility studies, namely the cell behaviour in the presence of the extracts from the Mg-based substrates and a set of Mg ion concentrations, using human mesenchymal stem cells, osteoclastic cells and endothelial cells as culture models;

Chapter 6 contains the general discussion of this work;

Chapter 7 enumerates the main conclusions of the conducted studies and future perspectives.

The work developed in this thesis was partially published:

Zomorodian A, GARCIA MP, Moura e Silva T, Fernandes JCS, Fernandes MH, Montemor, M.F. (2015) Biofunctional composite coating architectures based on polycaprolactone and nanohydroxyapatite for controlled corrosion activity and enhanced biocompatibility of magnesium AZ31 alloy. Materials Science and Engineering: C 48 (0): 434-443. DOI:10.1016/j.msec.2014.12.027

Zomorodian, A., GARCIA, M.P., Moura e Silva, T., Fernandes, J.C.S., Fernandes, M.H., Montemor, M.F. (2013) Corrosion resistance of a composite polymeric coating applied on biodegradable AZ31 magnesium alloy. Acta Biomaterialia 9 (10): 8660-8670. DOI: 10.1016/j.actbio.2013.02.036

GARCIA MP, Gomes PS, Michalski J, Kwiatkowski L, Montemor MF, Fernandes MH. Osteoblastic cytocompatibility of anodised AZ31 and RZ5 magnesium alloys. 3rd International Conference "Strategies in Tissue Engineering", May 23 to 25, 2012, Würzburg, Germany.

Chapter 2

General introduction

2.1 Bone Physiology

Bone is a complex organ with an important role as structural support for the body and supporting movement and locomotion by providing levers for muscles, ligaments and tendons [12,13]. Bone tissue major functions also include protection and support of internal organs, mechanical support of the diaphragm, brain function, mineral ion homeostasis (calcium, phosphate), acid-base balance, reservoir of growth factors and cytokines, and provide the environment for haematopoiesis within the marrow spaces [12,13,14,15].

Bone tissue is composed of mineralized osseous tissue, marrow, endosteum, nerves and blood vessels [14]. The cellular components of bone tissue are osteoblasts, osteocytes, bone-lining cells and osteoclasts. The extracellular matrix of the bone is composed of an organic matrix and a mineralized matrix. The organic matrix is mainly composed of type I collagen (90%), non-structural proteins (growth factors, osteocalcin, osteonectin, phosphoproteins), lipids and glycosaminoglycans (2%) [13,15,16].

The structure of the mineralized matrix can be discriminated into seven levels of hierarchy [17]. Firstly, the matrix is composed of nanoscopic plate-like crystals of carbonated hydroxyapatite (HA) ($Ca_{10}[\ PO_4\ ]_6[\ OH\ ]_2$) that are oriented and aligned within self-assembled collagen fibrils; these fibrils are layered in parallel arrangement within lamellae. The lamellae are arranged concentrically around blood vessels to form osteons. The osteons are either packed densely into compact bone (or cortical bone) or comprise a trabecular network of microporous bone, referred to as spongy or cancellous bone [17,18]. In the cortical bone, the lamellae are regular and cylindrical in comparison to the irregular, sinuous convolutions of the structure in cancellous bone [12,14]. The adult human skeleton is composed of 80% cortical bone (or compact) and 20% cancellous bone (trabecular or spongy) overall [12]. The microstructure of the bone comprises the harversian system, osteon and single trabeculae [14].

Cortical osteons are called Harversian systems, which are cylindrical in shape, approximately 400 mm long and 200 mm wide at their base, and form a branching network within the cortical bone (Figure 1) [12]. The walls of Harversian systems are formed of concentric lamellae [12]. Cortical bone has an outer periosteal surface and an inner endosteal surface [12]. Trabecular osteons are called packets, which are composed

of plates and rods averaging 50 to 400 mm in thickness [12]. Trabecular osteons are semilunar in shape, normally approximately 35 mm thick, and composed of concentric lamellae [12].

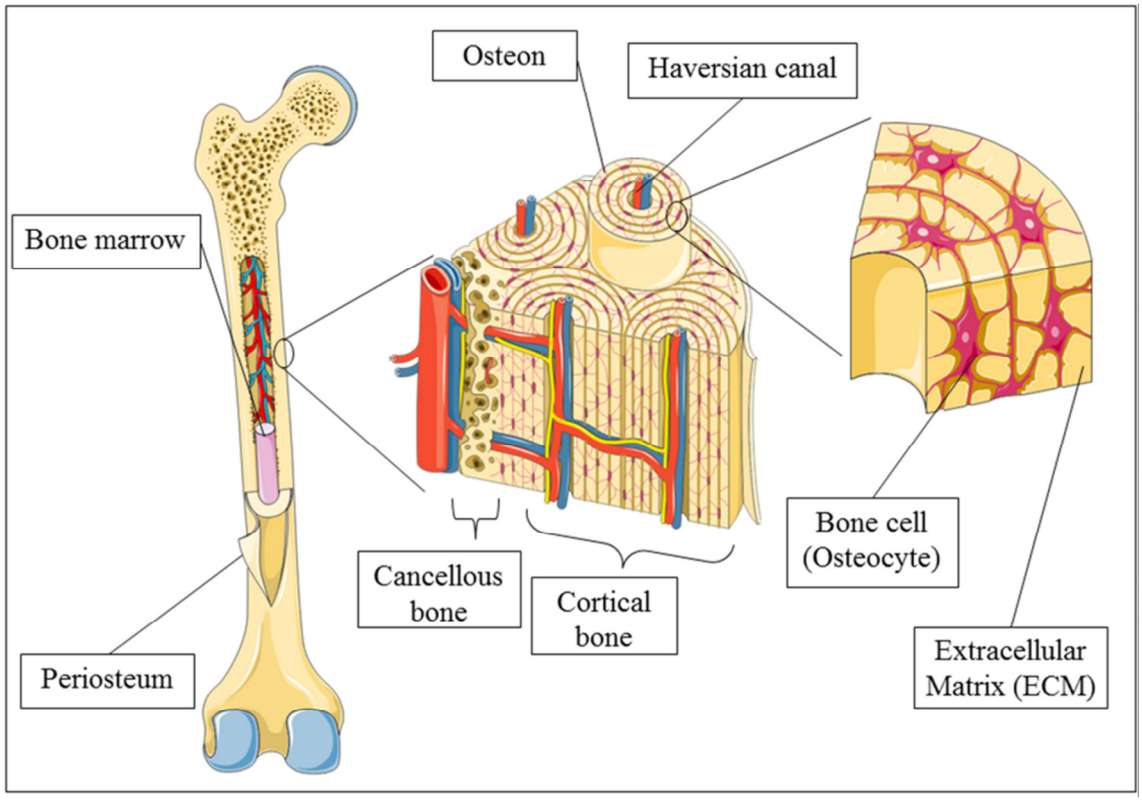

Figure 1. Schematic representation of bone structure [19].

The cellular components of the bone include osteocytes, osteoblasts, osteoclast, bone-lining cells and mesenchymal stem cells (MSC). Mesenchymal stem cells have the potential to differentiate into fibroblasts, osteoblasts, osteocytes, adipocytes and chondrocytes [20]. The process of differentiation is controlled by the expression of lineage-specific transcription factors, growth factors and cytokines.

Osteoblasts are elongated cells derived from MSC and responsible for the production of the organic matrix of the bone [16]. The differentiation of MSC into osteoblasts and the bone calcification is controlled by transcription factors Runt-related transcription factor 2 (Runx2) and Osterix [16,20]. Osteoblasts are responsible for the expression of genes necessary for calcification and induction or downregulation of

osteoclasts [15,21]. Osteoblasts might be encased in the extracellular matrix as osteocytes, or remain on the bone surface as bone-lining cells [16].

Osteoclasts are large multinucleated cells derived from bone marrow hematopoietic stem cells (HSC) with an important role on bone reabsorption [15,16]. Osteoclastogenesis is regulated by transcription factors PU.1, AP-1, Nuclear factor kappa-light-chain-enhancer of activated B cells (NF-kB) and nuclear factor of Activated T-Cells (NFATc) [20]. Some of the growth factors/cytokines controlling osteoclastogenesis are Macrophage colony-stimulating factor (M-CSF) and Receptor activator of nuclear factor kappa-B ligand (RANKL) which are synthetized by osteoblasts. Both have a positive role in the expansion of the precursors and osteoclast differentiation. Osteoprotegerin (OPG), also synthetized by osteoblasts, has a negative role in osteoclastogenesis [20].

Bone formation, growth and remodelling are regulated by hormones, growth factors and cytokines (such as IGF-I, BMPs, FGFs, Wnt, Notch, PTH) and also by nutrition, mechanical loading and aging [20]. These factors will activate different pathways that are important in the remodelling of the bone tissue. Bone remodelling is a process in which osteoclasts perform bone resorption and later osteoblasts form new bone. This process involves three sequential steps: resorption, reversal and formation of bone [13]. Bone lining cells express RANKL which will bind to a surface receptor on the membrane of pre-osteoclasts (RANK, Receptor activator of nuclear factor kappa-B). The binding of RANKL will activate a signalling cascade for osteoclast activation and commitment (Figure 2) [13]. Osteocytes might have an essential part in this process, since it has been proposed that they sense microcracks and microfractures triggering osteoclast differentiation and bone resorption [13]. It has been proposed that osteocytes can regulate the expression of RANKL in osteoblasts, which in turn will influence osteoclastogenesis. Osteocytes are connected by cytoplasmic processes to each other and other types of cells, such as osteoblasts [13].

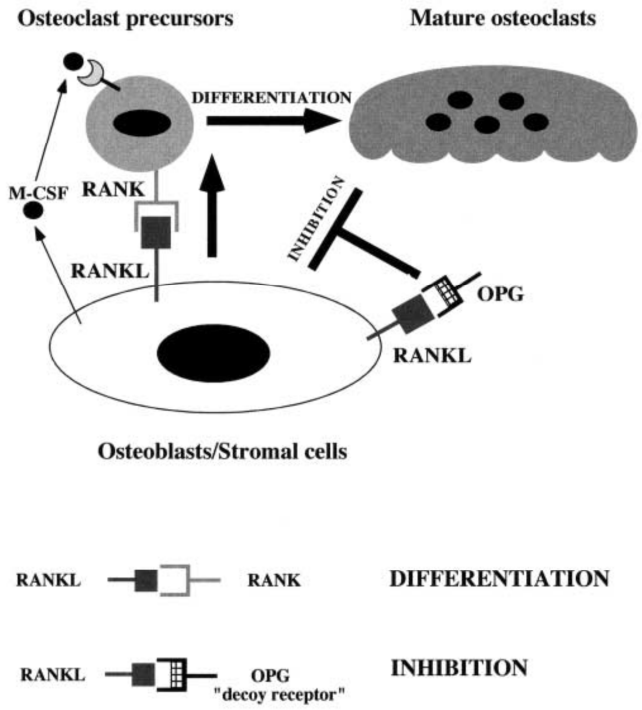

Figure 2. Schematic representation of osteoclastogenesis regulation by osteoblasts/stromal cells. The presence of M-CSF will induce the differentiation and proliferation of osteoclasts [22].

In the resorption phase, the osteoclast progenitors will differentiate into active osteoclasts that can dig trenches with a depth of 40 – 60 μm in the bone [13]. This phase is followed by the reversal phase in which osteoblast precursors differentiate to osteoblasts and osteoclasts undergo apoptosis, discontinuing bone resorption [13]. At this phase, osteoblasts lay down new bone material (mainly collagen type I, but also osteocalcin, osteopontin, along with a large variety of other bioactive molecules) until the reabsorbed bone is replaced by a new one [13]. The osteoblasts that stay encased in the new bone matrix during bone formation are transformed to osteocytes [13]. The osteoblasts become quiescent at the end of bone remodelling forming flattened lining cells on the bone surface [13].

The various components of the bone are organized in a way that bone is able to perform diverse mechanical, biological and chemical functions [14]. The major factor to determine the mechanical properties of bone is based in the hierarchical structure of this tissue. The combination of bone components gives the tissue mechanical properties that

have been difficult to reproduce by biomaterials science. Bone tissue presents a low density, from 0.2 g/cm^3 in cancellous structure to 1.80 g/cm^3 in cortical bone. In cortical bone, tensile strength can vary from 35 to 283 MPa, compression strength from 164 to 240 MPa and elastic modulus between 5 and 23 GPa [4,23].

2.2 Magnesium Biomaterials for Bone Regeneration

In the last decades an increasing interest in magnesium alloys for bone tissue applications was evident. However, the interest in magnesium for medical applications started 200 years ago, shortly after the discovery of elemental magnesium [24]. Reports of the use of magnesium as a biomaterial go as far as 1878 where magnesium wire was used to stop bleeding vessels of three patients [24].

Various applications have been purposed for magnesium biomaterials, such as screws, bone plates and stents. In case of a complex fracture, due to accident or disease, the bone may require to be fixed with an internal implant (screws or plates), with the need of a surgical intervention. Current commercial options for this application can be made of titanium, stainless steel or cobalt-chromium alloys, and are permanent implants [25]. One of the disadvantages of commercial options is that, after 1 or 2 years, the implants need to be removed; therefore a second surgery is required. Biodegradable implants can reduce the life-long problems caused by permanent implants which include long-term endothelial dysfunction, permanent physical irritation and chronic inflammatory local reactions [26].

Also, for orthopaedic applications the mechanical properties of the implanted biomaterial should be similar to the tissue being regenerated. This ensures proper support in the early healing stages and graded load transfer later during the formation of replacement tissue [27,28]. The mechanical properties to be considered for these applications include compression, tension and torsion. Compressive properties should be an important concern when the material is applied to cancellous bone, while tensile properties should be taken in to consideration in the cortical bone [28]. The titanium and stainless steel implants currently available have mechanical properties different from bone such as a higher Young modulus (Table 1) [29]. As a result these implants are too stiff compared to the adjacent cancellous bones creating stress shielding. Mechanical stress such as internal loads, which are usually carried by the bone, will be mainly supported by the implants creating this effect called stress shielding [25]. There are several clinical complications associated with this problem, such as early implant loosening, damage to healing process and adjacent anatomical structures, skeleton thickening and chronic inflammation [25]. The stress-shielding phenomena caused by

metallic implants (stainless steel or titanium alloy) could be minimized by the use of magnesium alloy [30]. Magnesium alloys present mechanical properties closer to the values observed in natural bone [4]. These characteristics include density, elastic modulus and compressive yield strength. Elastic modulus of magnesium alloys (40 – 45 GPa) is similar to bone (3 – 20 GPa) (Table 1) [29]. Also, when compared to hydroxyapatite and other ceramic biomaterials, the elastic modulus and fracture toughness of magnesium alloys is higher [29].

Other biodegradable implants have been developed, such as resorbable polymer fixation plates and screws but they have demonstrated to be relatively weak and less rigid compared to metals [31,32].

Table 1. Physical and mechanical properties of biomaterials used for bone tissue applications [29].

Properties	Natural bone	Magnesium	Ti alloy	Co-Cr alloy	Stainless steel	Synthetic hydroxyapatite
Density (g/cm^3)	1.8 – 2.1	1.74 – 2.0	4.4 – 4.5	8.3 – 9.2	7.9 – 8.1	3.1
Elastic modulus (GPa)	3 - 20	41 – 45	110 - 117	230	189 – 205	73 - 117
Compressive yield strength (MPa)	130 - 180	65 – 100	758 - 1117	450 - 1000	170 – 310	600
Fracture toughness	3 - 6	15 – 40	55 - 115		50 – 200	0.7

The interest of magnesium alloys for bone regeneration relies on the similarity of mechanical properties compared to bone, however between magnesium alloys the mechanical properties are also different. Magnesium mechanical properties show a discrepancy depending on composition, cast method and trace elements present [5,33]. Pure magnesium, with 99% of magnesium and a small percentage of other elements has a density of 1.74 to 2.0 g/cm^3. The elastic modulus varies from 41 to 45 GPa, compressive yield strength from 65 to 100 MPa and fracture toughness from 15 to 40

MPam½ [29] (Table 2). Gu and coworkers (2009) reported that magnesium with alloying elements such as Al, Ag, In, Si or Zn would have an improvement in yield strength and tensile strength compared to pure magnesium (Table 2) [5].

Table 2. Mechanical properties of different magnesium alloys used in bone tissue applications [4,34].

	Cortical bone	Mg-cast	AZ91E-F sand cast	AZ31 extruded	AZ31 sheet	LAE442	Mg-1Ca-extruded	Mg-Zn-Mn-extruded
Compression strength (MPa)	164 – 240		97	83 – 97	110 – 180			
Tensile strength (MPa)	35 – 283	86.8 ± 2.5	165	241 – 260	255 – 290	247	239.6 ± 7.2	280.3 ± 0.9
E-mod. Tensile (GPa)	5 – 23	41	45					
Density (g/cm^3)	1.8 – 2.0	1.74	1.81		1.78			
Yield strength (MPa)		20.9 ± 2.3	97	165 – 200	150 - 220	148	135.6 ± 5.4	246.5 ± 4.5

Magnesium is one of the most important cations in the human body, mainly present in the bone (60 to 70% of the total amount) [1,2]. Magnesium is also present in the soft tissue and extracellular compartments [1]. The homeostasis of magnesium is performed by three major organs, small bowel (absorption), kidneys (excretion and reabsorption) and bone [35]. The bone assists as a reservoir for magnesium since up to one third of this magnesium is exchangeable. In case of deprivation, magnesium present in the bone can be used to supplement the serum levels of magnesium [36]. In the cells, magnesium has an important role in the maintenance of membrane integrity, increasing the resistance towards oxidative stress and regulation of cell proliferation, differentiation and apoptosis [3]. The Mg present in the muscle, soft tissues and erythrocytes is considered intracellular Mg [35]. This Mg is preferentially bound to chelators such as negatively charged molecules, membranes and ATP [1]. It is, also, a regulator of more than 350 proteins, stabilizer of DNA and RNA and co-regulator and activator of

integrins (cell migration) [4]. Part of the intracellular Mg, 5 to 10%, is in the ionized form and have an important role in regulating intracellular homeostasis [35]. Extracellular Mg, present in the serum, is mainly in the ionized form (67%), protein bound (19%) and complexed (14%) [35]. Both, protein bound and complexed Mg are unavailable for most biochemical processes. Mg can act as a calcium blocker and control intracellular calcium, i.e. an increase in extracellular Mg decreases the intracellular calcium [37,38]. In normal cells, the regulatory effect of Ca^{2+} is mediated through Mg^{2+}-dependent processes. Hypomagnesemia is also associated with an imbalance of electrolytes such as Na^{+}, K^{+} and Ca^{2+} [35,39].

One of the most important features of magnesium alloys is their ability to corrode in aqueous systems. This is a determinant factor for magnesium alloys to be used for bone tissue regeneration as temporary implants. Therefore, the control of corrosion rate is one of the most important features to take into account when designing a magnesium biomaterial.

In aqueous solutions, magnesium alloys react producing hydrogen and a magnesium hydroxide layer:

(1) $Mg + 2H_2O \Rightarrow Mg(OH)_2 + H_2$.

In the presence of chloride ions, in environments such as cell culture medium or body fluids, the magnesium hydroxide dissolves into $MgCl_2$ salt:

(2) $Mg(OH)_2 + 2Cl^- \Leftrightarrow MgCl_2 + 2OH$ [40].

Interaction with artificial body fluids (Hank's solution or simulated body fluid) can result in the formation of magnesium hydroxide, magnesium oxide, magnesium chloride, as well as calcium and magnesium apatites [41]. The formation of magnesium hydroxide can lead to the elevation of pH in the surrounding environment. Although magnesium hydroxide can act as a corrosion protective layer in water, in high concentration of chloride it is converted to a highly soluble magnesium chloride [4,26]. The presence of biomolecules, such as bovine serum albumin, can also increase the dissolution rate of magnesium hydroxide and inhibit the deposition of calcium phosphate on Mg substrates [42]. Hydrogen gas is an important effect of corrosion and a

major concern for using Mg-based alloys in orthopaedic applications because bone poorly vascularizes and transports the excessive gas, potentially resulting in the formation of harmful gas pockets [26,43]. Although, the hydrogen gas can be exchanged through the skin or accumulate in fatty tissue, therefore decreasing its effects [26].

The corrosion of magnesium alloys is dependent of the following parameters: composition of Mg alloy, metallurgical treatments, surface treatment, composition of the contacting electrolyte, pH and buffer capacity of the electrolyte, mechanical inputs such as compression or bending forces, biological environment, presence of biological molecules and transport phenomena associated with the reactants and products of the corrosion reaction [40].

In physiological environment, Mg alloys can be affected by two types of corrosion, pitting corrosion and galvanic corrosion. Corrosion is typically localized in single-phase materials, resulting in the formation of pits on the surface of the material [44,45]. The presence of a secondary phase due to impurities or alloying components results in galvanic corrosion. In this type of corrosion, the secondary phase acts as a local cathode resulting in localized corrosion [45].

In the human body, magnesium implant will be exposed to various constituents of the body fluids, such as proteins, anions (chloride, phosphate, bicarbonate), cations (Na^+, K^+, Ca^{2+}, Mg^{2+} etc.), organic substances of low molecular-weight species, relatively high molecular-weight polymeric components, as well as dissolved oxygen [46,47,48]. This physiological environment makes an extremely complex corrosive medium. In case of high concentration of chloride, i.e. human body, magnesium hydroxide will be converted to magnesium chloride inducing pitting corrosion [40,49]. Other ions also influence corrosion of magnesium alloys in physiological environment. It was reported that hydrogen carbonate ions would stimulate the overall corrosion of magnesium alloys [50]. The same authors reported an increase in corrosion resistance with increasing of HPO_4^{2-} concentration due to the formation of a stable passivation layer. The presence of HCO_3^-, Ca^{2+} and HPO_4^{2-} together decreases the corrosion rate of Mg alloys surface due to the formation of insoluble HA [50].

The development of magnesium alloys suitable for biodegradable implants is dependent on the control of corrosion rate and mechanical integrity of the implant in physiological environment. Several techniques have been used to improve corrosion resistance and the mechanical properties of Mg alloys, such as alloying Mg, surface modification of the substrate and various coatings techniques [44]. A set of approaches for surface modifications are based in the formation of a biomimetic layer (composed of Ca, P and C) [7,51,52]; moreover other coatings have been used such as hydroxyapatite [8] or polymers (such as polycaprolactone (PCL), polyether imide (PEI), poly-(L-lactic) acid (PLLA), poly(lactic-co-glycolic acid) (PLLC)) [10,11,53,54,55,56].

These treatments are interesting for degradable implants because the corrosion rate is intended to be low in the initial phase due to the modified surface layer and then returns to the normal value when the layer corrodes away [57]. Such degradation pattern is desirable since the loss of strength of the implant would mirror the increase in strength of the healing bone, providing sufficient support in the initial phase [57].

One of the methods used to modify Mg alloys is through alloying, i.e. selecting the composition of the alloys. The composition of the alloys can affect their strength, ductility and corrosion properties [44,58].

Mg alloys have been developed for industry and consequently the same alloys were used in biomaterials research. These alloys usually contain aluminium and rare earth elements. Aluminium is one of the most common alloying elements used in metal biomaterials, such as titanium implants [4]. Although its use is approved in such biomaterials, several reports concerning its toxicity for the human body have been published. Aluminium has been described as risk factor for Alzheimer and Parkinson disease [59]. Rare earth elements (yttrium (Y), cerium (Ce), lanthanum (La)) are known to have anticarcinogenic properties but the effects in humans are still unclear [4,60]. Mg alloys such as AZ91, AZ31, AE21 and LAE442, with aluminium in their composition, have been tested for biomedical applications. Magnesium alloys with rare earth elements studied for biomedical applications include WE43 and LAE442 [58].

Other Mg alloys have been studied for these applications using non-toxic elements such as calcium (Ca), manganese (Mn), zinc (Zn) and zirconium (Zr) [44]. Zinc is an important trace element found in several human tissues, such as skin, bone, liver, muscles and brain [61]. In the bone, zinc has an important role in the growth,

development and maintenance, and deficiency can lead to bone growth retardation [62]. It is also required in a variety of cellular processes, including DNA and protein synthesis, enzyme activity and intracellular activity [63]. Other alloying elements (Ca, Cr, Mn, Sn, Si) are also nutrients present in human body. Calcium is an important macronutrient, mainly presented in the bone (99%) in the form of hydroxyapatite [64]. Other alloying components also investigated include lithium, cadmium, strontium and silicon [44]. Also, most alloys have impurities such as iron, copper, nickel and beryllium [33]. For biomedical applications, the amount of impurities should be kept minimal, especially those known to create deleterious effects in the human body [33,43]. Impurities could also have an important effect in the characteristics of the alloy, most important in the corrosion resistance of the alloy [43].

The addition of Al in Mg alloys can improve strength, corrosion resistance and increase oxidation rate [44,65]. Although Al can increase at corrosion resistance up to a certain level, at higher concentrations the opposite effect is observed due to increased presence of $Mg_{17}Al_{12}$ phase that promotes galvanic corrosion [66,67]. Rare earth elements are also used to increase strength, ductility, corrosion resistance and creep resistance of the material [4,33,44,68]. They can improve corrosion resistance in high chloride environments due to the formation of an oxide passivation layer [69,70]. Other components such as In, Mn, Zn or Zr can also reduce the corrosion rate [5]. The opposite behaviour was observed in alloying elements such as Si and Y. Zinc is also known to increase the oxidation rate, whereas rare earth elements decrease the oxidation rate of magnesium alloys [65]. In a study performed by Kirkland and co-workers (2010) increasing concentrations of Ca were used to enhance the corrosion rate [6]. Also, the corrosion rate of MgCa alloys was significantly reduced when the corrosion fluid used had higher concentration of proteins [6,71].

Surface roughness can influence the corrosion rate of magnesium alloys. Nguyen *et al.* (2012) observed an acceleration of corrosion with the increase of roughness, in pure magnesium [72].To increase the degradation resistance, Kannan *et al.* (2011) performed mechanical alterations in the surface of the magnesium alloy, using friction stir processing [73]. AZ31 alloy treated by friction stir presented a higher degradation resistance compared to non-treated AZ31 alloy, when incubated with SBF. Corrosion rate is also affected by casting process has observed by Zhang *et al.* (2012) [74].

An option to adjust the corrosion rate is the formation of a protective layer. In vitro tests have shown that incubation of pure Magnesium with cell culture medium, up to 24 hours, increase corrosion protection [51]. A biomimetic layer composed of Ca, P and C is rapidly formed, decreasing the amount of H_2 liberation and corrosion rate of magnesium materials [51].

A method used to produce a biomimetic layer is anodisation, which can create a precipitate composed of Ca, P and F (β-TCP and $CaPO_3(OH)$) on the surface of the material [7]. The anodisation of magnesium is an electro-chemical process that changes the surface chemistry of the metal, via oxidation, to produce a stable anodic oxide layer. The structure of this layer is characterized by a thin barrier layer at the metal-oxide interface, followed by a less dense porous oxide layer. The porous layer can display a variety of different structures and properties which are dependent on the composition, substrate micro-structure and processing parameters [75,76,77]. The processing parameters that influence oxide layer formation include: 1) the type, temperature and concentration of electrolyte; 2) current density; and 3) the applied anodisation voltage. These parameters can also significantly influence the resulting corrosion behaviour of the substrate [76]. The coating formed in magnesium has been shown to decrease corrosion rate in *in vitro* testing simulating physiological environment in previous reports [7,78,79,80]. Anodised AZ31 presented a higher corrosion resistance in the initial stages of corrosion and retardation of the uniform corrosion and localized corrosion mechanisms during immersion in physiological environment [9,81]. The ceramic coating formed has shown to be maintained up to 28 days with no significant degradation (incubated in physiological environment), and degradation is observed only after 60 days; AZ31D alloy showed evidence of degradation after 4 days [81]. Tan and co-workers (2010) reported a reduction in corrosion rate of AZ31 alloys after being submitted to the process of anodisation [7]. Moreover, the corrosion of this layer is determined by the corrosion resistance of the base material [82]. The implication of this observation is that the same coating on different magnesium alloys will result in different corrosion rates.

Polymer coating have been used for numerous biomedical applications, such has bone plates and screws, bone cement, catheters, vascular grafts and surface coatings [83]. Polymeric coatings have been applied to enhance corrosion resistance, abrasion and wear properties of magnesium alloys for biomedical applications [75]. Various

polymers have been used for this application such as PCL, PEI, PLLA and PLLC, polyvinyl acetate (PVAc) [10,11,53,54,55,56,84,85,86,87]. The coatings showed a better performance compared to uncoated samples when incubated in physiological environment, with a delayed start of degradation [10,11]. Furthermore, these coatings have shown to increase biocompatibility of coated magnesium alloys in vitro [86,88]. In vivo tests have shown a delayed degradation and a higher formation of bone on coated alloys after implantation in a rabbit model [88].

PEI is an amorphous polymer that has been studied for magnesium coating showing promising results as a corrosion treatment [53,84,85,87,89]. PCL has also been used as coating for magnesium alloys presenting promising results, decreasing corrosion rate and augmenting biocompatibility of the alloys [10]. Compared to PLLA, the authors found a lower adhesion of the coating to the magnesium alloy, which could be attributed to the molecular structure of the both polymers [10].

Wong and co-workers (2010) tested a polymeric coating composed of polycaprolactone and dichloromethane. The report showed not only a reduced corrosion rate of the coated magnesium alloys but also that the coating aided in retaining the mechanical strength of the implant. Other study compared the efficiency of a PCL and a PLLA coating in corrosion protection [10]. In this work, both coatings exhibited better corrosion protection compared to the uncoated sample. Further, PLLA showed better overall performance. PEI has shown promising results to control corrosion of AZ31 [53]. The authors also reported a better performance of the coating when it exhibited microporous. In the case of non-porous polymers, the integrity of the layer could not be guaranteed due to hydrogen gas production, eventually resulting in the corrosion of the metal surface [53].

Rosemann and co-workers (2012) used a combination of anodic oxidation and a PLLC coating to enhance protection against corrosion [11]. Anodic oxidation led to the reduction of hydrogen evolution, however it could not delay the beginning of degradation. Moreover, the combination of both approaches was found to delay degradation in biological fluid [11].

2.3 *In vivo* and *in vitro* studies of magnesium alloys

Literature regarding the use of magnesium alloys as implants has shown a good compatibility and minor adverse effects, especially in *in vivo* tests [7,33,52,90,91,92].

Magnesium alloys were found to have osteoconductive and osteoinductive properties, contributing to a less invasive repair and a temporary support during tissue recovery [93]. Also, the fact that the alloys can be dissolved or absorbed by the body is an advantage compared to permanent implants, since the later can cause mismatches in the behaviour between the implant and the body, inducing physical irritation and chronic inflammatory reactions [30]. Biodegradable Mg alloys have been reported to have higher bone-implant interface strength than titanium, a well-stablished material for bone tissue applications. A Mg alloy (Mg–Y–Nd–HRE, based on WE43) showed a higher stability and osteointegration after transcortical implantation in rats, when compared to titanium implants [94]. A MgCa0.8 screw implant also showed good biocompatibility and biomechanical properties, comparable to stainless steel [95]. In a study using two different Mg-based implants, ZX50 and WZ21, reported a similar result [96]. These implants, when implanted in Sprague–Dawley rats, presented a good biocompatibility. Normal bone growth after degradation of the Mg implants was observed, even in ZX50 which has a higher degradation rate and massive gas formation is observed [96].

In a study using guinea pigs as animal model, the implantation of magnesium alloys (AZ31, AZ91, WE41 and LAE442) showed a better performance compared to a degradable polymer [33]. A higher bone mass and mineral apposition rate was observed close to magnesium implants. The same authors described a better implant performance in magnesium alloys with rare earth materials in their composition [33]. In implants prepared from LAE442, it has been report a decrease in osteopontin and osteocalcin expression throughout the implantation time, which is an indicator appropriate biocompatibility [97]. Also, it has been found a decrease in the corrosion rate up to 4 orders in *in vivo* results, compared to *in vitro* [8]. Henderson *et al.* (2014) described a good performance of Mg alloys for degradable craniofacial bone screws [98]. Pure Mg and AZ31 alloy implanted in a rabbit mandible presented a good biocompatibility, with

no evident signs of inflammatory response. Mg-Zr alloys have also been reported to induce mineralization when implanted in New Zealand white rabbits [99].

To control corrosion rate, a plasma anodisation film was created in the surface of Mg-Zn-Ca alloy and a better biocompatibility response was reported for anodised material compared to base alloy [100]. A MgZnCa glass has been studied to control corrosion rate and decreasing hydrogen evolution, [101]. Reports showed a decrease in hydrogen evolution *in vitro* and *in vivo* and similar tissue biocompatibility compared to crystalline Mg implants.

AX30 Mg alloy coated with MgF_2 or CaP/ MgF_2 showed a good biocompatibility when implanted in rabbit femurs[102]. When comparing both coatings, it was observed a better osseointegration by osteoid and mineralized bone formation in MgF_2. The results were related to a decrease in degradation observed in Mg alloys with MgF_2 coating. In another study, AZ31 coated with Ca-P was reported to increase biocompatibility and bone regeneration when implanted in rabbits [103]. The implantation of AZ91 and a merwinite/PEO coated AZ91 in rabbits showed an improvement in the biodegradability and biocompatibility, including an increase in the bone formation, in coated samples [104].

In vitro cytocompatibility testing can involve an indirect assay (ISO 10993-5 [105]), in which the cultured cells are exposed to an extract of the material to be tested; or a direct test (ISO 10993-12 [106]), in which the cells are seeded on the surface of the biomaterial. In indirect assays, the extracts are prepared by immersion of the material in culture media for 24 to 72h. In this assay, the cytotoxic or proliferative effects of the materials are then measured in the cells exposed to the extracts [44]. The results obtained in both assays can show great discrepancies. Jung *et al.* (2015) analysed the biocompatibility of a series of Mg-based alloys in both direct and indirect assays [107]. Although in direct tests pure Mg showed a poor cytocompatibility while WE43 had a better result, in indirect tests both materials presented a poor cytocompatibility [107].

Pure Mg was found to support the adhesion, differentiation and growth of stromal cells (obtained from Wistar rats) towards an osteoblast-like phenotype with the subsequent production of a bone like matrix after 17 days of culture [91]. The same authors found no significant difference between pure Mg, AZ21 alloy or a 0.5 wt% Ca alloy. The worst result was found in a 0.8 wt% Ca alloy, presenting a total

disintegration of the material, which showed minimal cell growth [91]. Zhang *et al.* (2012) performed an indirect test to evaluate the cytotoxicity of various Mg-Nd-Zn-Zr alloys, with different casting methods [74]. The incubation of L929 cells with magnesium extraction medium showed a small decrease in viability, still in the range requirements of cell toxicity for biomaterials. Hänzi *et al.* (2010) also obtained a good cytocompatibility of two Mg–Y–Zn alloys (ZW21 and WZ21) when performing indirect cell testing using HUVEC's [90]. In another study, MG63 cells cultured on the surface of AZ31 alloy presented decreased in viability after 48 hours in culture [7]. In other work, hMSC did not proliferate in direct contact with a Mg-Ca alloy [108]. Pure Mg and bulk metallic glass, $Mg_{65}Zn_{30}Ca_5$, were capable of supporting adhesion and viability of L929 cells cultured in the surface of the material [109]. In an indirect test, hMSC have shown to be highly affect by Mg-based extracts [110]. In this study, Mg-based extracts showed a cytotoxic effect on hMSC, when added at high concentration. At lower concentrations, the extracts were able to increase proliferation and differentiation of hMSC. Mg-based extracts have also been described to induce the up-regulation of osteogenic markers, such has ALP and osteocalcin, in MG-63 [111]. U2OS osteoblastic cells seeded in the presence of Mg alloys showed an expression and enzymatic activity of ALP and mineralization similar to control cultures [112]. Extracts from Mg-REE (rare earth elements) are reported to be toxic to MC3T3 cells, at high concentrations [113].

The rate of corrosion has a direct effect in both direct and indirect biocompatibility outcomes. It has been reported that Mg alloy with higher corrosion rates will show less cell growth in the surface of materials as well as a higher toxicity rate in indirect assay [114].

Zhao *et al.* (2014) compared the results of both types of cytocompatibility studies, using endothelial cells, of pure magnesium and magnesium-rare earth alloys [115]. The indirect study revealed no significant differences between pure magnesium and magnesium-rare earth alloys. The opposite was observed in the direct test, with a better attachment and spreading of endothelial cells in the magnesium-rare earth alloys [115]. As referred above, in the direct assay, magnesium alloys show a poorer performance compared to that observed in the indirect assays, which is related with the high corrosion rate of these materials. However, the concentration of magnesium ions alone may not be responsible for the decrease in cell density, spreading and alterations in

morphology, as observed by Keim et al. [51]. Even in the presence of high magnesium concentrations in the medium, such as 750 mg/L, HeLa cells were able to attach and grow. Magnesium ions are also known to stimulate adhesion of osteoblastic cells when added to alumina (Al_2O_3) biomaterials, commonly used in orthopaedic implants [116].

A major factor in the cell adhesion behaviour is the corrosion rate upon exposure of cells to Mg surface [51]. The discrepancy between the various studies, especially the ones using the same alloys, is possibly due to the surface alterations occurring with the corrosion and not from direct cytotoxicity of Mg materials. Cells are exposed to H_2 bubbling and pH increase in the medium when in contact with Mg surface, decreasing their ability to adhere and proliferate. In surfaces previously exposed to culture medium, presenting a biomimetic layer (Ca, P and C), the cell adhesion and spreading will be enhanced compared to pure Mg polished surfaces [51].

AZ31 alloys have been described to have a good performance *in vivo* (implanted in rabbits), with no chronic inflammation being observed [52]. After 8 weeks, the formation of new bone could be seen close to the implant. In the same period, AZ31 alloy coated with Ca-P presented a reduction in the biodegradation compared with naked AZ31. Also, more osteoid formation was found in Ca-P coated samples [52]. In another study, surface treatment with microarc oxidation coating performed in a Mg-Ca alloy resulted in a better corrosion resistance compared to the naked sample [117]. The coated samples revealed to be more efficient in promoting cell adhesion and spreading compared to Mg-Ca naked sample, and presented a better biocompatibility [117]. AZ31 scaffolds coated with Ca-P showed enhanced biocompatibility in MSC cultures compared to base sample, in an indirect assay [103]. MSC cultured in the surface of base and coated samples showed a reduced viability, although the results were in accordance to that observed in the indirect assay, i.e. better performance of the coated samples.

The surface passivation of pure Mg alloy, which creates a Ca/Mg-phosphate layer, has been described to enable HeLa cells adhesion to the surface of the alloys and enhance its biocompatibility [118].

A surface treatment by anodisation as reported to increase the corrosion resistance of three Mg alloys, AZ31B, AZ91E and ZK60A [119]. MC3T3 cells cultured in the presence of extracts from ZK60A and anodised sample showed a decreased viability.

Both, AZ31 and AZ91 showed an increase in viability of MC3T3 cells, especially the anodised samples [119].

A strategy to improve corrosion properties and biocompatibility is the formation of a metal matrix composite, using HA particles. Witte *et al.* (2007) used an AZ91D alloy in combination with HA particles, improving corrosion properties and lowering the pH compared to the base material [8]. Human bone derived cells, MG-63 and RAW 264.7 cells cultured in the surface of these materials were able to adhere and proliferate in both corroding surface, although an increased in cell viability and proliferation was observed in the composite alloy [8]. Another study using a HA coating or a HA/TiO_2 showed similar results. MG-63 cells seeded in the surface of these coatings showed an increase in viability/proliferation compared to base Mg (2.83% Al, 0.8% Zn, 0.37% Mn, 0.002% Cu and balance Mg) [120]. Iskandar *et al.* (2013) reported an increase in adhesion and cytocompatilibity of bone stromal cells cultured in the surface of nanostructured HA-coated Mg alloys compared to the base materials [121]. Also, an improvement in biodegradation of the coated samples was observed.

Polymeric coatings have also been applied to control corrosion rate of Mg alloys. PLGA polymer applied in surface of AZ31 and Mg4Y improved the biocompatibility of mouse osteoblasts cultured in the surface of Mg alloy and provided corrosion protection [122]. In another study, PCL, PEI and PLGA where used to provide a protection layer in AZ31 alloy. MC3T3 cells cultured in the surface of these coated materials showed a increase in viability and proliferation compared to uncoated samples [89]. Xu and Yamamoto (2012) performed a study using polymer films (PLLA and PLC) to enhance the resistance to corrosion of pure magnesium [10]. The pH measurement and Mg^{2+} release were significantly decreased in coated samples. These polymer films provided a significantly better cytocompatibility than uncoated magnesium materials, when SaOS-2 cells were cultured on their surface [10].

PVAc has also been used to control corrosion rate when applied to the surface of Mg alloys. Osteoblast cells MC3T3 seeded in the surface of polymeric coated samples showed a high adherence, proliferation and survival compared to the results observed in uncoated sample (AM50) [86]. PLA polymer with incorporated HA particles has been observed to control corrosion rate and increase biocompatibility. Both, PLA coated samples and HA-doped PLA samples, showed an increase in corrosion resistance

accompanied by an increase of cell growth, when MC3T3 cells were cultured in the presence of extracts of the materials [123].

Wong and co-workers (2010) have used a polycaprolactone and dichloromethane coating to enhance the biocompatibility of AZ91 alloy [88]. *In vitro* tests, using eGFP and SaOS-2 osteoblasts, indicated a better performance of the coated samples when compared to bare AZ91. Moreover, rabbits that have been implanted with both materials showed bone formation, without evidence of inflammation, necrosis or hydrogen gas accumulation. The major differences between implants were the earlier degradation of uncoated samples and the lower volume of new bone in these samples [88].

Zhao and co-workers (2014) showed that endothelial cells (HCAECs) had better attachment, spreading, growth and proliferation on magnesium materials coated with fluoride when compared to collagen coating or uncoated samples [54].

Magnesium alloys present an interesting set of characteristics that make then suitable for bone tissue regeneration, especially their mechanical characteristics. The major difficulty in their use is the fast corrosion rate in physiological conditions. However, a variety of surface treatments are being developed to control the corrosion rate of magnesium alloys, improving significantly the *in vivo* and *in vitro* performance of these materials.

Chapter 3

Materials and Methods

The cytocompatibility of Mg alloys and further surface treatments was analysed in direct assays, i.e. cells were cultured on the surface of the materials, and also using indirect assays, i.e. cells were cultured in the presence of extracts from the Mg-based substrates.

3.1 Direct cytocompatibility assays

The following surfaces were analysed: (i) naked AZ31, AZ61 and RZ5 alloys, (ii) anodised AZ31 and RZ5 alloys, (iii) several compositions of PEI/HA coated AZ31 alloy (Table 3) and (iv) several compositions of PCL/HA coated AZ31 alloy (Table 4).

Table 3. Composition of PEI/HA coated samples.

	Composition
PEI	5% PEI
PEI+HA	5% PEI + 2% HA
	5% PEI + 5% HA
PEI + DETA	5% PEI + 0.3% DETA
PEI + DETA + HA	5% PEI + 0.3% DETA + 2% HA
	5% PEI + 0.3% DETA + 5% HA

Table 4. Composition of PCL/HA coated samples.

	Composition
PCL	5% PCL
PCL + HA	5% PCL + 5% HA
	10% PCL + 5% HA

MG-63 cells were cultured over these surfaces for periods up to 4 days in standard tissue culture conditions. Cell response was evaluated for viability/proliferation, morphology and F-actin cytoskeleton organization, by biochemical methods and observation by scanning electron microscopy (SEM) and confocal laser scanning microscopy (CLSM). Cells seeded in standard culture plates were used as control.

3.2 Indirect cytocompatibility assays

An indirect assay was used to analyse the cytocompatibility of (i) AZ31 alloy, (ii) anodised AZ31 alloy, and (iii) anodised AZ31 alloy coated with PCL containing 2%HA. Cell response was addressed using human mesenchymal stem cells, human osteoclast precursors and human umbilical vein endothelial cells. Cells were cultured in appropriate experimental conditions for each cell type, in the presence of a concentration range of the extracts from the tested materials.

Cell response was evaluated for viability/proliferation, morphology and phenotype markers. Cells cultured in the absence of the extracts were used as control.

3.3 Effects of Mg ion on the osteoblastic, osteoclastic and endothelial cell response

A range of Mg concentrations was used to analyse effect of Mg ion on osteoblastic, osteoclastic and endothelial cell response. Cell response was addressed using human mesenchymal stem cells, human osteoclast precursors and human umbilical vein endothelial cells. Cells were cultured in appropriate experimental conditions for each cell type, in the presence of a concentration range of the Mg ion, in the form of $MgCl_2$. The Mg ion concentrations evaluated were: 1, 10, 20, 50 and 100mM.

Cell response was evaluated for viability/proliferation and phenotype markers. Cells cultured in standard conditions were used as control.

3.4 Mg alloys

The alloys used in this work were purchased from Goodfellow, Inc. The nominal composition of the alloy is depicted in Table 5.

Table 5. Nominal chemical composition of the tested magnesium alloys.

Elements	Aluminium	Zinc	Manganese	Rare Earth	Zirconium	Magnesium
AZ31	2.5-3.5%	0.7-1.3%	0.2-1.0%	-	-	Balanced
AZ61	5.5-6.5%	0.2-1.0%	0.1-0.4%	-	-	Balanced
RZ5	-	3.5-5.0%	0.15%	0.8-1.7%	0.4-1.0%	Balanced

3.5 Substrate preparation

The substrates used in this work were commercial AZ31 Mg alloy, AZ61 Mg alloy and RZ5 Mg alloy, with 3.8 cm^2, that were mechanically polished with 2100 grit SiC paper. The coupons were degreased in alcohol and pre-treated by immersion in a 12% HF solution for 1 h.

3.6 Anodisation: PEO

Anodisation of AZ31 and RZ5 alloys was performed in a two-stage process: KOH 100g/L + Na_3PO_4 100g/L (DC current 5.2A/dm2, voltage up to 30V, 10min, 20-25 ºC); KOH 6g/L + NaF 13g/L (DC current 3.7-1.5 A/dm2, voltage up to 180V, 10 min, 20-25 ºC), according to the previously reported [124].

3.7 Coating formulation: PEI

The polymeric coating was synthesized by mixing PEI in N,N-dimethylacetamide (DMAc), as a solvent, in concentrations of 15 wt.%. The mixture was stirred for 24 h at 50 ºC in order to obtain a stable and yellowish but transparent solution. Diethylenetriamine (DETA) (3 wt.%) was added to this formulation. To improve the biocompatibility, nanohydroxyapatite particles (HA) were added to the obtained

solution in different percentages (2 and 5 wt.%). Detailed description of the methodology was previously reported [55].

The composite polymeric coating was applied on the metallic coupons using a dip coater and then it was cured in an oven at 150 ºC for 2 h under atmospheric conditions. The composite polymeric coating was also applied to glass coverslips.

Several coating compositions were tested on glass coverslips: PEI, PEI + 2% HA, PEI + 5% HA, PEI + DETA, PEI + DETA + 2% HA and PEI + DETA + 5% HA (Table 3). The best compositions were applied over AZ31 alloys.

3.8 Coating formulation: PCL

The coating system was composed of two layers applied in separated steps. Firstly, a polymeric layer was synthesized by mixing PEI in N,N-dimethylacetamide (DMAc), as a solvent, in concentrations of 2.5 wt.%. The polymeric coating was applied on the metallic coupons using a dip coater and then it was cured in an oven at 150 ºC for 2 h under atmospheric conditions. The second polymeric layer was prepared by dissolving PCL granules (Mn 70,000–90,000 Da) in chloroform, under magnetic stirring for 2 h. The composite polymeric coating was also applied to glass coverslips. Nanohydroxyapatite particles were added to the obtained solution. The PCL coatings were applied over the PEI-coated metallic coupons by dip coating. Detailed description of the methodology was previously reported [56].

Several coating compositions were tested on glass coverslips and over AZ31 alloys: 5% PCL, 5% PCL+5% HA and 10% PCL+5% HA (Table 4).

3.9 Extract preparation

Samples of AZ31, anodised AZ31 and anodised AZ31 coated with PEI+DETA+2%HA, with 2 cm^3, were incubated in 10 mL of culture medium (α-MEM or M199, depending of the cell culture tested) for 24h at 37ºC. After the incubation period, the medium was collected and a series of concentrations, between 50% and 2%, were added to cell cultures. Cultures of hMSC, PBMC and HUVECs were analysed for relevant phenotypic characteristics.

The concentrations of Mg and Ca ions in the pure extracts were analysed by atomic absorption spectroscopy, and are depicted in Table 6. pH values were measured with pH indicator stripes and are depicted in Table 6. The pH value of the medium with the extract concentrations used was 7.4, with the exception of the concentration 50% for the AZ31 and anodised samples (pH values = 7.8).

Table 6. Concentration of Mg and Ca ions in the pure extracts (mM).

		Control a)	AZ31	Anodised AZ31	Anodized AZ31, coated PEI+DETA+2%HA
Mg	α-MEM	0.92±0.01	21.08±0.14	13.18±0.20	1.18±0.01
	M199	0.97±0.01	17.04±0.25	13.76±0.10	4.21±0.04
Ca	α-MEM	1.62±0.01	1.37±0.01	1.18±0.04	1.81±0.01
	M199	1.78±0.03	1.19±0.01	1.03±0.02	1.63±0.02
pH	α-MEM	7.4	9.5	8.5	7.4
	M199	7.4	9.5	8.5	7.4

a) Control is the culture medium used to prepare the extract.

3.10 Cell cultures

3.10.1 MG-63 cell cultures

Human osteosarcoma MG-63 cells (ATCC) were cultured in standard culture conditions, i.e. α-minimal essential medium (α-MEM) containing 10% fetal bovine serum (FBS; Gibco/BRL), ascorbic acid (50 μg/mL), 2.5 μg/mL fungizone, penicillin-streptomycin (100 IU/mL and 100 μg/mL, respectively), and incubated in a humidified atmosphere of 5% CO2 in air at 37ºC.

At 70 to 80% cell confluence, adherent cells were enzymatically released with a solution of 0.05% trypsin in 0.25% EDTA to detach adherent cells, and the culture plates were incubated at 37ºC in a humidified atmosphere (5% CO2 in air) for 5

minutes. Complete culture medium (2 mL) was added to the culture plates to stop the enzymatic reaction.

MG-63 cells were used in the direct cytocompatibility assays. Cells were cultured at a density of 10^5 cell/cm^2 over (i) naked AZ31, AZ61 and RZ5 alloys and (ii) anodised AZ31 and RZ5 alloys. Samples were evaluated throughout 4 days, at two times points (day 1 and day 4). Evaluation of the cell cultures was performed for cell viability/proliferation (MTT assay) and observation by Confocal Laser Scanning Microscopy (CLSM) and Scanning Electron Microscopy (SEM).

Also, cells were cultured at a density of $5x10^4$ cell/cm^2 over several compositions of PEI/HA coated AZ31 alloy and several compositions of PCL/HA coated AZ31 alloy. The cultures were evaluated throughout 4 and 5 days, respectively. The cell response to PEI/HA coatings was analysed for viability/proliferation (MTT assay) and observation by CLSM and SEM. Cell response to PCL/HA coatings was assessed for cell viability/proliferation (rezasurin assay), alkaline phosphatase (ALP) activity, and observation by CLSM and SEM.

Cells seeded in standard culture plates were used as control for all groups analysed.

3.10.2 Human mesenchymal stem cell cultures

Human mesenchymal stem cells (hMSC, Lonza) were expanded on cell culture plates with α-minimal essential medium (α-MEM) containing 10% fetal bovine serum (FBS; Gibco/BRL), 2.5 μg/mL fungizone, penicillin-streptomycin (100 IU/mL and 100 μg/mL, respectively), and incubated in a humidified atmosphere of 5% CO2 in air at 37ºC. Third-subculture cells were used in the experiments.

Human MSCs were cultured in the presence of 10 mM β-glycerophosphate and 10 nM dexamethasone for the induction of the osteoblastic phenotype [125]. Cells were seeded at 10^4cells/cm^2 in standard tissue culture plates. After 24h, the culture medium was removed and replaced by one containing the extracts from several Mg-based materials. Cultures were exposed to the extracts during 21 days, and the extract was renewed at each medium change (once a week).

Cell behaviour was analysed throughout the culture time for viability/proliferation (MTT assay, DNA content), ALP activity, expression of osteoblastic genes, histochemical staining of ALP and collagen and intracellular signalling pathways.

3.10.3 Human osteoclastic cell cultures

Peripheral blood mononuclear cells (PBMC) were isolated from blood of 25-35 years old healthy male donors, after informed consent, as previously described [126]. Shortly, after dilution with phosphate-buffered saline (PBS) (2:1), blood was applied on top of Ficoll-Paque™ PREMIUM (GE Healthcare Bio-Sciences). Samples were centrifuged at 400 g for 30 minutes and PBMC were collected at the interface between Ficoll-Paque and PBS. Cells were washed twice with PBS. On average, for each 90 mL of processed blood about $450x10^6$ PBMC were obtained.

PBMC were seeded at $1.5x10^6$cells/cm^2 in standard tissue culture plates and cultured in α-MEM supplemented with 30% human serum (from the same donor from which PBMC were collected), 2.5 μg/mL fungizone, penicillin-streptomycin (100 IU/mL and 100 μg/mL, respectively), 2 mM L-glutamine and the osteoclastogenic inducers M-CSF (25 ng/mL) and RANKL (40 ng/mL). After 24h, the culture medium was removed and replaced by one containing the extracts from several Mg-based materials. Cultures were exposed to the extracts during 21 days, and the extract was renewed at each medium change (once a week).

Cell behaviour was analysed throughout the culture time for DNA content, Tartrate-resistance acid phosphatase (TRAP) activity, expression of osteoclastic genes, caspase activity, histochemical staining of TRAP-positive multinucleated cells and intracellular signalling pathways.

3.10.4 Human umbilical vein endothelial cell cultures

Human umbilical vein endothelial cells (HUVECs, Lonza) were seeded in culture plates coated with 0.2% gelatine. Cultures were maintained in culture medium M199 with 20% of FBS, 2.5 μg/mL fungizone, penicillin-streptomycin (100 IU/mL and 100 μg/mL, respectively) and endothelial cell growth supplement (ECGS). Third subculture cells were used in the experiments.

Cells were seeded at 10^4cells/cm^2 in culture plates coated with 0.2% gelatine. After 24h, the culture medium was removed and replaced by one containing the extracts from several Mg-based materials. Cultures were exposed to the extracts during 7 days, and the extract was renewed at each medium change (every 3 days). Cell behaviour was analysed during the culture time for viability/proliferation (MTT assay, DNA content), caspase activity, NO concentration, expression of endothelial genes and tube-like formation assay.

3.11 Cell viability/proliferation (MTT assay)

The MTT (3-(4,5-Dimethylthiazol-2-yl)-2,5,diphenyltetrazolium) assay is a method used to evaluate the viability, proliferation and activation of cells. This method is based in the capability of mitochondrial dehydrogenase, in live cells, to transform the MTT in a dark blue formazan product.

MTT (0.5 mg/mL) was added to each well, and the culture plates were incubated for 3 h at 37ºC. After the incubation period, the culture medium was removed; the formazan salts were dissolved in 100 µL of dimethylsulphoxide (DMSO) and the absorbance was determined at λ = 550 nm on a ELISA reader (Synergy HT, Biotek). Results were expressed as Absorbance per cm^2 (Abs/cm^2).

In order to exclude the interference of magnesium ions in the MTT analysis, material samples without seeded cells were incubated in the same experimental conditions as the seeded materials and used as blank controls.

3.12 Cell viability/proliferation (Rezasurin assay)

In the resazurin assay, a non-fluorescent blue component is reduced by the living cells to a pink fluorescent component. At each time-point, the culture medium was removed, and fresh medium with 10% (v/v) of resazurin was added to the cells. Cultures were incubated at 37 °C in humidified atmosphere of 95% air and 5% CO_2 for 3 h. Then, 100 µL was transferred to a 96-well plate and the fluorescence intensity was measured in a microplate reader (Synergy HT, BioTek, USA) at 535nm excitation

wavelength and 590nm emission wavelength. The results were expressed in relative fluorescence units.

3.13 DNA content assay

DNA content assay was performed using Quant-iT™ PicoGreen ® dsDNA kit (Invitrogen, Molecular Probes) according to manufacturer's instructions. Previously, cultures were treated with 0.1% Triton X-100 for 15 min. Fluorescence was measured on a ELISA reader (Synergy HT, Biotek, USA) at wavelengths of 480/520 nm (excitation/emission).

3.14 F-actin cytoskeleton labelling

Cells were fixed with formaldehyde (methanol free), for 15 min, and were washed twice with PBS. Cells were maintained at 4ºC in PBS until labelling.

For labelling, cells were permeabilized with 0.1% triton in PBS, for 5 min. A solution of 10 mg/mL of BSA with 1 µg/mL RNAse in PBS was added and left in incubation for 1 h. A solution of 5 U/mL Alexa Fluor® 647-Phalloidin (Invitrogen, Barcelona, Spain) was added and cells were incubated for 20 min in the dark. Cells were washed with PBS, and a solution of propidium iodide (10 µg/mL in PBS; Sigma-Aldrich, St. Louis, MO) was added. Cells were incubated for 10 min in the dark, at room temperature. Cells were washed with PBS, and maintained in a mounting medium (20 mM tris pH 0.8, 0.5% N-propyl gallate, 90% glycerol) before CLSM observation. CLSM was performed in a Laser Scanning Confocal Microscope Leica SP2 AOBS SE (Leica Microsystems, Germany).

3.15 Scanning electron microscopy

For SEM observation, cells were fixed with 1.5% glutaraldehyde in 0.14M sodium cacodylate buffer (pH 7.3). Then, samples were dehydrated in graded alcohols (70%, 80%, 90%, 90% and 100%) for 10 minutes each. To simulate the critical point drying, a solution of hexamethyldisilazane (50%, 60%, 70%, 90% and 100%) in alcohol was added to the samples for 10 minutes each. Samples were sputter-coated with gold and

analysed in a scanning electron microscope (FEI Quanta 400FEG scanning electron microscope equipped with EDS microanalysis capability, EDAX Genesis X4M).

3.16 ALP activity

ALP activity of hMSC cultures was evaluated in cell lysates (0.1% Triton X-100, 5 min) by the hydrolysis of p-nitrophenyl phosphate in alkaline buffer solution (pH≈10.3; 30min, 37 ºC) and colorimetric determination of the product (p-nitrophenol) at 400 nm in an ELISA plate reader (Synergy HT, Biotek). ALP activity was normalized to total protein content (quantified by Bradford's method) and was expressed as nmol/min·$\mu g^{-1}_{protein}$.

3.17 TRAP activity

TRAP activity of osteoclastic cell cultures was evaluated in cell lysates (0.1% Triton X-100, 5 min) by the hydrolysis of p-nitrophenyl phosphate in a acid buffer solution (pH = 5.8, 1 hour, 37ºC) and colorimetric determination of the product (p-nitrophenol) at 400 nm in an ELISA plate reader (Synergy HT, Biotek). TRAP activity was normalized to total protein content (quantified by Bradford's method) and was expressed as nmol/min·$\mu g^{-1}_{protein}$.

3.18 Total RNA extraction and RT-PCR analysis

Osteoblastic, osteoclastic and endothelial cell cultures were characterized for the expression of important genes (Table 7), by RT-PCR. Total RNA was extracted using the Nucleospin RNA II kit (Machery-Nagel), according to the manufacturer's instructions. RNA was analysed for its concentration and purity in each sample by UV spectrophotometry at 260 nm and by calculating the A260nm/A280nm ratio, respectively. RT-PCR was done using the Titan One Tube RT-PCR System (Roche Applied Science), according to the manufacturer's instructions. Half microgram of total RNA from each sample was reverse transcribed and amplified (35 cycles) with Titan One Tube RT-PCR System (Roche), with an annealing temperature of 55ºC. The amplification conditions were chosen accordingly to preliminary calibration

experiments (data not shown), in order to become possible to use the RT-PCR analysis as a quantitative tool. RT-PCR products were separated on a 1% (w/V) agarose gel and gel band intensities were analysed with ImageJ 1.41 software. Values were considered as a percentage of the corresponding GAPDH (housekeeping gene) value of each experimental condition.

Table 7. Primers used on RT-PCR analyses.

Gene	5' Primer	3' Primer
Housekeeping gene		
GAPDH	CAGGACCAGGTTCACCAACAAGT	GTGGCAGTGATGGCATGGACTGT
Osteoblastic genes		
ALP	ACGTGGCTAAGAATGTCATC	CTGGTAGGCGATGTCCTTA
Runx-2	CAGTTCCCAAGCATTTCATCC	TCAATATGGTCGCCAAACAG
Col-1	TCCGGCTCCTGCTCCTCTTA	ACCAGCAGGACCAGCATCTC
BMP-2	GACGAGGTCCTGAGCGAGTT	GCAATGGCCTTATCTGTGAC
OPG	AAGGAGCTGCAGTACGTCAA	CTGCTCGAAGGTGAGGTTAG
Osteocalcin	CATGAGAGCCCTCACA	AGAGCGACACCCTAGAC
Osteoclastic genes		
c-src	AAGCTGTTCGGAGGCTTCAA	TTGGAGTAGTAGGCCACCAG
TRAP	ACCATGACCACCTTGGCAATGTCTC	ATAGTGGAAGCGCAGATAGCCGTT
Ca2	GGACCTGAGCACTGGCATAAGGACT	AAGGAGGCCACGAGGATCGAAGTT
Catk	AGGTTCTGCTGCTACCTGTGGTGAG	CTTGCATCAATGGCCACAGAGACAG
Endothelial genes		
VE-cadherin	GAGTGGCAAGAATGCCAAGT	TACTTGGTCATCCGGTTCTG
CD31	ATGAAGAGCCTGCCGGACTG	TTCCGTCACGGTGACCAGTT
VWF	TCGGAAGTGACTTCGTCAAC	AACACCCAGGTGCTCTTCAG

3.19 Caspase activity

Caspase-3 is a protease that has been found to have an important role in the initiation of apoptosis. This caspase has a substrate specificity to the amino sequence Asp-Glu-Val-Asp and cleaves several proteins, such has poly(ADP-ribose) polymerase, (PARP) and DNA-dependent protein kinase [127]. Caspase activity was performed using EnzCheck caspase-3 assay kit #2 (Invitrogen, Molecular Probes) according to

manufacturer's instructions. Previously, cultures were treated with 0.1% Triton X-100 for 15 min. Fluorescence was measured on a ELISA reader (Synergy HT, Biotek, USA) at wavelengths of 496/520 nm (excitation/emission).). Caspase-3 activity was normalized to total protein content (quantified by Bradford's method) and was expressed as nmol/min·$\mu g^{-1}_{protein}$.

3.20 Histochemical staining of TRAP-positive multinucleated cells

At days 7, 14 and 21 of culture, osteoclastic cell cultures were fixed in 3.7% formaldehyde for 10 min. Cells were rinsed with distilled water and stained for TRAP and Acid Phosphatase, Leukocyte (TRAP) kit (Sigma), according to manufacturer's instructions. TRAP-positive (dark red/purple) and multinucleated cells were counted in a microscope (Nikon TMS inverted phase microscope).

3.21 Histochemical staining of ALP

At days 7, 14 and 21 of culture, hMSC cultures were fixed in 1.5% glutaraldehyde in sodium cacodilate (0.14M) for 10 min. Cells were rinsed with PBS and stained with a solution of α-napthyl acid phosphate (2mg/mL) and Fast Blue R (2mg/mL) prepared in Tris 0.1M, pH 10. The cultures were incubated for 1h in the dark and washed with water at the end of the period. The presence of ALP was noticed by a brown to black staining according to the relative amount of the enzyme. The presence of the staining was assessed under a Nikon TMS inverted phase microscope.

3.22 Histochemical staining of Collagen

At days 7, 14 and 21 of culture, hMSC cultures were fixed in 1.5% glutaraldehyde in sodium cacodilate (0.14M) for 10 min. Cells were rinsed with PBS and stained with a solution of 0.1% Sirius red F3BA in saturated picric acid. The cultures where incubated for 1h and washed with 0.01N HCl at the end of the period. The presence of collagen, a pink staining, was assessed under microscope (Nikon TMS inverted phase microscope).

3.23 Signalling pathways

Osteoblastic and osteoclastic cultures exposed to 10% of extracts, Mg ion concentration and control cultures were analysed for intracellular signalling pathways involved in osteoblastogenesis and osteoclastogenesis. Cultures performed as previously described were exposed to signalling pathways inhibitors throughout the culture time. At day 14, osteoblastic and osteoclastic cultures were analysed for ALP and TRAP activity, respectively. The signalling pathways inhibitors used were: 1 μmol/L U0126 (MEK signalling pathway inhibitor), 10 μmol/L PDTC (NF-kB signalling pathway inhibitor), 10 μmol/L SP600125 (JNK signalling pathway inhibitor) and 5 μmol/L SB202190 (p38 MAPK signalling pathway). Results were presented as percentage of variation of ALP or TRAP activity relative to the sample in the absence of the inhibitor.

3.24 *In vitro* tube-like formation assay: the Matrigel assay

The ability of endothelial cell cultures in organizing the cell layer in a network of tube-like structures upon the contact with an extracellular matrix was evaluated using the Matrigel assay. Endothelial cell cultures were performed as described above. At day 4 of culture, the medium was removed and 10mg/mL of Matrigel (BD Matrigel Matrix, BD Biosciences, Franklin Lakes, New Jersey, USA) was added to the culture. After an incubation of 60 min, at 37ºC, for the jellification of the matrix, culture medium was added to the wells and cultures kept for 24h. Capillary tube-like formation was assessed under a microscope (Nikon TMS Inverted Phase microscope).

3.25 Chick chorioallantoic membrane (CAM) assay

The effect of the extracts from the Mg-based substrates in the *in vivo* angiogenic response was evaluated by the CAM assay. Fertilized chicken embryos were incubated at 37ºC in 45% humidity for 4 days. After this period, a hole was drilled in order to expose the vascular zone of the embryo. A sterilized filter-paper disk, used as carrier for Mg extracts, was applied to the vascular zone. The eggs were sealed and incubated for 3 days at 37ºC. After the incubation period, the number of blood vessels surrounding the discs was photographed (Nikon TMS Inverted Phase microscope) and counted.

3.26 Statistical analysis

Four independent experiments were performed in all biological assays. In each experiment, three replicas were accomplished for the quantitative assays and two replicas for the qualitative assays. The results are shown as mean ± standard error (± SE). Data were analysed with one-way analysis of variance (ANOVA). Statistical differences were determined by the *post hoc* Tukey HSD multicomparison test. A p value of value of ≤ 0.05 was considered statistically significant.

Chapter 4

Direct cytocompatibility assays

Osteoblastic cell behaviour over the Mg-based substrates

The development of magnesium alloys suitable for biodegradable implants is dependent on the control of corrosion rate and mechanical integrity of the implant in physiological environment. An approach to control corrosion rate is thus surface treatment of the alloys. These treatments are interesting for degradable implants because the corrosion rate is intended to be low in the initial phase due to the modified surface layer and then returns to the normal value when the layer corrodes away [57]. Such degradation pattern is desirable since the loss of strength of the implant would mirror the increase in strength of the healing bone, providing sufficient support in the initial phase [57].

In this work, several approaches were used to control corrosion rate of Mg alloys. Firstly, the cytocompatibility of three Mg alloys, AZ31, AZ61 and RZ5 was analysed to evaluate the best Mg alloy to be used in the surface treatments. In a second part, a surface modification by anodisation was used to increase the corrosion resistance of the two alloys with the best performance, AZ31 and RZ5. Furthermore, two polymeric coatings, based on PEI and PCL, used alone or containing nanohydroxyapatite particles, were also evaluated. Firstly, the cytocompatibility of several coatings' compositions was analysed by them self, i.e. applied onto a glass surface, thus without the interference of an underlying Mg alloy. Subsequently, the best coatings' compositions were applied to Mg alloy AZ31 and the resulting substrates were analysed for their cytocompatibility.

The cytocompatibility of these surface treatments was evaluated using MG-63 osteoblastic cell cultures.

4.1 Osteoblastic cytocompatibility of AZ31, AZ61 and RZ5 Magnesium alloys

AZ31, AZ61 and RZ5 alloys have magnesium as their major component; the additional alloying materials vary in presence and concentration. The second element in AZ31 and AZ61 alloys is aluminium, whereas RZ5 alloy have a higher percentage of zinc. RZ5 alloy also presents rare earth metals such as cerium and lanthanum. The composition of the alloys was presented in Table 5.

To analyse the cytocompatibility of the alloys, MG-63 cells were seeded on the surface of the materials and the colonized materials were cultured for 1 and 4 days. Cell behaviour was evaluated throughout the culture time for viability/proliferation (MTT assay) and SEM observation to assess the cell morphology, pattern of cell growth and distribution on the material surface and cell/surface interactions. Cultures performed on the standard tissue culture plates were used as control.

Results for the viability/proliferation are shown in Figure 3. Control cultures presented an increase in viability/proliferation during the culture period. The magnesium alloys showed a significantly reduced viability/proliferation compared to control. A similar number of cells attached to the three alloys, as suggested by the identical MTT reduction values at day 1. On AZ31 and RZ5 alloys, cell proliferation increased from day 1 to day 4, especially on AZ31 alloy. However, AZ61 presented a higher toxicity, which increased with the culture time, as seen by the lower values at day 4 compared to those at day 1.

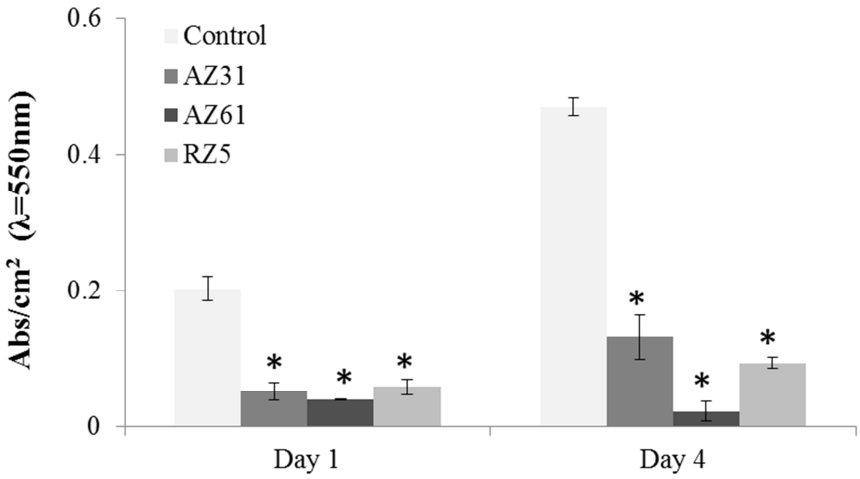

Figure 3. Viability/proliferation of MG-63 osteoblastic cells seeded on magnesium alloys, AZ31, AZ61 and RZ5. * Significantly different from control cultures (MG-63 cells cultured in standard tissue culture plates).

SEM observation was performed on control cultures and on the colonized alloys, at days 1 and 4, Figure 4. At day 1, control cultures presented cells with an elongated morphology, characteristic of this cell type, and cell-to cell contact. On AZ31 and RZ5 alloys, cells also exhibited an elongated morphology, but cytoplasmic expansion was lower than that on control cells, suggesting some degree of cytotoxicity. AZ61 showed only few cells with a round morphology, evidencing a high cytotoxicity of this alloy which did not allow the process of cytoplasmic expansion/cell spreading after the cell adhesion. At day 4, control cultures exhibited a well-organized and dense cell layer. AZ31 and RZ5 alloys also allowed the formation of a cell layer, although with a lower density compared to the control cultures. However, cells cultured on RZ5 alloy showed evident morphological alterations, mainly a reduced cytoplasmic volume, compared to those on AZ31 alloy and control cultures. Similar to that observed in the MTT assay, AZ61 alloy presented a high toxicity; at day 4, cells were barely observed on the material surface.

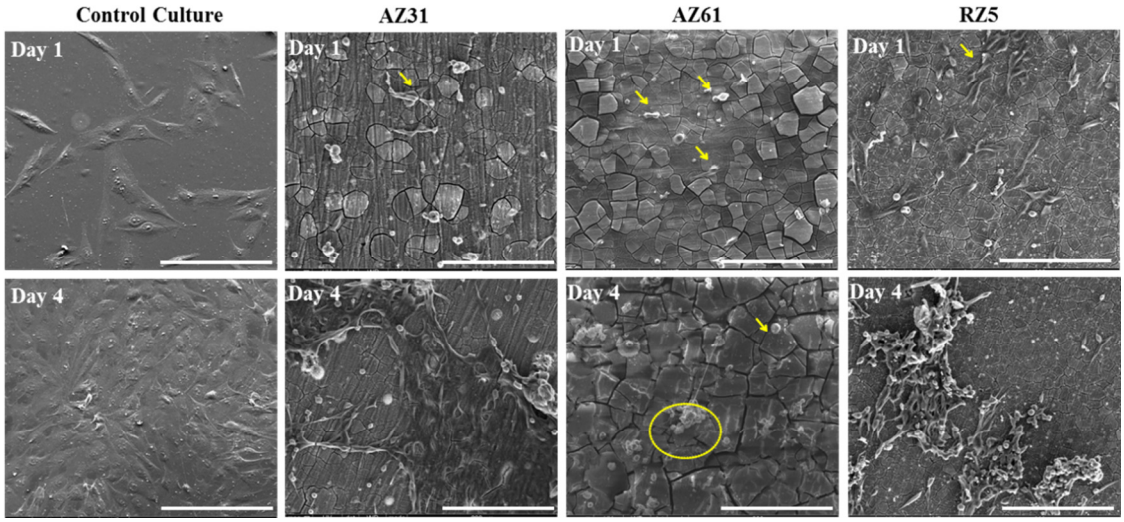

Figure 4. Representative SEM images of MG-63 osteoblastic cells seeded on AZ31, AZ61 and RZ5 alloys. Yellow marks correspond to spots with cells. Bar: 200 µm.

The alloys showed fragmentation of the material surface with evident corrosion/dissolution processes occurring after incubation with culture medium (Figure 5). This was evident particularly in AZ61 which presented a higher fragmentation rate, even at day 1. AZ31 and RZ5 were further analysed before and after incubation with culture medium. The EDS analysis showed an increase of carbon, oxygen and phosphate after incubation with culture medium for four days.

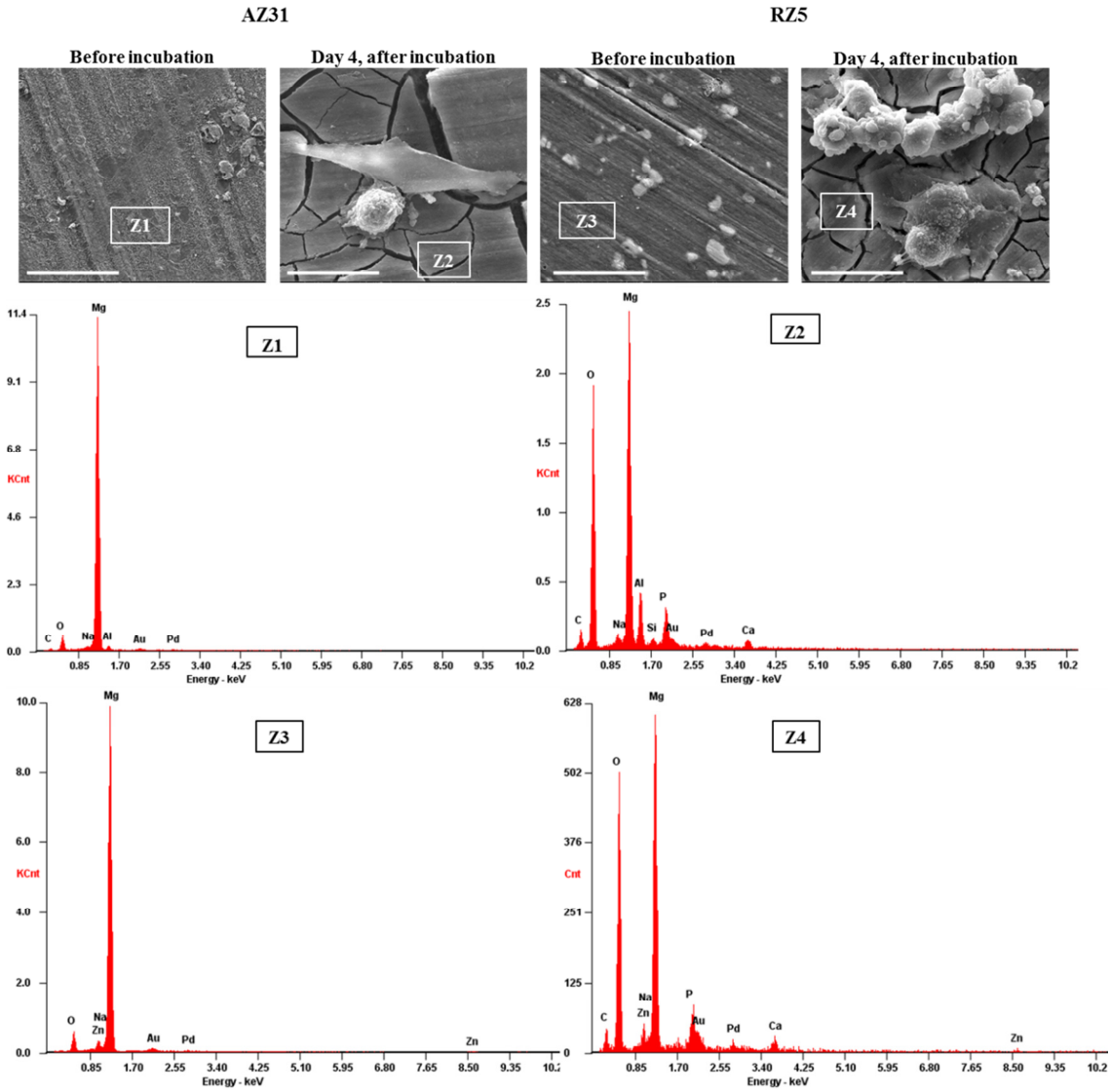

Figure 5. Representative SEM images and respective EDS analysis of AZ31 and RZ5 alloys, before and after contacting with the cell culture medium, for 4 days. Bar: 20 µm.

CLSM observation was in agreement with the information provided by SEM. Control cultures presented an organized cell layer, with extensive cell-to-cell contact by day 4 (Figure 6). Cultures on alloys presented a lower amount of cells. Cells seeded in AZ61 alloy showed rounded morphology on day 1, and by day 4 they were barely visible. AZ31 and RZ5 had a better performance compared to AZ61. In these two alloys, cells with a normal adhesion, elongated morphology and spreading events were observed at day 1. At day 4, a cell layer was observed on both alloys.

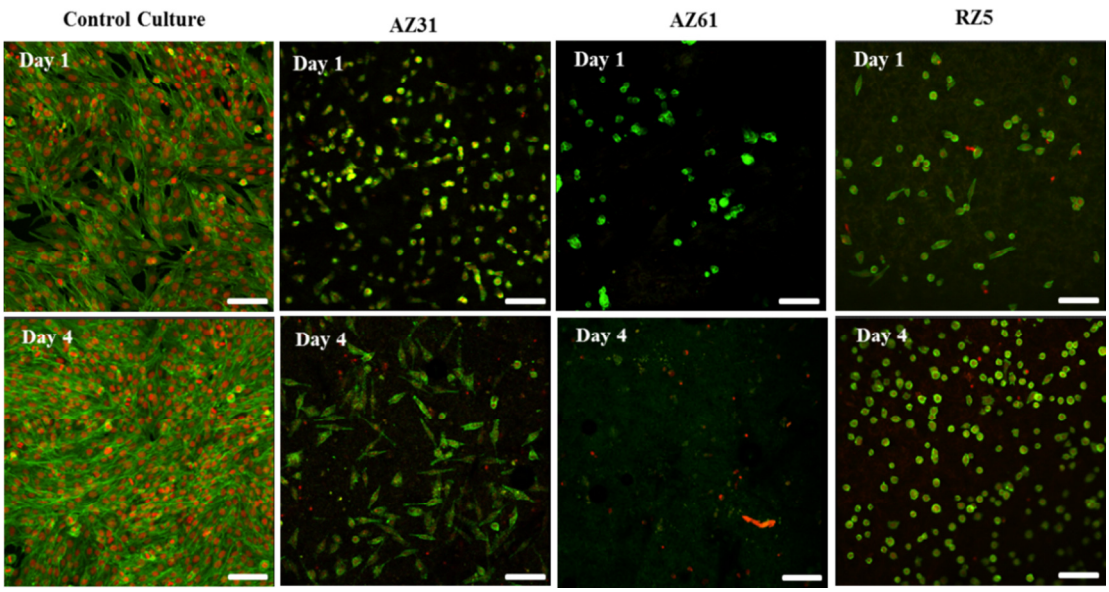

Figure 6. CLMS observation of MG-63 osteoblastic cells seeded on magnesium alloys, stained for F-actin cytoskeleton (green) and nucleus (red). Bar: 80 μm.

The three alloys studied in this work presented a lower performance compared to control cultures. When comparing the alloys, AZ61 Mg alloy showed the highest toxicity in all tests performed. AZ31 and RZ5 alloys presented better cytocompatibility.

4.2 Osteoblastic cytocompatibility of anodised AZ31 and RZ5 alloys

Anodisation is one of the methods used to control corrosion of Mg alloys, which consist in the formation of a thick film on the surface of the alloy. In this study, anodisation of AZ31 and RZ5 alloys was performed using plasma electrolytic oxidation (PEO). PEO is a two-way process using different electrolytes ($KOH+Na_3PO_4$; KOH+NaF) and different current densities. The anodic layer formed on the magnesium alloys exhibited a bi-layer containing an inner barrier layer composed of magnesium, oxygen, phosphorous and fluoride and a porous external layer containing essentially magnesium oxide [124].

To analyse the biocompatibility of the anodised AZ31 and RZ5 alloys, MG-63 cells were seeded on the surface of the materials and the behaviour was evaluated at day 1 and day 4. Cell response was assessed for viability/proliferation and SEM and CLSM observation.

Figure 7 shows the results for the viability/proliferation, assessed by the MTT assay. Control cultures presented an increase in viability/proliferation during the culture period. MG-63 cells seeded on the anodised alloys also presented an increase in proliferation from day 1 to day 4. However, compared to control culture, the viability/proliferation was significantly lower for both materials. Between the two, no significant differences were observed.

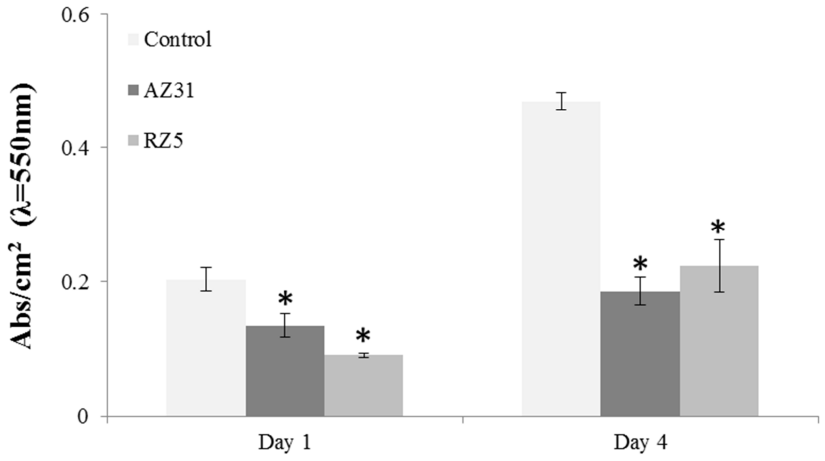

Figure 7. Viability/proliferation of MG-63 osteoblastic cells seeded on anodised AZ31 and RZ5 alloys. * Significantly different from control cultures (MG-63 cells seeded in standard tissue culture plates).

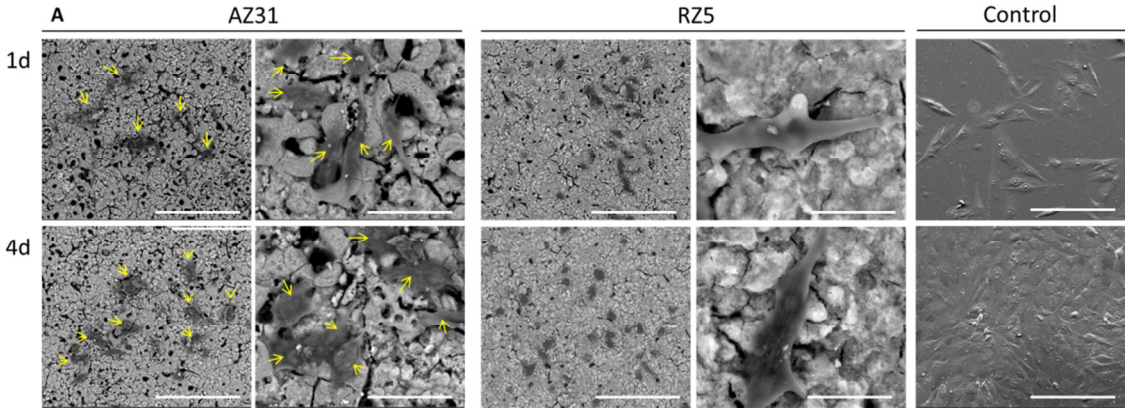

Figure 8. Representative SEM images of MG-63 osteoblastic cells seeded on anodised AZ31 and RZ5 alloys. Yellow arrows correspond to spots with cells. Bar: 200 and 50 μm.

On SEM observation, Figure 8, control cultures presented an organized cell layer which increased with the culture time; cells exhibited the typical elongated morphology expected for this cell type. The alloys presented a significantly lower number of cells, compared to control, both at days 1 and 4. However, high magnification SEM images showed that cells were able to adapt to the irregular surface topography and, in addition, presented an elongated morphology with an appropriate cytoplasmic expansion, suggesting a healthy behaviour.

Anodised AZ31 and RZ5 alloys were also analysed before and after incubation with culture medium, Figure 9. The surface of both alloys presented an intact appearance, without fracture or visible evidence of corrosion. The EDS analysis showed an increase of carbon, oxygen, phosphate and calcium after incubation with culture medium for four days.

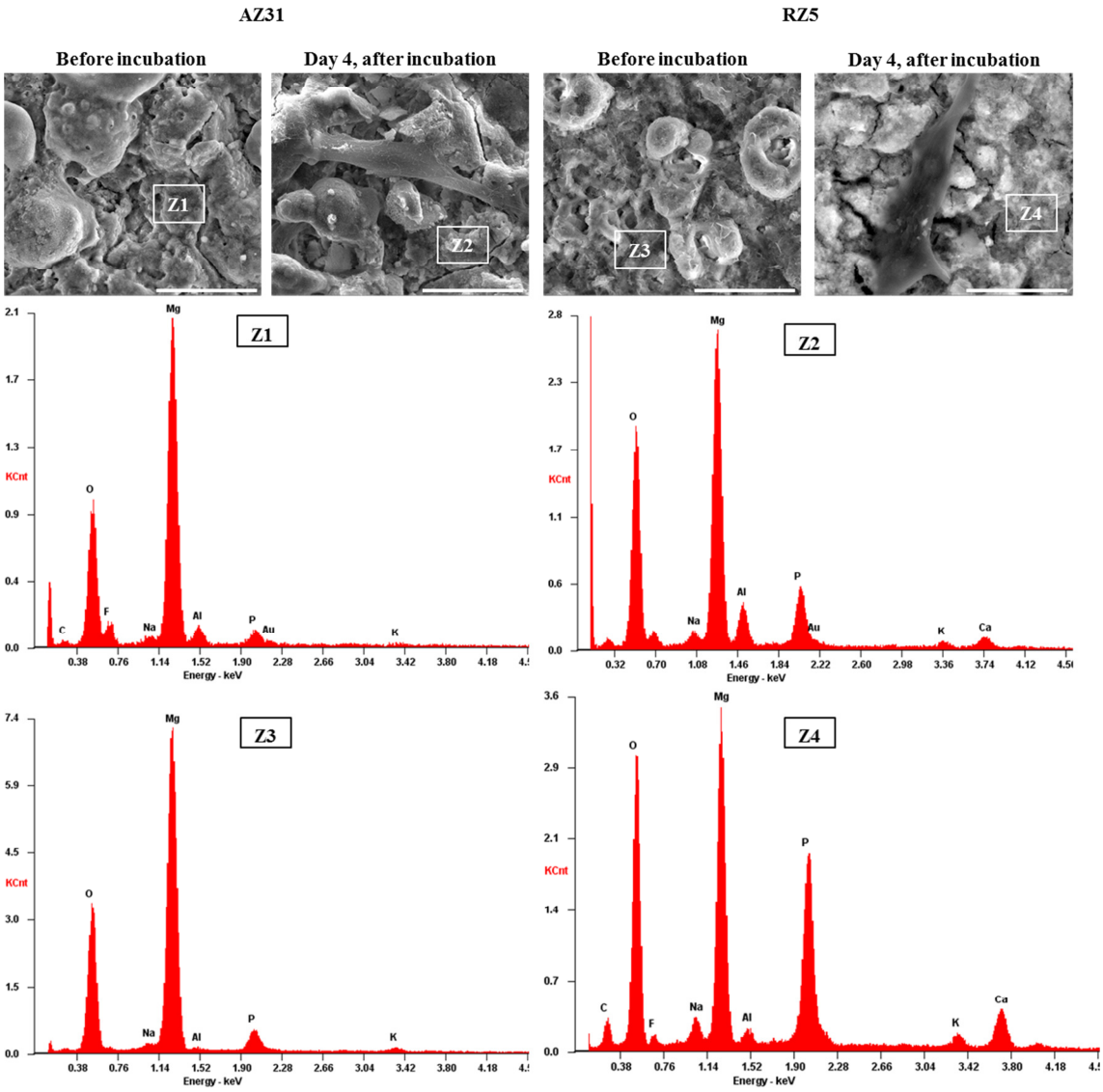

Figure 9. Representative SEM images and respective EDS analysis of anodised AZ31 and RZ5 alloys, before and after contacting with the cell culture medium. Bar: 20 μm.

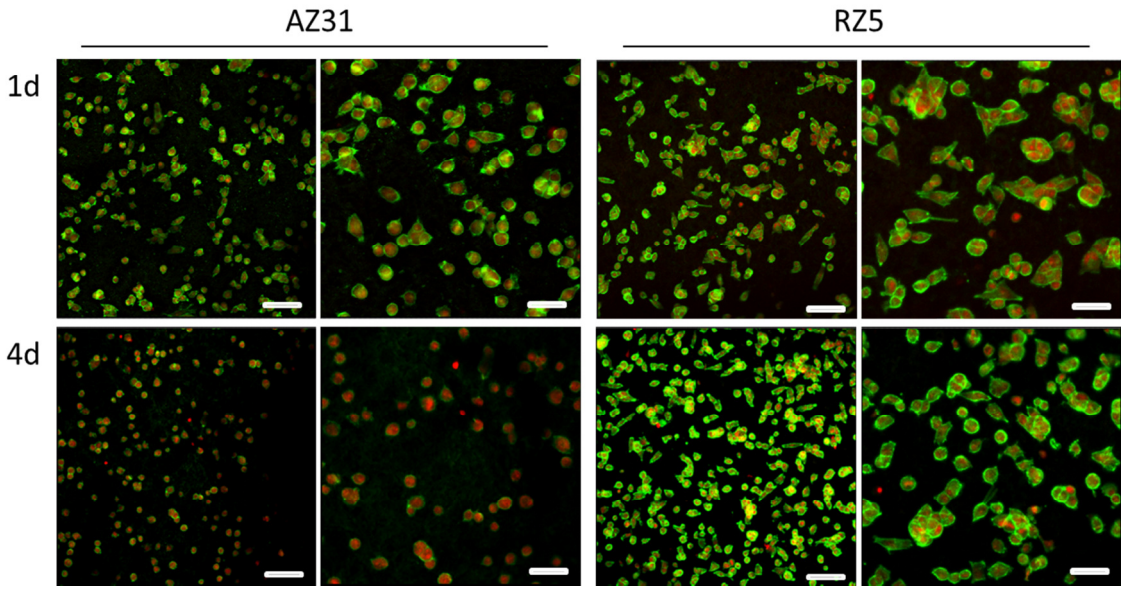

Figure 10. CLMS observation of MG-63 osteoblastic cells seeded on anodised alloys, stained for F-actin cytoskeleton (green) and nucleus (red). Bar: 80 μm and 40 μm.

CLMS observation showed similar results to the ones observed by SEM. MG-63 cells were able to adhere to both anodised alloys, AZ31 and RZ5 (Figure 10). Cell cultures presented normal adhesion and spreading events. Also, most cells showed an elongated morphology and proliferated during the culture period.

Anodisation of Mg alloys created a surface capable of increasing the cell attachment and proliferation, compared to the bare alloy. However, cell growth rate was still lower when compared to control cultures.

4.3 Osteoblastic cytocompatibility of polyether imide-coated AZ31 alloy

Polyether imide (PEI) is an amorphous polymer with good chemical and thermal stability, high mechanical strength, excellent membrane forming properties and can be easily modified by wet chemical processes [128,129,130,131]. PEI has shown to be non-toxic and a biocompatible substrate for cell proliferation in MG-63 cells [128] and human umbilical vein endothelial cells (HUVEC) [131,132]. PEI has also been described to increase the corrosion resistance of Mg alloys [133].

In order to enhance the resistance and cytocompatibility of the polymeric coating, a variety of techniques can be used, including the addition of diethylenetriamine (DETA) and nanoparticles of HA. DETA is a cross-link agent which has been described to enhance adhesion of the polymer to the substrate and with a self-healing effect [134,135]. HA nanoparticles, which have a chemical composition similar to the inorganic part of the bone, have been described to enhance osteoblastic cell differentiation [136] and may act as a corrosion inhibitor [137].

In this work, a series of PEI coating compositions were analysed for their ability to influence in the cytocompatibility of MG-63 cells cultured on the surface of Mg alloys. Firstly, the cytocompatibility of a series of PEI compositions was analysed with the polymer applied over glass coverslips to discern the performance of the coating without the interference of the underlying Mg alloy. The compositions with the best performance were further analysed when applied on the surface of AZ31 Mg alloy.

MG-63 cells were cultured at a density of $5x10^4$ cell/cm^2 on the surface of the coatings. Osteoblastic cytocompatibility of the coating, by itself and applied over magnesium alloys, was evaluated regarding cell adhesion and proliferation, and morphology.

The following polymeric coating compositions were applied over glass coverslips: 15%PEI; 15%PEI+2%HA; 15%PEI+5%HA; 15%PEI+0.3%DETA; 15%PEI+0.3%DETA+2%HA; 15%PEI+0.3%DETA+5%HA (Table 3).

Results for the viability/proliferation are depicted in Figure 11.

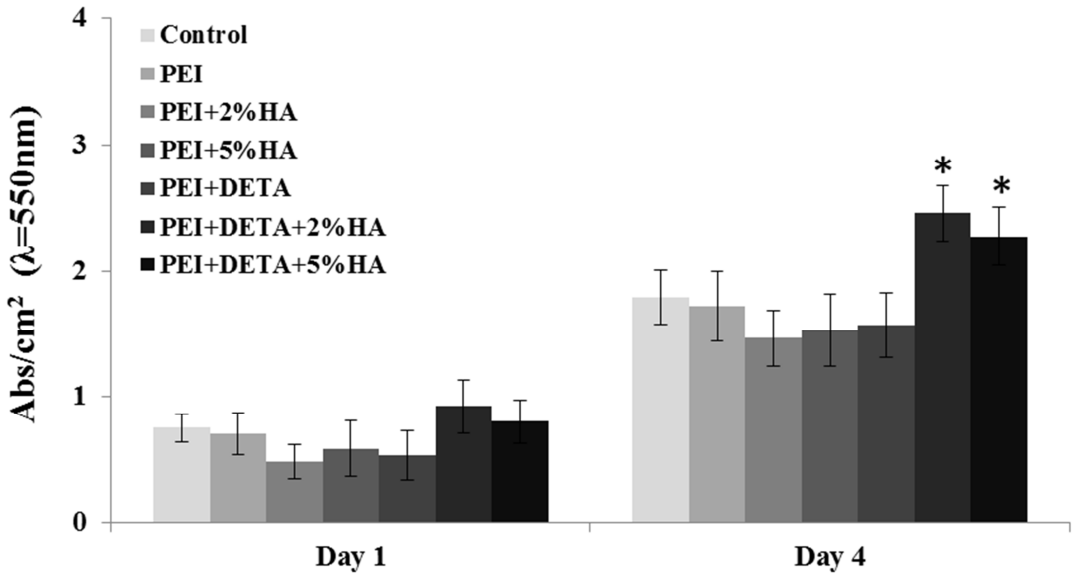

Figure 11. Cell viability/proliferation of MG-63 osteoblastic cells cultured on representative coating compositions applied over glass coverslips. *Significantly different from PEI.

All coatings allowed the proliferation of the osteoblastic cells, as the values observed in the MTT assay increased from day 1 to day 4. Coatings containing HA (2% or 5%) and PEI+DETA presented lower values compared to PEI, although the differences did not attain statistical significance (Figure 11). However, the presence of HA (2% or 5%) in the coatings containing the crosslinking agent (DETA) greatly improved cell proliferation. This inductive effect was noted at day 1, and attained statistical significance at day 4. Cells cultured over standard coverslips presented MTT reduction values similar to those on PEI coating (Figure 11).

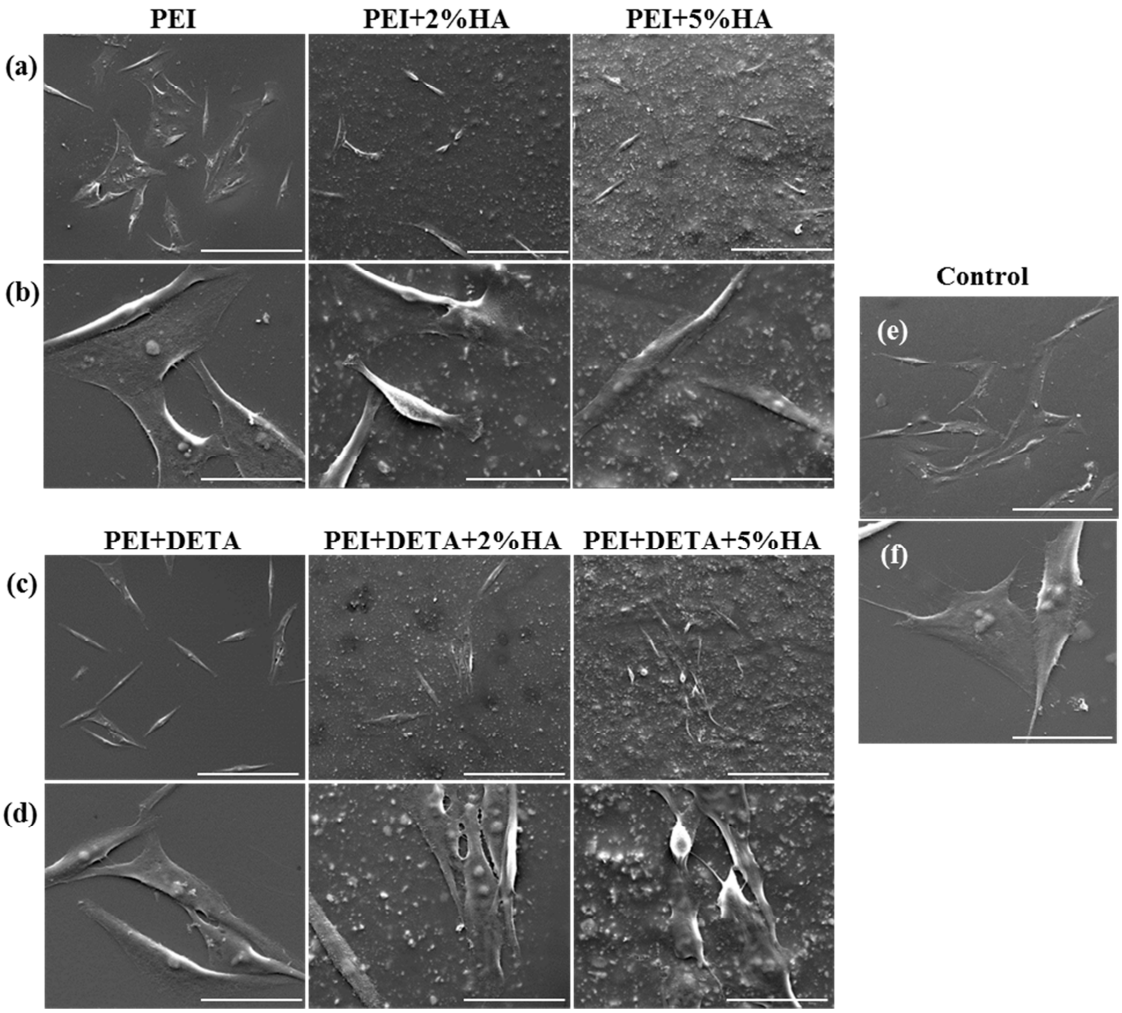

Figure 12. Representative SEM images of coating compositions applied over glass coverslips and seeded with MG-63 osteoblastic cells, at day 1. Cultures performed on control coverslips (e, f). Bar: 200μm (a, c, e) and 50μm (b, d, f).

SEM observation of the colonized coatings provided similar information. However, changes in the cell morphology were also noted. Cells attached to the PEI coating displayed a flat and spread appearance (Figure 12.a,b). Comparatively, on the PEI coatings containing HA, cells were elongated and with a more tridimensional structure (Figure 12.a,b). On the PEI+DETA coating, cells appeared elongated, but relatively thinner (Figure 12.c,d). Interestingly, cells attached on PEI+DETA coating containing HA (2% or 5%) also appeared elongated but with a higher volume (Figure 12.c,d). These observations suggest a healthier cellular morphology over the coatings containing HA. The best performance was achieved in the coatings with the crosslinking agent and

HA. At day 1, cells presented already cell-to-cell contact and a perfect adaptation to the underlying rough topography (Figure 12.c,d). At day 4, all coatings were covered with a cell layer, which appeared denser over PEI+DETA+HA coatings (Figure 13.a). The cell layer appeared relatively flat over PEI and PEI+DETA coatings, and with well-organized cell clusters over the coatings containing HA (Figure 13.a,b). No significant differences were found between the coatings containing 2% or 5% HA, although the composition with 2%HA appeared to present an improved performance. The SEM appearance of the cells grown over standard coverslips was similar to that observed over the PEI coating, at day 1 (Figure 12.e,f) and at day 4 (Figure 13.c).

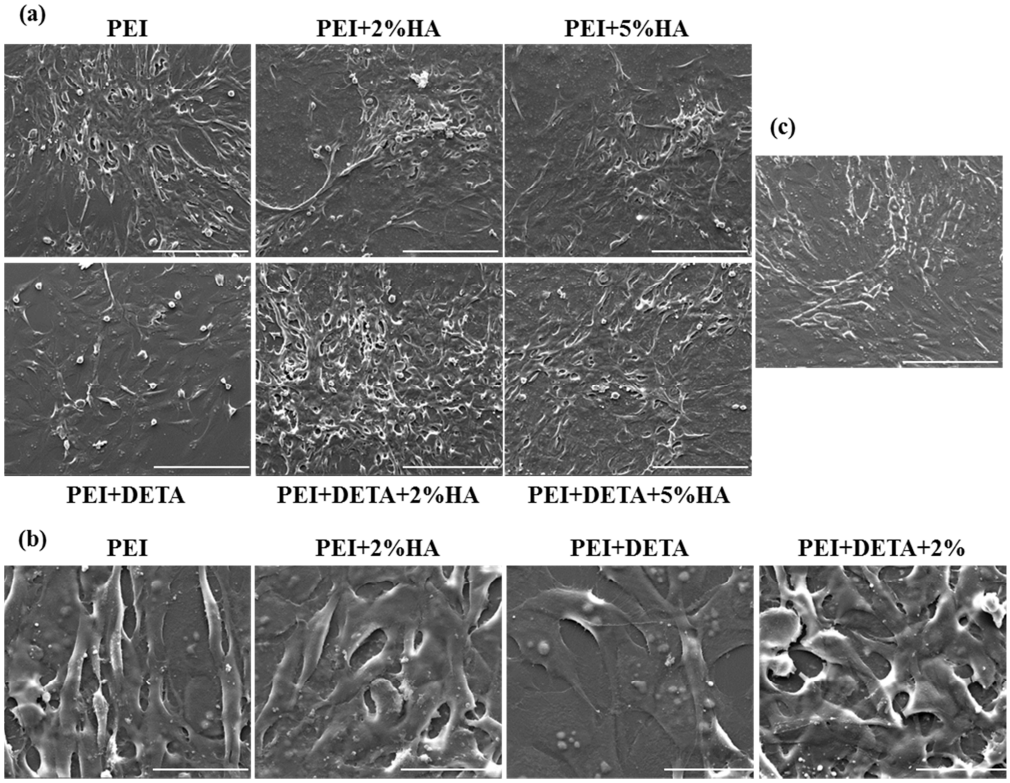

Figure 13. Representative SEM images of coating compositions applied over glass coverslips and seeded with MG-63 osteoblastic cells, at day 4. Cultures performed on control coverslips (c). Bar: 200μm (a, c) and 50μm (b).

Cellular response over the coatings applied on the AZ31 Mg alloy was assessed by CLSM (day 1) and SEM (days 1 and 4). Cell morphology, pattern of cell growth and differences among the coatings were similar to those seen on the coatings applied over

the glass coverslips. Representative images are shown for the coatings PEI, PEI+DETA+2%HA and PEI+DETA+5%HA (Figure 14).

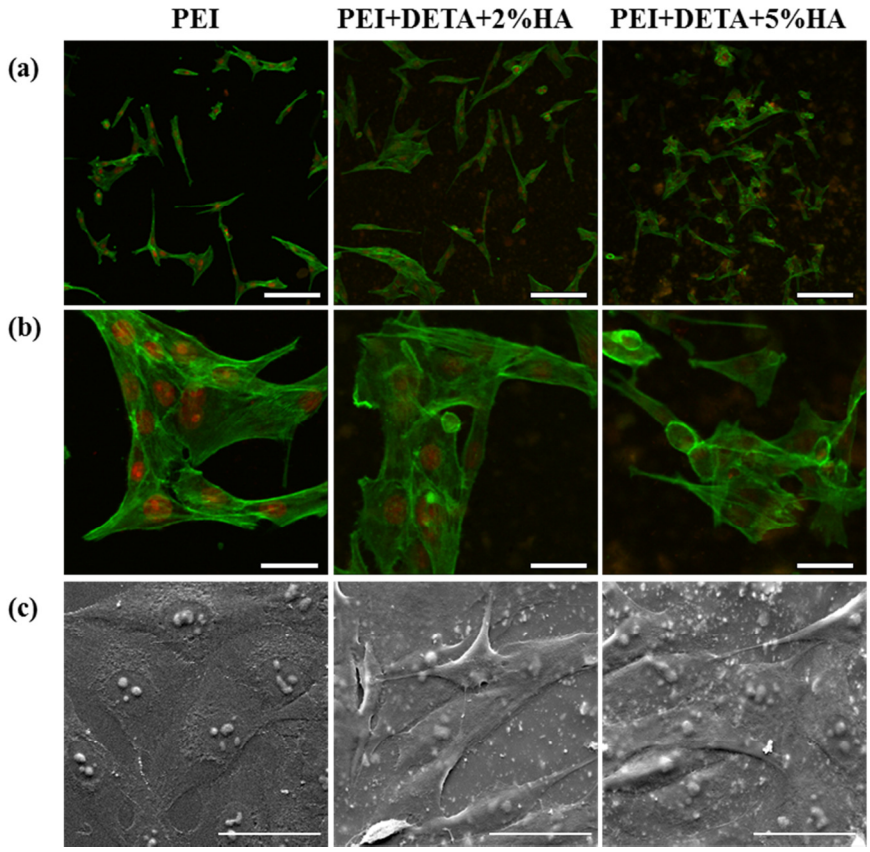

Figure 14. Representative CLSM (a, b) and SEM (c) images of coating compositions applied over AZ31 alloy and seeded with MG-63 osteoblastic cells, at day 1 (a, b) and day 4 (c). Bar: 80µm (a), 20µm (b) and 50µm (c).

At day 1, CLSM images (Figure 14.a, b), showed well spread cells with a prominent nucleus and cell-to-cell contact. In addition, a well-organized F-actin cytoskeleton (which stained intensively at the cell limits) was evident. However, cells adhered to PEI+DETA+5%HA displayed signs of toxicity, reflected by some shrinkage of the cytoplasm with a reduction in the cell volume and a higher number of cells with aberrant cytoskeleton organization and morphology than that seen on PEI and PEI+DETA+2%HA. The apparent signs of deleterious effects on the cytoskeleton detected over PEI+DETA+5%HA might be related to its lower corrosion performance

compared to the one containing 2%HA, as mentioned in Zomorodian *et al.* (2013) [55]. However, high magnification SEM images (Figure 14.c, day 4) show spread cells perfectly adapted to the coating topography in both HA-containing coatings.

The PEI coatings analysed in this work were found to increase the cytocompatibility of AZ31 alloy. Furthermore, the incorporation of HA nanoparticles, especially at 2%, increased the osteoblastic compatibility of the PEI-based coatings.

4.4 Osteoblastic cytocompatibility of polycaprolactone-coated AZ31 alloy

Polycaprolactone (PCL) is a semicrystalline polyester with great organic solvent solubility and a melting temperature of 55 – 60 °C [138]. PCL is used in research and clinical applications and is approved by the Food and Drug Administration (FDA) as a biodegradable polymer [89]. It has been purposed for long-term implant device due to the low rate of degradation in vivo [138]. PCL has also been used as coating for magnesium alloys presenting promising results, decreasing corrosion rate and augmenting biocompatibility of the alloys [10].

In this work, a PCL coating was produced to prolong the corrosion resistance of AZ31 for long periods. To overcome the problem with adhesion of PCL coating to the substrate, an inner polyether imide (PEI) layer with a nanometric thickness was used as adhesion promoter between the AZ31 and the PCL coating. The following compositions were analysed: 5% PCL, 5% PCL+5% HA and 10% PCL+5% HA (Table 4).

MG-63 cells were cultured at a density of $5x10^4$ cell/cm^2 on the surface of the coatings, and were analysed for up to 5 days. As a first approach, cell behaviour was addressed on the coatings applied onto glass coverslips, to have information on their performance without any interference of the AZ31 magnesium alloy. Subsequently, the coatings were applied onto the pre-treated Mg alloy and tested for the cellular response. Osteoblastic cytocompatibility of the coating was evaluated regarding cell adhesion and proliferation, morphology and ALP activity.

Results concerning cell viability/proliferation and ALP activity of the cultures grown on the three coatings' compositions are depicted in Figure 15. All coatings, applied over the glass or over the pre-treated alloy, allowed the proliferation of the osteoblastic cells, as the values observed in the Resazurin assay increased from day 1 to day 5.

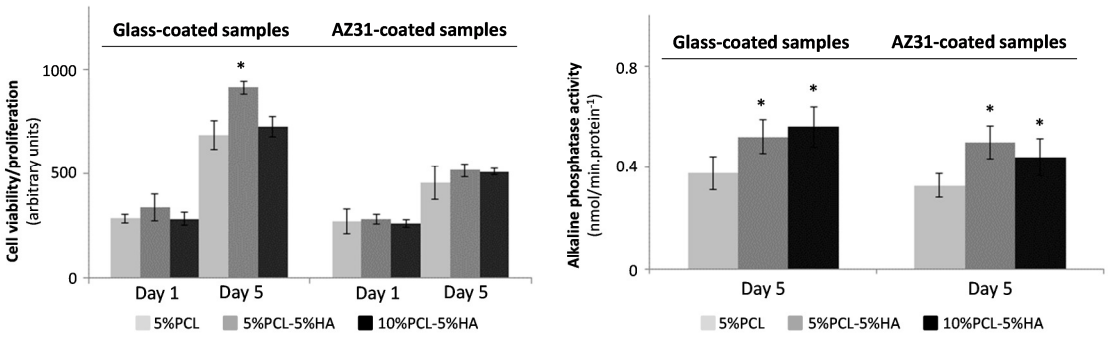

Figure 15. Cell viability/proliferation (days 1 and 5) and Alkaline phosphatase activity (day 5) of MG-63 osteoblastic cells grown over the glass-coated samples and the AZ31-coated alloy. *Significantly different from 5%PCL, for each condition ($p \leq 0.5$).

On the glass coated samples, values were similar at day 1, suggesting the presence of a comparable number of viable cells over the three compositions. However, at day 5, the 5%PCL+5%HA coating showed increased values (~30%), as compared to the other compositions. Cultures grown over the coatings applied to the pre-treated alloy presented some differences on cell behaviour. At day 1, values from the Resazurin assay were identical to those measured on the glass coated surfaces, suggesting that cell adhesion behaves quite similar; also, no differences were noted among the three compositions. However, at day 5, values were lower on the coatings applied over the pre-treated alloy (~30%), and they were similar for the three compositions. Nevertheless, cultures grown over the coated glass or the coated pre-treated alloy showed similar ALP activity. Further, in both conditions, ALP activity was higher in the HA-containing coatings compared to the PCL matrix, but no significant differences were found between 5%PCL+5%HA and 10%PCL+5%HA.

Figure 16 depicts representative SEM and CLSM images of the cultures grown over the glass coated samples. At day 1, cells presented an elongated morphology on the three compositions. CLSM images show that cells stained for the F-actin cytoskeleton presented a higher staining intensity at the cell limits. They also exhibit a well-defined and developed nucleus; in addition, cells on on-going cell division were already visible. At day 5, the three coatings showed a higher number of cells, which appeared well spread over the 5%PCL coating and more elongated over the coatings containing HA. It is worth to note that there was a distinct pattern of cell distribution over the two HA-containing coatings.

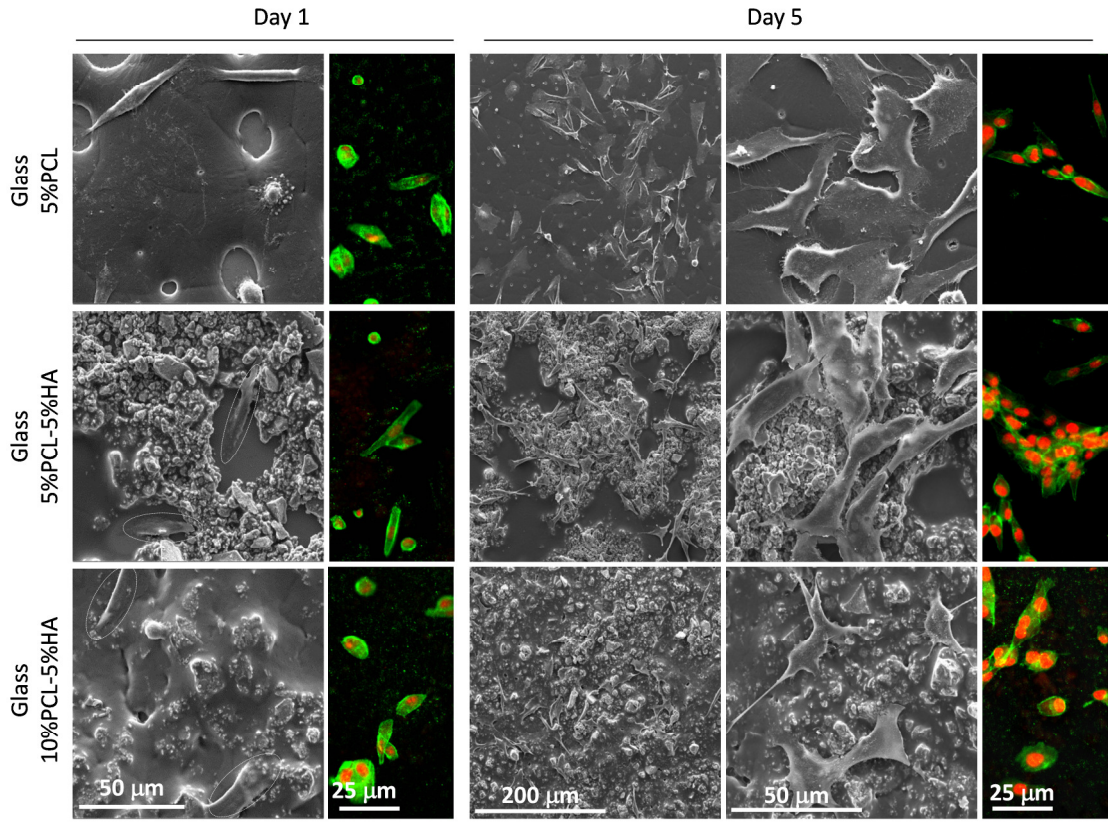

Figure 16. Representative SEM and CLSM images of MG-63 osteoblastic cells cultured for 1 and 5 days over coatings applied on glass. On CLSM images, cells were stained for the F-actin cytoskeleton (green) and nucleus (red).

On the 5%PCL+5%HA coating, cells were clearly more concentrated on the surface areas containing the HA micro-aggregates, whereas cells exhibited a relatively

randomly distribution over the 10%PCL+5%HA coating. In both coatings, cells appeared to adapt perfectly to the underlying surface topography. This pattern of cell growth was evident both in the low and the high magnification SEM images. Also, CLSM images provided similar information, i.e. cells were agglomerated in preferential areas on the 5%PCL+5%HA coating and were randomly distributed over the 10%PCL+5%HA coating.

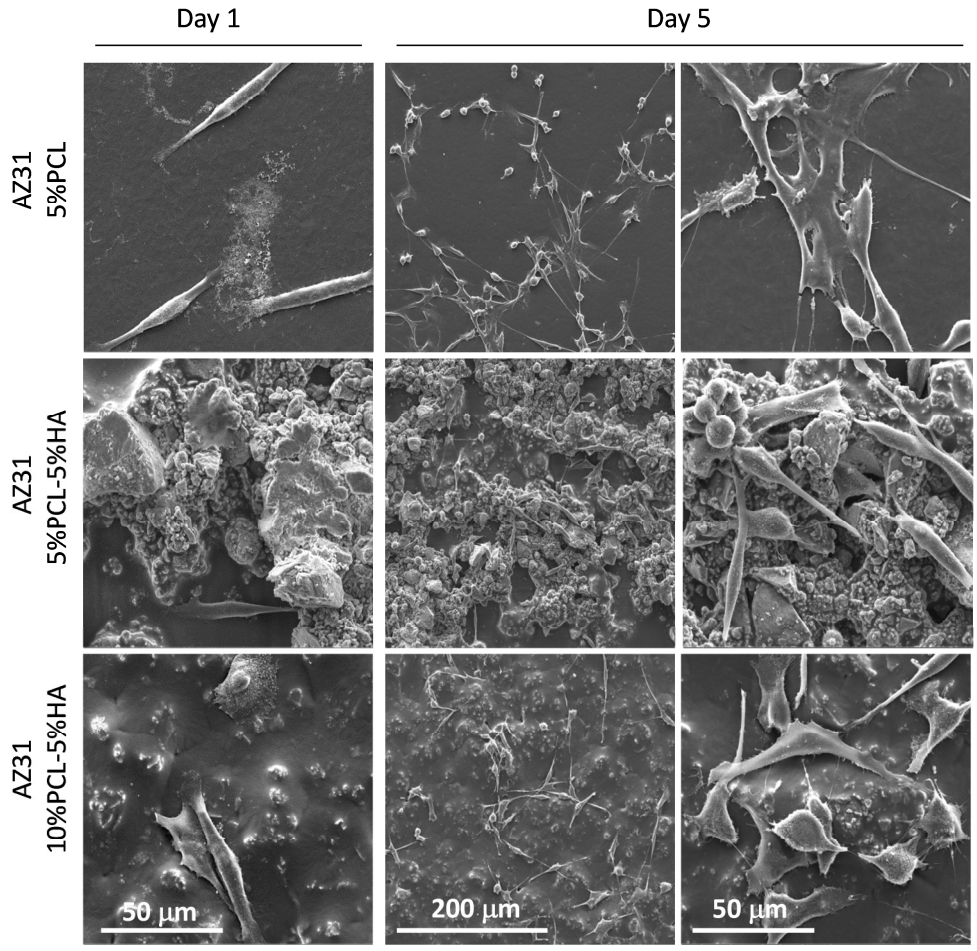

Figure 17. Representative SEM images of MG-63 osteoblastic cells cultured for 1 and 5 days over coatings applied on pre-treated AZ31 alloy.

Figure 17 displays the morphology and pattern of cell growth over the coatings applied to the pre-treated AZ31 Mg alloy, as visualized by SEM. At day 1, cells presented an elongated appearance, similar to that observed over the glass coated samples. However, at day 5, some differences on the morphology were evident. On the

AZ31 coated samples, cells showed lower cytoplasmic spreading, on the three compositions. Nevertheless, they exhibited the same pattern of cellular distribution. On the 5%PCL+5%HA coating, they were concentrated on the coating locations containing the HA micro-aggregates, whereas they were randomly distributed over the 10%PCL+5%HA coating.

The several PCL coatings tested in this work were found to increase the cytocompatibility of Mg alloys. Furthermore, the addition of HA increased viability and the functional activity of MG-63 osteoblastic cells.

4.5 Discussion

Magnesium alloys have been suggested for biomedical applications, showing various advantages for bone tissue regeneration. Mg alloys can be used as biodegradable implants for their ability to corrode in physiological environment [44]. In this study, a set of techniques were used to control corrosion rate: alloy composition and surface treatments such has anodisation and polymeric coating.

Initially, three commercially available magnesium alloys (AZ31, AZ61 and RZ5) were analysed for their osteoblastic cytocompatibility. The results showed reduced viability/proliferation over the Mg alloys compared to control cultures. Of the three alloys, AZ31 and RZ5 presented a better performance *in vitro*. These two alloys showed the formation of a cell layer throughout the culture time (observed by CLMS and SEM). In the literature, alloys such as Mg-Ca alloy [117] and AZ31 alloy [7] have shown similar results. MG-63 cells cultured on the surface of Mg-Ca alloy showed a decreased viability/proliferation in a 5 days culture period [117]. Furthermore, the same authors found a decreased ALP activity of the osteoblastic cells at 5 days of culture. Tan *et al.* (2010) reported a decreased viability/proliferation of MG-63 cells cultured in surface of AZ31 alloy for 48 hours, when compared to cultures in standard conditions i.e. seeded in culture plates [7].

The fragmentation of the three alloys started immediately after incubation with culture medium, especially for AZ61 alloy. The decreased cell adhesion and proliferation observed over the Mg alloys could be strongly affected by changes occurring on the material surface as a result of the fast corrosion process. The phenomenon of corrosion of Mg alloys creates hydrogen gas, which forms bubbles in the surface of the material and increase the pH levels of the surrounding medium [4,51]. As a result of corrosion, a more dynamic surface is created, decreasing the cells' ability to adhere and proliferate in such environments. Higher corrosion rate would also increase the amount of ions and debris in the culture medium, leading to a further damage of cells. Besides the increase of pH levels, it has been described alterations in the osmolality of the culture medium, increased concentration of Mg^{2+} and decreased levels of Ca^{2+} and PO_4^{3-} [43,139]. These alterations could lead to more damage in the cells, particularly in the case of AZ61 which has a higher corrosion rate.

The results showed a higher rate of degradation and corrosion in AZ61 alloy, compared to the other two alloys. A main difference between the three selected alloys is the alloying composition, which has been described as a major factor for alterations in the biocompatibility of magnesium materials [5]. AZ61 alloy has a higher concentration of aluminium compared to AZ31 alloy, whereas RZ5 alloy has higher percentage of zinc plus rare earth elements. Higher percentages of aluminium and zinc have been described to increase oxidation rate of magnesium alloys [33]. In Hank's solution, AZ31 alloy has shown to have better corrosion resistance than AZ91 alloy (with higher concentration of aluminium) [67], which could explain the poorest outcome of AZ61 alloy in this work. Also, Witte *et al.* (2005) described a better resistance to corrosion in alloys with rare earth elements (such as RZ5) [33]. Also, it has been described a better cellular response to magnesium-rare earth alloys when compared to pure magnesium, with a better attachment and spreading of endothelial cells in the magnesium-rare earth alloys [115].

Another option for controlling corrosion rate and therefore improving cytocompatibility of Mg alloys is through surface modification. In this work, anodisation by PEO was used to create an oxide layer, containing phosphorous and calcium. This layer decreased the amount of degradation of the magnesium alloys. This process provided a suitable environment for cells to attach and proliferate. Accordingly, it was possible to observe an increase in cell viability/proliferation in both anodised

alloys, AZ31 and RZ5. In addition, the results achieved for anodised alloys indicated a better surface and environment for cell attachment and growth, when compared to the base alloys.

The results in this work are in accordance to the reports in literature. *In vitro* corrosion studies have shown that creating a layer composed of Ca-P can increase corrosion resistance and biocompatibility [51]. Keim and co-works (2011) reported that incubating the alloys prior the seeding of the cells, 24 hours in advance, created a protection layer of Ca-P in which cells are able to attach. Anodised alloys incubated in physiological environment also showed to be more resistant to corrosion [7,78,79,80,140]. AZ31 alloy has shown a better performance during immersion in physiologic environment after surface treatment by anodisation [9,81]. A factor that should be taking into consideration is the fact that corrosion rate of anodised alloys is dependent on the base material used [82]. Thus, if the base alloy is prone to high corrosion rate, the anodisation coating will be less effective as soon as the base material comes into contact with physiological environment. In a study performed by Pompa *et al.* (2015), AZ31B, AZ91E and ZK60A where evaluated for their biocompatibility after anodisation [119]. It was found that MC3T3 cells cultured in the surface of bare and anodised ZK60A presented a decreased viability. AZ31 and AZ91 showed an increase in viability of MC3T3 cell, especially in the anodised samples. Both samples had a higher corrosion resistance compared to ZK60A.

In vitro studies have revealed that cells seeded in direct contact with the anodised alloys have better biocompatibility compared to uncoated alloy [7]. It is important to mention that, *in vivo*, alloys with/and without surface treatments have a better performance [141]. Park and co-workers (2012) reported a better response of anodised material compared to base alloy [100]. However, both alloys had good biocompatibility when implanted in rats; in addition, the implants were absorbed within weeks, and the absorption period increased in the anodised alloy. The same results were observed by Yang *et al.* (2011) using a rabbit model [52]. The coated implant was found to decrease the amount of hydrogen gas produced compared to uncoated sample. It was also observed a better performance *in vivo* in coated alloys, with evidence of slower degradation [52].

Polymeric coatings, PEI and PCL, were also used to improve the cytocompatibility of AZ31 Mg alloy. As a first approach, cell behaviour was addressed in the coatings applied onto glass coverslips in order to obtain information on their performance without any interference from the underlying AZ31 Mg alloy. Subsequently, the coatings applied onto the Mg alloy were also tested for cellular response.

A series of PEI-based coatings' compositions were tested to analyse the effect of the several components of the coating: 15%PEI, 15%PEI+2%HA, 15%PEI+5%HA, 15%PEI+0.3%DETA, 15%PEI+0.3%DETA+2%HA and 15%PEI+0.3%DETA+5%HA.

Regarding the results from PEI coatings applied onto glass coverslips, it was found that adding DETA to PEI polymer did not contribute to a positive effect on cell response. It was observed a poorer performance of this coating compared to PEI by itself. The addition of HA to the polymeric coating did not affect the viability/proliferation compared to PEI coating. However, the combination of DETA+HA increased the viability/proliferation of MG-63 osteoblastic cells. Furthermore, on these coatings, cells presented a better morphology, showing a higher volume, compared to samples with only one of the two components. Additionally, the coatings with 2% of HA presented a better cell response.

In the PEI coated AZ31 samples, a similar behaviour was observed, namely a better performance on the samples with a combination of DETA+HA. Also, a better performance was observed in the samples with 2% of HA.

A series of PCL coatings were also tested: 5% PCL, 5% PCL+5%HA, 10%PCL+5%HA. Firstly, the coatings were tested in glass coverslips to analyse the effect of the various coatings without the interference from Mg alloy. The viability/proliferation increased in all coatings tested throughout the culture period. At day 5, a significant increase in viability/proliferation was observed in the coating 5%PCL + 5% HA. The functional activity of the two coatings with HA particles significantly increased when compared to PCL by itself.

The AZ31 coated samples also showed a better performance compared to naked samples. When comparing the three coatings tested, the results showed no significant differences in the viability/proliferation, although ALP activity and morphology were better in the samples with HA particles.

The cell behaviour was greatly improved in both polymeric coatings with HA particles. This improvement was evident in viability assays, cell morphology and, especially, in the results regarding ALP activity. In PCL coating, ALP activity was significantly higher on both HA-containing coatings. ALP is an important enzyme produced by osteoblastic cells from the early stages of the osteoblastic commitment, and is actively involved in the mineralization of the extracellular matrix, by providing phosphate ions from the hydrolysis of organic substrates, being a major osteoblastic marker [142]. HA is known to influence osteoblastic cells differentiation and for creating a more biomimetic environment for these cells, since HA is the inorganic component of bone tissue [136]. HA particle size has been described to influence osteoblastic cell behaviour. The particle size of the HA particles used in the present work was ~20 nm, which has been shown to allow for an enhanced osteoblastic response when incorporated in films, compared to that seen in films containing micro-HA particles [143]. It has been reported that films, granules or composite materials manufactured with HA nanoparticles exhibit a surface with improved osteoblastic activity and new bone formation, suggesting a clear advantage in bone tissue applications, compared to conventional HA microstructured materials [144]. In the present work, the agglomeration of the nanoparticles led to the formation of bigger sized particles, still in the nanorange in the 2% HA PEI composite, but as submicron/micron particles' clusters in the 5% HA PEI coating. The agglomeration of the nonaparticles also increased the coating roughness especially with 5% HA, which is reported to enhance cell adhesion and proliferation [145].

AZ31 Mg alloy coated samples showed a better performance compared to uncoated samples. The polymeric coatings controlled corrosion rate and increased osteoblastic cytocompatibility. These results are in accordance to literature reports [53,84,85,87,89]. The polymeric coatings have shown to delay degradation in physiological environment [10,11], increase biocompatibility [86,88] and increase formation of bone of coated alloys after implantation in a rabbit model [88].

The results described in this chapter have shown that modification of the magnesium alloys surface can improve the performance of the alloys. Anodisation showed to enhance the cells attachment to the surface and further growth. Although the promising results, the performance of these anodised materials was still lower than the one observed in control cultures. The polymeric PEI- and PCL-based coatings showed a

better biocompatibility, allowing cell adhesion and proliferation. Furthermore, the results demonstrated that the best cellular response was achieved with the coatings containing nanoparticles of HA.

In conclusion, the coatings proposed in this work increased the biocompatibility of AZ31 alloy, by tailoring the corrosion rate of the alloy. The coated magnesium alloys appear as a promising strategy to obtain biologically safe and active implant materials.

Chapter 5

Indirect cytocompatibility assays

Cell behaviour in the presence of extracts from the Mg-based substrates

An important factor when testing degradable materials, as the Mg-based materials, is the type of cytocompatibility tests performed. Two well-established *in vitro* tests used in these materials are the direct and indirect assays. The direct assays are based in seeding cells on the surface of Mg alloys, as those accomplished in the previous chapter. The indirect assays allow the evaluation of Mg alloy compatibility by analysing the effect of corrosion products released to culture medium, therefore avoiding the effect from the highly dynamic surface of the alloy [7].

In the previous chapter, a series of Mg-based materials and coatings were tested for the direct cytocompatibility of substrates with increasing resistance to corrosion in physiologic environment. The results showed that both, anodisation and polymeric coatings, which decreased the degradation rate of Mg alloys, such as AZ31, resulted in increased biological performance towards osteoblastic cells.

In this chapter, a series of extracts from Mg-based substrates were tested in cells relevant for bone tissue regeneration: osteoblastic-induced human mesenchymal stem cells (hMSC), osteoclastogenic-induced human precursor osteoclastic cells (PMBC) and human endothelial cells (HUVECs). The assayed materials used to produce the extracts were AZ31, anodised AZ31 and anodised AZ31 coated with PEI+DETA+2%HA. The last material is a combination of anodisation and the coating with the best performance described in the previous chapter.

Cultures of hMSC, PBMC and HUVECs were performed in the presence of a concentration range of the extracts for a period of 21 days (osteoblastic cell cultures and osteoclastic cell cultures) and 7 days (endothelial cell cultures) and were characterized for the respective cell phenotype behaviour. The concentration range of the tested extracts was the same for the various cell types: 50%, 20%, 10%, 5% and 2% of the undiluted extract, prepared as described in the section “Materials and Methods”.

Another important thing is to discern the effect of the Mg ion in the cell response observed in the indirect assays. Thus, in the second part of this chapter, a series of Mg concentrations where tested in the same cell types and the cell behaviour was analysed for the respective cell phenotype.

5.1 Effects of the extracts from Mg-based substrates in the osteoblastic, osteoclastic and endothelial cell response

5.1.1 Osteoblastic behaviour of human mesenchymal stem cells exposed to the extracts from the Mg-based substrates

hMSC were used has a model to evaluate the effect of extracts from Mg-based materials on osteoblastic cells. hMSC were cultured for 21 days in the presence of the extracts from the Mg-based substrates, using the experimental protocol described in the Chapter 3. The cells were also cultured in the presence of dexamethasone and β-glycerophosphate to induce the osteogenic differentiation of hMSC.

The extracts used in this work were obtained from three Mg-based materials: AZ31, anodised AZ31 and anodised AZ31 coated with PEI+DETA+2%HA. A set of 5 extract concentrations (50%, 20%, 10%, 5%, 2%) was analysed for the ability to interfere with viability, proliferation and functional activity of hMSC for 21 days.

Figure 18 shows the effects of the materials' extracts in cell viability/proliferation and DNA content during the 21-day culture time. In control cultures, there was an increase in viability/proliferation between days 7 and 14, and at a less extend at day 21. This increase was accompanied with an increase in DNA content.

hMSC cultured in the presence of extracts from AZ31 alloy presented significant differences compared to control cultures. At day 7, there was a tendency for an increase in the cell viability/proliferation in the presence of the extracts. At day 14, with the higher extract concentrations, 50% and 20%, the viability/proliferation (Figure 18.a) and DNA content (Figure 18.d) were significantly lower. At concentrations of 10% and 5%, the viability/proliferation increased when compared to control cultures, attaining statistical significance at day 14. At day 21, the exposure to the extracts decreased viability/proliferation of all concentration, except at 2%. Regarding DNA content, at day 21 the culture exposed to extracts from 20% to 2% maintained a similar result to control cultures.

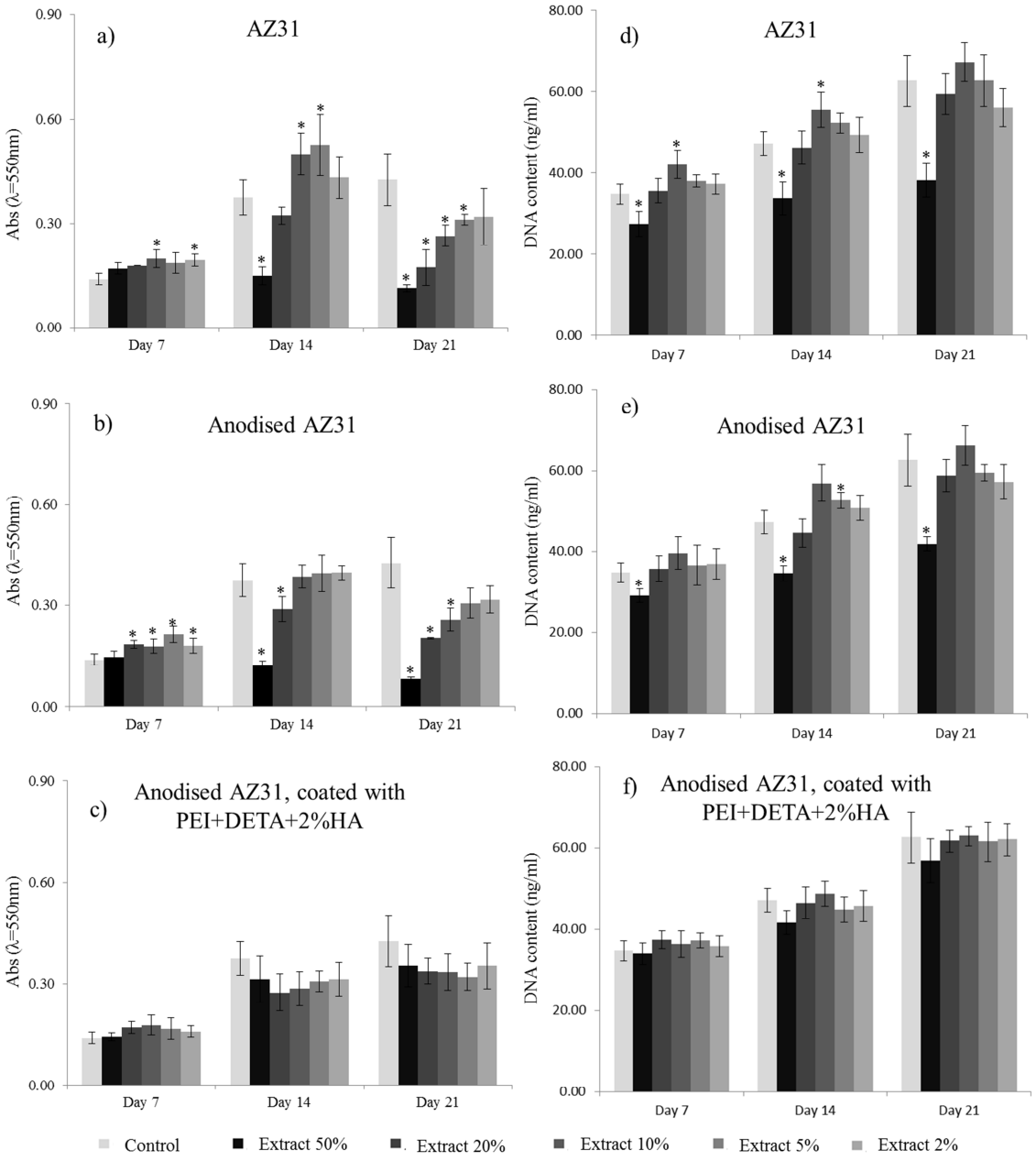

Figure 18. Cell viability/proliferation (a, b and c; MTT assay) and DNA content (d, e and f) of hMSC exposed to the extracts from the Mg-based substrates, at days 7, 14 and 21. *Significantly different from control (absence of extract).

hMSC cultures exposed to the extracts from anodised AZ31 presented similar results to those observed with AZ31 extracts. At day 7, cultures exposed to the extracts presented an increased viability/proliferation. At day 14, the viability/proliferation of cultures exposed to concentrations of 50% and 20% showed a decrease in viability/proliferation, accompanied by a decrease in DNA content. The remaining

concentrations presented similar results to those observed in control cultures. By day 21, the majority of the cultures exposed to the different extract concentrations had decreased viability/proliferation, although similar DNA content compared to control.

hMSC cultured in the presence of extracts from anodised AZ31 coated with PEI+DETA+2%HA were less affected. In this case, there were no significant differences between control cultures and cultures exposed to the extracts. The cells were able to proliferate in a rate similar to control cultures.

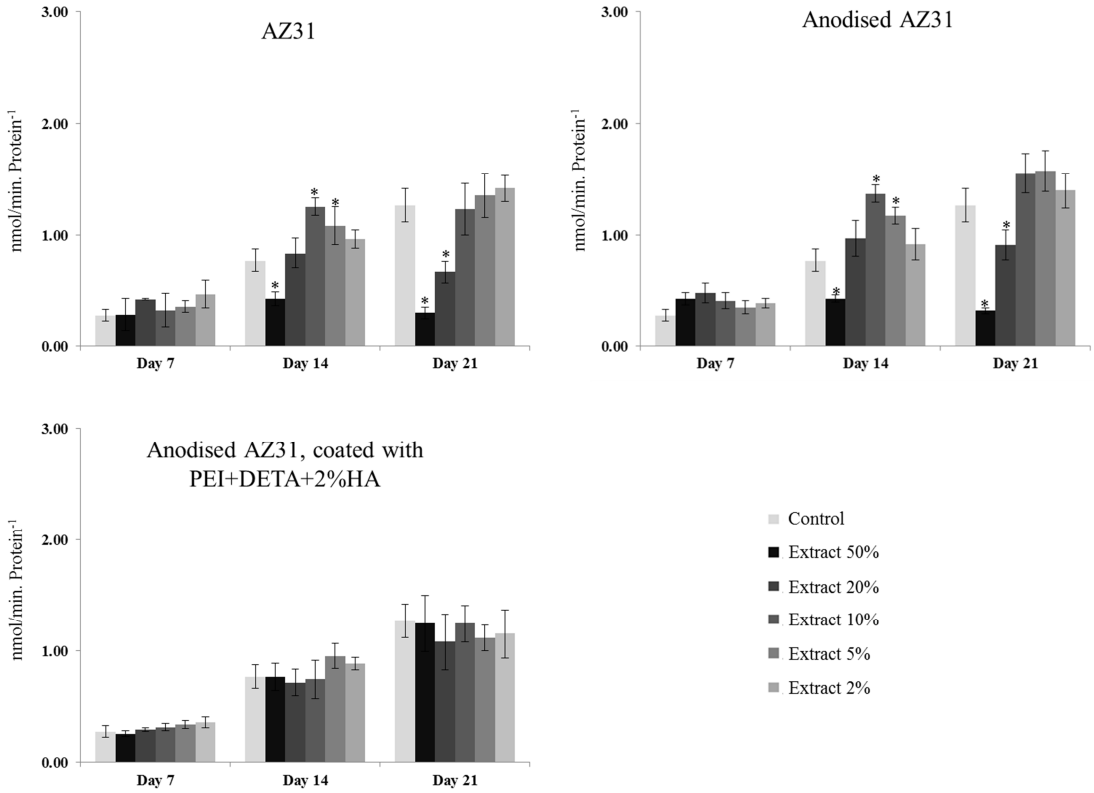

Figure 19. Alkaline phosphatase activity of hMSC exposed to the extracts from the Mg-based substrates, at 7, 14 and 21 days. * Significantly different from control cultures (absence of the extracts).

An important marker for hMSC is ALP activity, a measure for functional activity of osteoblastic cells. Figure 19 summarizes the results for ALP activity. In control cultures, ALP activity increased between day 7 and day 21. At day 7, ALP activity was similar in control and exposed cultures. The cultures exposed to high concentrations of extract from AZ31 alloy showed decreased ALP activity at day 14 (50% extract) and day 21 (50 and 20% extracts), which was in accordance to the viability results. However, 10 and 5% extracts increased ALP activity at day 14. By day 21, ALP activity was similar to control with the 10 to 2% extracts. A similar behaviour was observed in hMSC exposed to the extracts from anodised AZ31. At day 14, ALP activity increased with 10 and 5% extracts. In the same way, the 50% extract caused a decreased activity. The extracts from anodised AZ31 coated with PEI+DETA+2%HA had no effects in ALP activity compared to control cultures.

The results from viability/proliferation, DNA content and ALP activity showed that the extracts had clear effects, especially for AZ31 and anodised AZ31. High extract concentrations decreased cell viability and ALP activity. However, increased viability/proliferation and ALP activity was observed in the presence of 10% and 5% extracts, at day 14. Taking this into account, the effect of the 10% extract was further analysed to better characterize the osteogenic response.

Figure 20 represents the gene expression of osteoblast-related proteins in control cultures and cultures exposed to the extracts, at 10% concentration, measured at day 14. All cultures expressed the osteoblast-related genes: ALP, Runx-2, Col-1, BMP-2, OPG and osteocalcin. Cell cultures exposed to extracts showed an increase in the expression of ALP, Runx-2 and OPG. This effect was specially observed in the cell cultures exposed to the extract from anodised AZ31.

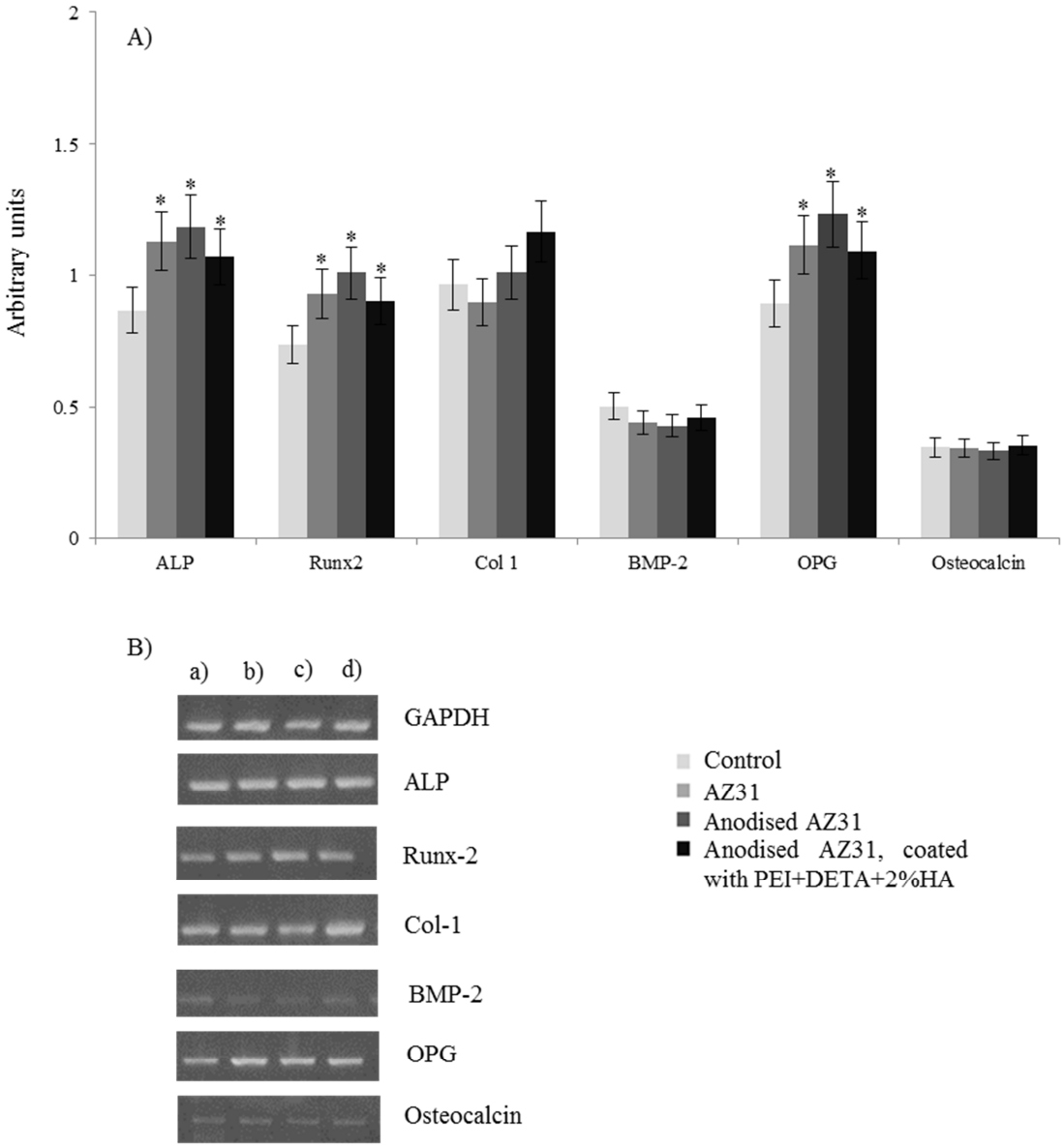

Figure 20. RT-PCR gene expression of hMSC exposed to the extracts from the Mg-based substrates, at a concentration of 10%, at days 14. A) RT-PCR products were subjected to a densitometric analysis and were normalized to the corresponding GAPDH value. *Significantly different from control (absence of the extract). B) Representative gel band images: a) Control, b) AZ31, c) Anodised AZ31 and d) Anodised AZ31, coated with PEI+DETA+2%HA.

Figure 21 shows representative images of histochemical staining for ALP and collagen, at days 14 and 21. In all cultures, ALP staining increased from day 14 to day 21. Cultures presented a characteristic pattern of cell growth, namely exhibiting areas of higher cell density randomly distributed on the culture surface. Cell cultures in contact with the 10% AZ31 and anodised AZ31 extract presented an increase in ALP, showing a darker coloration at day 21 compared to control cultures.

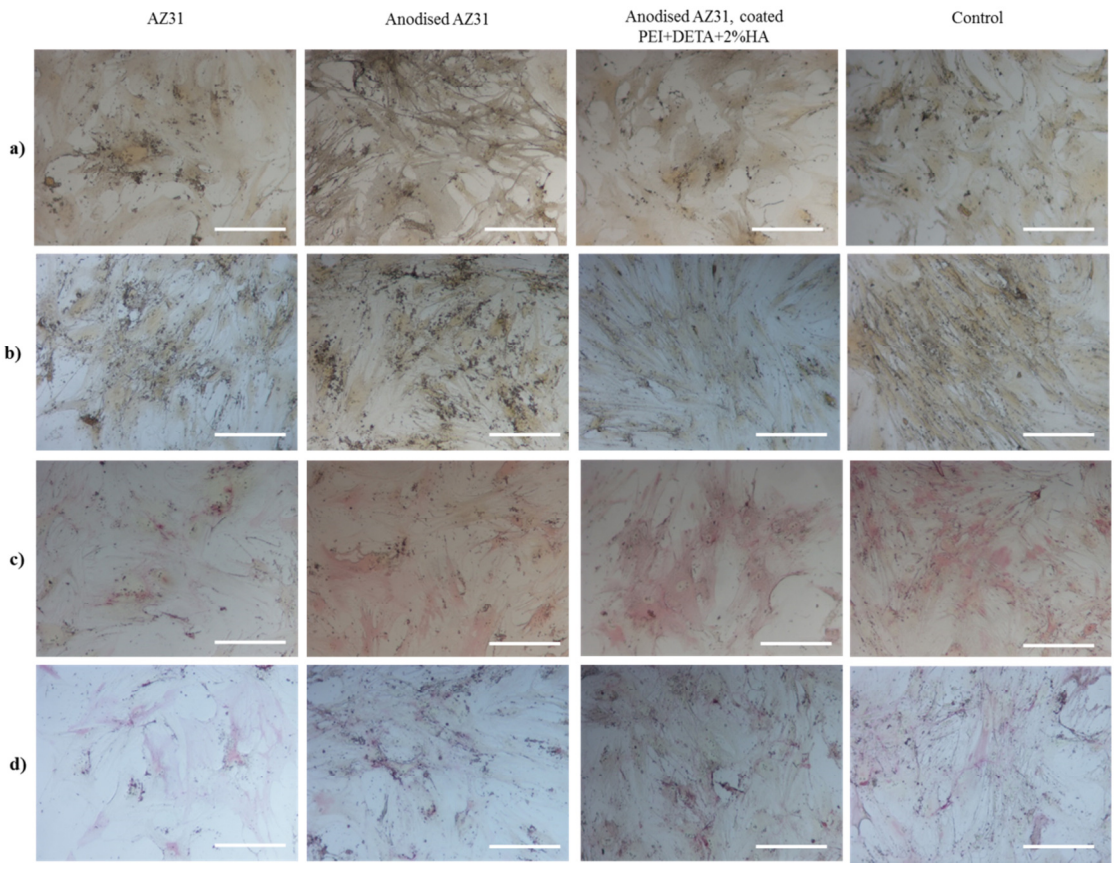

Figure 21. Representative images of hMSC cultures exposed to the extracts from the Mg-based substrates (10% dilution), and stained for ALP (a, b) and collagen (c, d), at days 14 (a, c) and 21 (b, d). bar: 200µm.

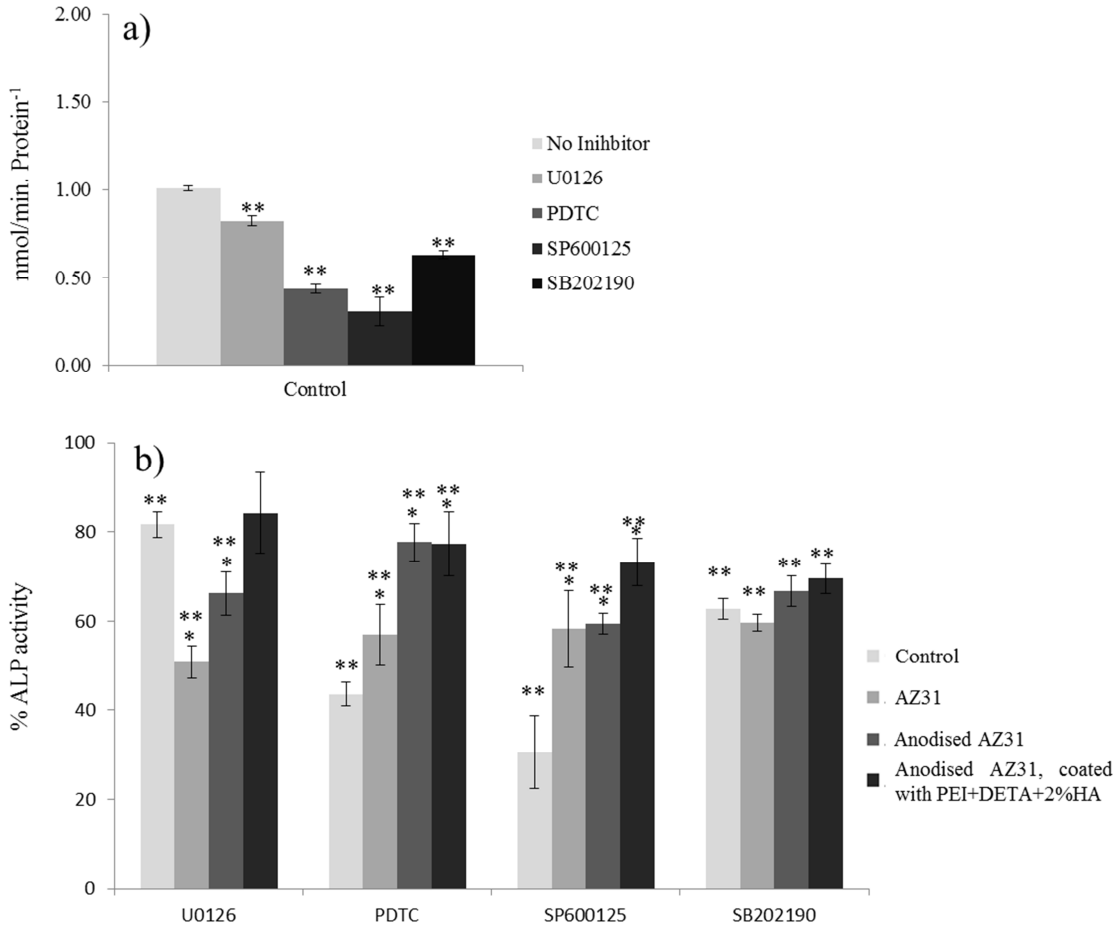

Figure 22. ALP activity of hMSC cultured in the presence of signalling pathways inhibitors, at day 14. a) Effect of signalling pathways inhibitors in control cultures, b)% of variation of ALP activity in cultures performed in the presence of 10% extracts. U0126: MEK signalling pathway inhibitor; PDTC: NF-kB signalling pathway inhibitor; SP600125: JNK signalling pathway inhibitor; SB202190: p38 MAPK signalling pathway. ** significantly different from the cultures performed in the absence of inhibitor. * significantly different from the control cultures.

Figure 22 shows the results for ALP activity of the cultures exposed to the extracts and performed in the presence of inhibitors of several signalling pathways, at day 14.In control cultures, the addition of the inhibitors (Figure 22.a) caused a decreased in ALP activity of hMSC. The NF-KB (PDTC) and JNK (SP600125) signalling pathways showed a more pronounced effect in these cultures, with significant inhibition of ALP activity after the inhibitors were added.

Figure 22.b presents the effects of the Mg-based extracts (10%) plus the signalling pathways inhibitors. In the cultures exposed to AZ31 extract, it was found a significant decrease in ALP activity in all cultures exposed to the inhibitors when compared to the culture performed with no inhibitors. Comparing to control cultures exposed to the same inhibitors, it was observed a significant decrease in ALP activity for MEK signal pathway. Both, NF-KB and JNK signal pathways were down-regulated in the presence of this extract, i.e. increased ALP activity. In cultures exposed to anodized AZ31 extract it was observed a decrease in ALP activity in the cultures exposed to the signal pathways inhibitors. Compared to control cultures, the inhibitor for MEK signal pathway significantly decreased ALP activity. It was observed with the AZ31 extract, NF-KB and JNK signal pathways were also down-regulated in the presence of this extract. With the exception of MEK signal pathway, all inhibitors significantly decreased ALP activity in the culture exposed to the extract from coated AZ31 with PEI compared to the culture performed with no inhibitors. Compared to control cultures, NF-KB and JNK were also down-regulated as observed in the other extracts tested. The p38 MAPK was found to have a similar effect in all tested extracts, with no significant differences compared to control.

In conclusion, the extracts from AZ31 alloy and anodized AZ31 alloy were found to be toxic at high concentrations, such as 50% and 20%. At lower concentrations, these extracts stimulated viability/proliferation, ALP activity and expression of some osteoblastic genes on hMSC cultures. The extract from anodized AZ31 alloy coated with PEI+DETA+2%HA was nontoxic in the tested concentration range, and hMCS presented a behavior similar to control.

5.1.2 Osteoclastic behaviour of peripheral blood mononuclear cells exposed to the extracts from the Mg-based substrates

Osteoclastic cell cultures were established by culturing PBMC in the presence of M-CSF and RANKL for 21 days, using the methodology described in Chapter 3. Osteoclastic behaviour was evaluated in the presence of the extracts (50% to 2%) from the three Mg-based materials, at days 7, 14 and 21.

Figure 23 shows the results for DNA content and caspase-3 activity of the osteoclastic cultures. In control cultures, DNA content decreased between day 7 and day 21. In the presence of the extracts from the three Mg-based alloys, cell cultures had a similar pattern of behaviour, although showing significant differences compared to control cultures.

AZ31 extracts, at high concentrations (50 to 10%), caused an increase in the DNA content at day 7, followed by a significant decrease at days 14 and 21 (50 and 20%). Extracts from AZ31 anodized alloy increased DNA content at days 7 and 14 (50 to 5%) and at day 21 (10 and 5%); however the 50 and 20% extracts inhibited DNA content at day 21. Extracts from the coated alloy did not affect DNA content, compared to control.

Caspase-3 activity is used to measure the level of apoptosis in cell cultures, as an increase in the activity of this enzyme in indicative of high apoptosis rate. Figure 23 (d, e and f) shows the effect of Mg-based extracts, in percentage relative to control. At day 7, the presence of extracts from AZ31 decrease the percentage of apoptosis compared to control. However, at day 14 and 21, cells exposed to higher concentrations of the extract showed an increase in the amount of apoptosis compared to control. Cell cultures exposed to anodised extracts showed a similar result to control at day 7. At day 14 and 21, a decrease in apoptosis was observed for lower concentrations (10% and 5%). Also, it was observed an increase of apoptosis in cell cultures exposed to 50% extract, at day 21. Cell cultures exposed to extracts from coated AZ31 showed an apoptosis rate similar to control.

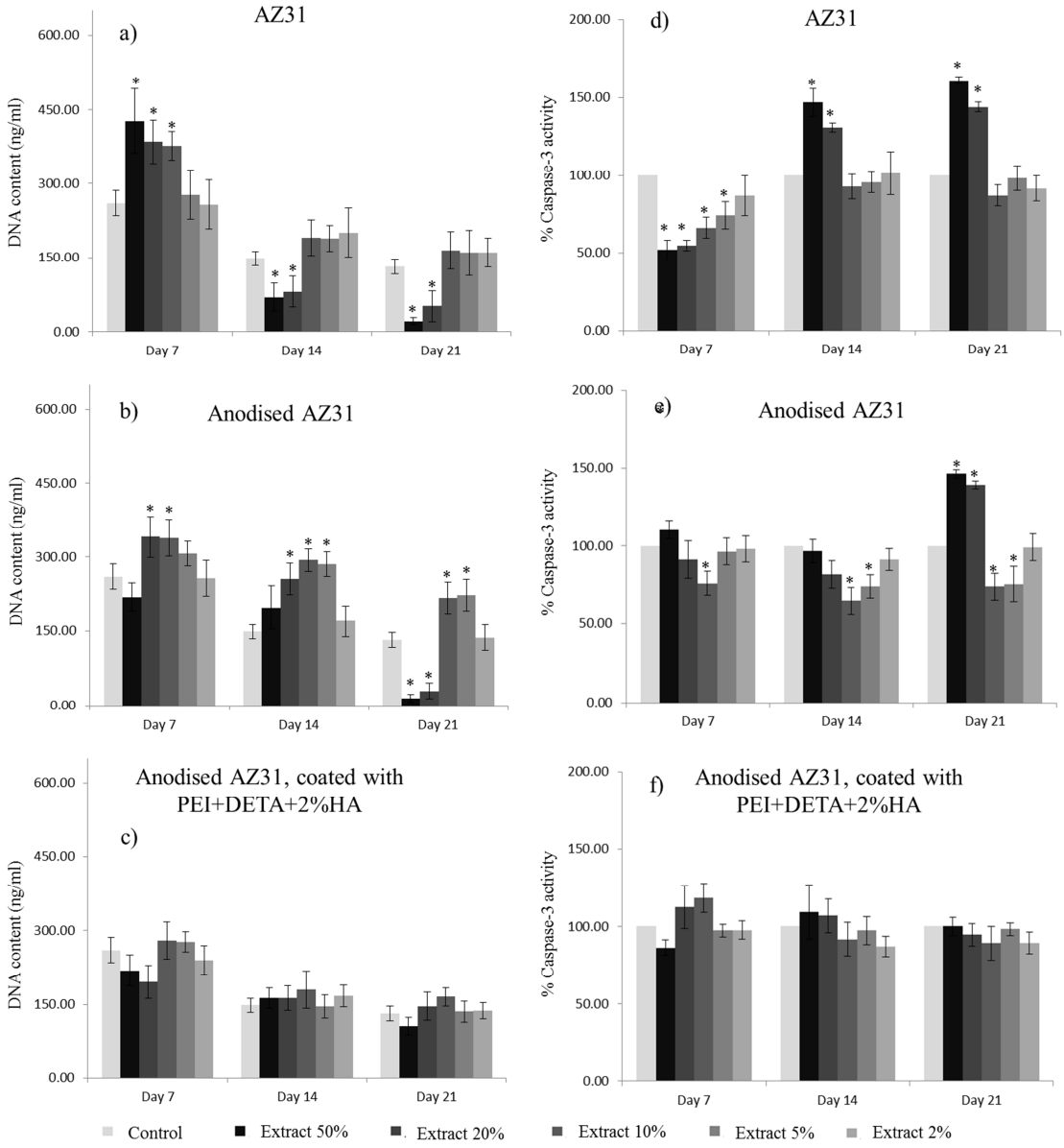

Figure 23. DNA content (a, b and c) and percentage of caspase-3 activity (d, e and f) of human osteoclastic cell cultures in the presence of the extracts from the Mg-coated materials.* Significantly different from control (absence of the extracts).

Figure 24 shows the effects of Mg-based extracts in TRAP activity and number of TRAP positive multinucleated cells. In control cultures, TRAP activity increased throughout the culture period, attaining its higher value by day 21. Extracts from AZ31 did not affect TRAP activity at day 7. However, with the 50% dilution, a significant decrease in TRAP activity was observed at days 14 and 21. Dilutions of 10 and 5% increased the enzyme activity at day 14. Extracts from the anodized alloy, at 10% dilution, increased TRAP activity at days 7 and 14, whereas with the 50 and 20% dilutions the enzyme activity was significantly decreased at days 14 and 21. Extracts from the polymeric coated alloy showed results similar to control cultures. Histochemical TRAP staining of osteoclastic cultures was performed, and the number of TRAP positive multinucleated cells is depicted in Figure 24.d, e and f. In control cultures, the number of these cells appeared to increase from day 7 to day 14, and was similar between days 14 and 21 (Figure 24). At high concentration of extract, from AZ31, the number of cells was low for all culture periods. At lower concentrations the amount of TRAP positive multinucleated cells was similar to control cultures. The extracts from anodised AZ31 had similar results, with a low amount of cells when higher concentrations of extracts were added to the culture. Also, concentrations around 10% to 5% had a stimulatory effect on the number of multinucleated cells. The extracts from polymeric coated alloy showed results similar to control cultures.

The previous results showed that the extracts at a concentration of 10% induced significant alterations in the cell behaviour. Therefore, cell response was further analysed for gene expression and signalling pathways, at day 14.

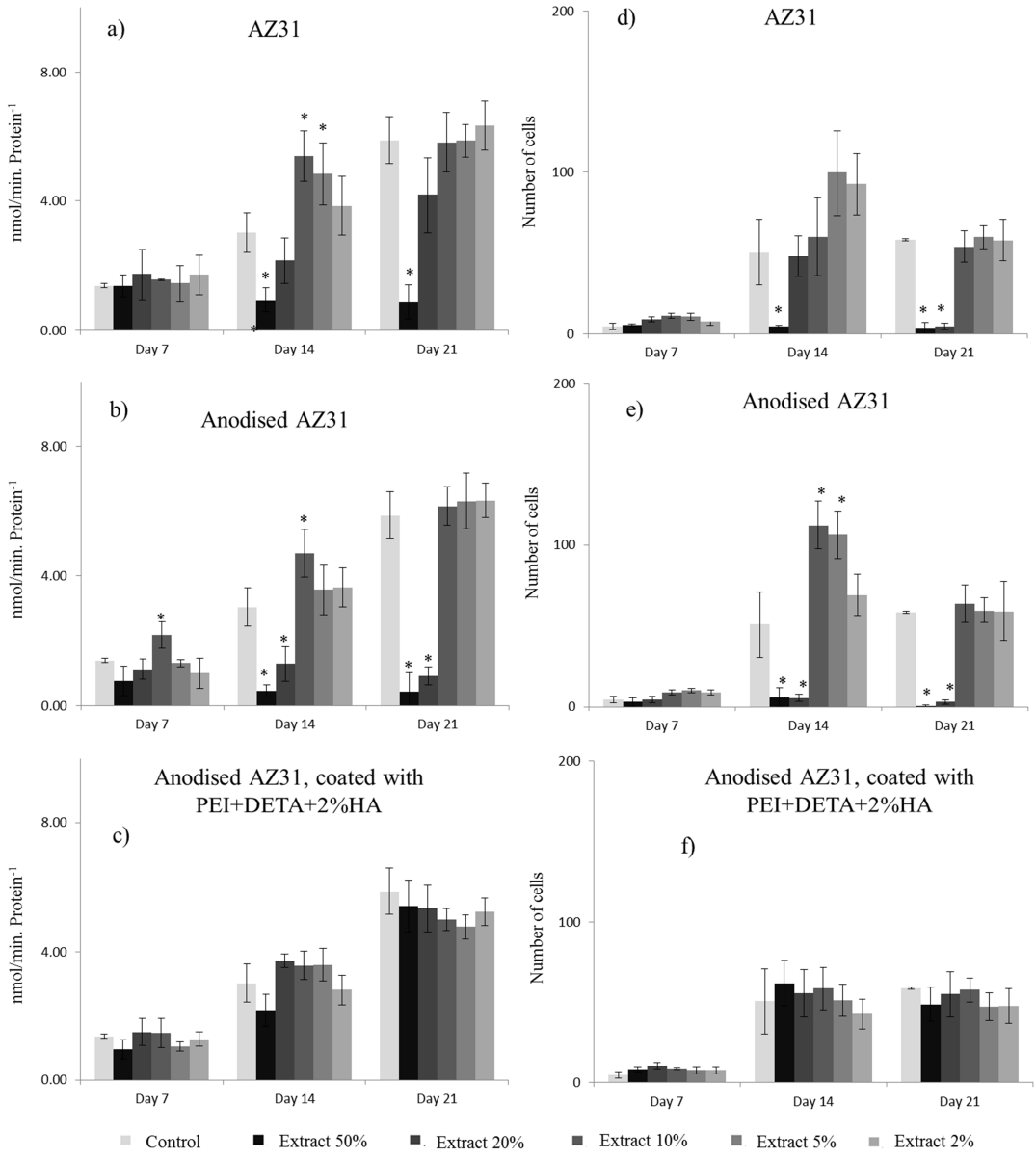

Figure 24. TRAP activity (a, b and c) and number of TRAP positive multinucleated cells (d, e and f) on osteoclastic cell cultures performed in the presence of the extracts from the Mg-based materials. * Significantly different from control cultures.

Gene expression of important proteins for osteoclastogenesis is shown in Figure 25. Extracts from AZ31 and anodised AZ31 were able to increase the expression of TRAP and Ca2. The extracts from AZ31 coated with PEI showed no significant differences from control cultures.

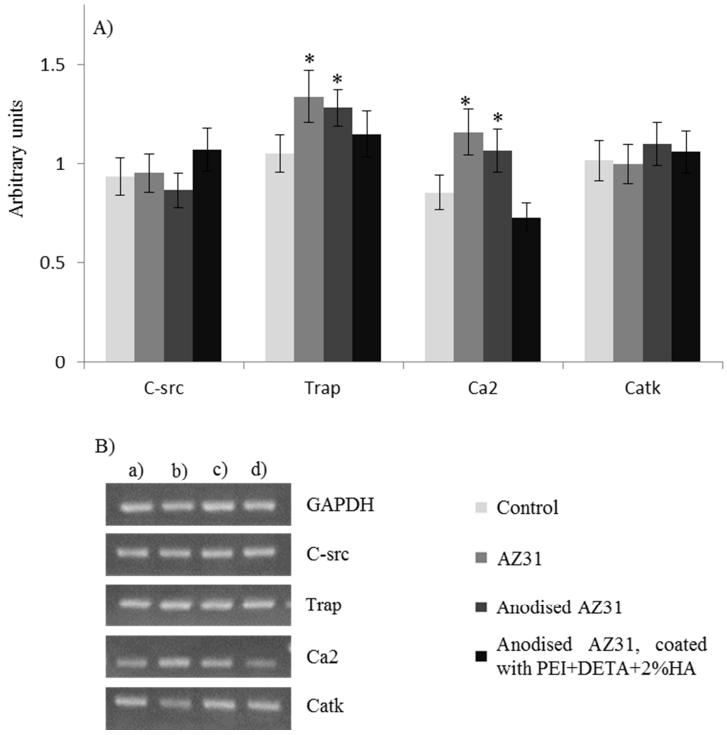

Figure 25. RT-PCR gene expression of osteoclastic cells exposed to the extracts from the Mg-based materials, at day 14. A) RT-PCR products were subjected to a densitometric analysis and were normalized to the corresponding GAPDH value. *Significantly different from control (absence of the extracts). B) Representative gel band images: a) control, b) AZ31, c) anodised AZ31, d) Anodised AZ31, coated with PEI+DETA+2%HA.

An important issue is the effect of the extracts on signalling pathways involved on osteoclastogenesis. The pathways analysed in hMCS were also addressed in osteoclastic cell cultures. The cultures exposed to 10% of the extracts were performed in the presence of specific inhibitors, and characterized for TRAP activity at day 14 (Figure 26). In control cultures, the addition of the inhibitors affected TRAP activity (Figure 26.a). The effect was more pronounced in control cultures exposed to NF-KB, followed by MEK and p38 MAPK signal pathway inhibitors. Figure 26.b depicts the combined effects of extract at 10% and the inhibitors. With the AZ31 extracts, the signal pathways inhibitors were able to decrease TRAP activity of the cultures. Compared to control, MEK and NF-KB were down-regulated, i.e. the effect in TRAP activity was less

pronounced. In the presence of the anodised AZ31 extracts, it was also observed a decrease in TRAP activity after the inhibitors were added, with the exception of JNK signalling pathway. Compared to control, the effect of the inhibitors was less pronounced. With the extracts from coated AZ31, results were similar to those observed in the cultures with no inhibitor, except for NF-KB signal pathway. It was also observed a down-regulation of all the signal pathways compared to control, i.e. TRAP activity was increased.

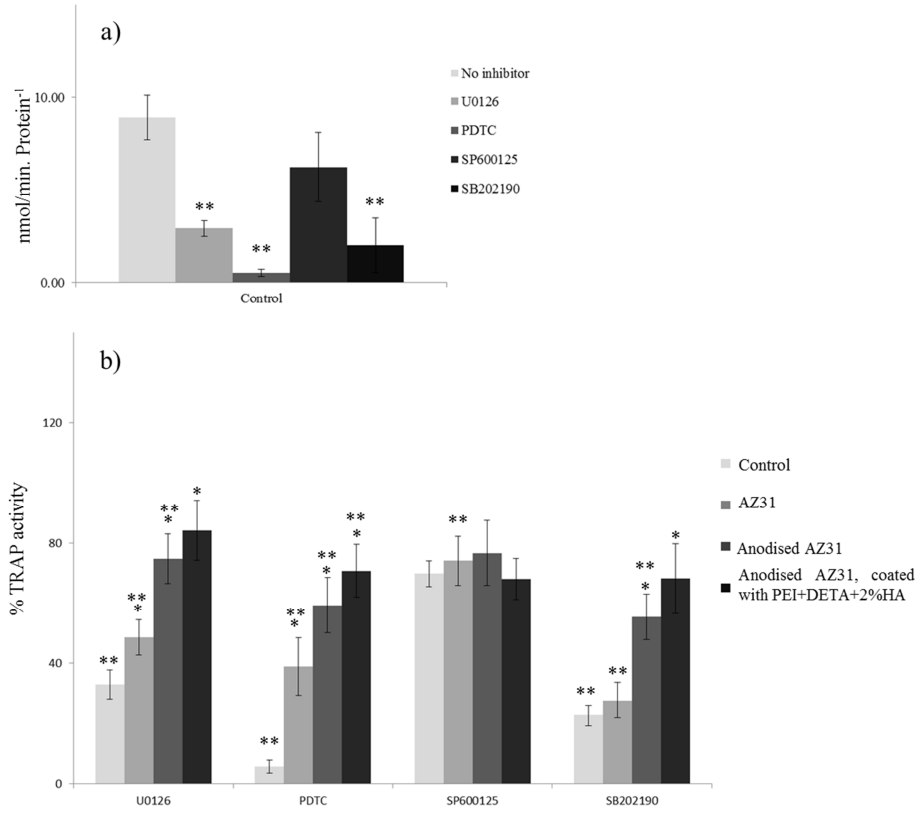

Figure 26. TRAP activity of osteoclastic cells exposed to the extracts from the Mg-based materials, performed in the presence of specific signalling pathways inhibitors a) Effect of signalling pathways inhibitors in control cultures, b)% of variation of TRAP activity in cultures performed in the presence of 10% extracts. U0126: MEK signalling pathway inhibitor; PDTC: NF-kB signalling pathway inhibitor; SP600125: JNK signalling pathway inhibitor; SB202190: p38 MAPK signalling pathway. ** significantly different from the cultures performed in the absence of inhibitor. * significantly different from the control cultures.

In conclusion, the extracts from AZ31 and anodised AZ31 showed a high toxicity at higher concentrations (50% to 20%), with a decrease in DNA content and increase of apoptosis. Lower concentrations caused a stimulatory effect , which was observed by the increase in TRAP activity and the expression of ALP and Ca2 genes, at 10%. The extracts from polymer coated AZ31 did not affect cell behaviour, as the results were similar to those observed in control cultures.

5.1.3 Behaviour of human endothelial cells exposed to the extracts from the Mg-based substrates

HUVECs were used as a model to evaluate the endothelial cell behaviour in the presence of the extracts from Mg-based materials. HUVECs were cultured for 7 days in the presence of the extracts from AZ31 alloy, anodised AZ31 and anodised AZ31 coated with PEI+DETA+2%HA, using the protocol described in Chapter 3.

Firstly, HUVECs were cultured in the presence of different concentrations of the extracts, and evaluated at days 1, 4 and 7. The effect on viability/proliferation is shown in figure 10. Cell proliferation increased throughout the culture time in control cultures and cultures exposed to the extracts.

The extracts from AZ31, at the highest extract concentration, 50%, decreased significantly the viability/proliferation, whereas the 20% extract had a stimulatory effect at days 1 and 4, and the presence of the 10 to 2% extracts did not affect the cell response (Figure 27). The 50% extract from anodised AZ31 alloy also presented a tendency to be toxic, with lower values at days 1 and 4, although without attaining statistical significance. The cultures exposed to the 20% extract presented increased viability/proliferation at day 4. Cultures exposed to the remaining extract concentrations (10%, 5% and 2%) presented a viability/proliferation similar to that on control cultures. HUVECs cultured in the presence of the extracts from anodised AZ31 coated with

PEI+DETA+2%HA had a response similar to that observed with the anodised AZ31 alloy, Figure 27.

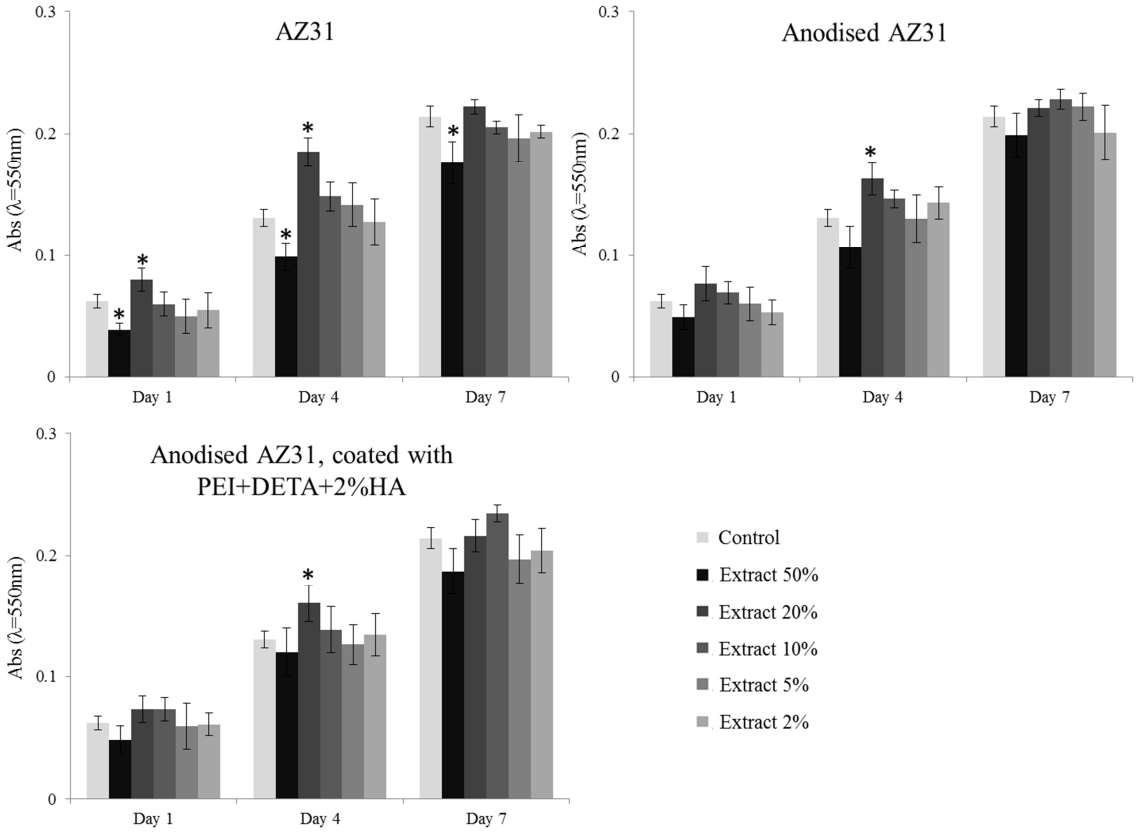

Figure 27. Cell viability/proliferation of HUVECs cultured in the presence of the extracts from the Mg-based materials, for 7 days. * Significantly different from control (absence of the extracts).

From the results obtained in the cell viability/proliferation, it was observed that the 20% and 10% (at a smaller level) extract concentrations had a stimulatory effect. This was specially seen for the extracts from AZ31 and anodised AZ31. So, cell response was further analysed for DNA content, caspase activity (apoptosis) and nitric oxide synthesis, at days 4 and 7.

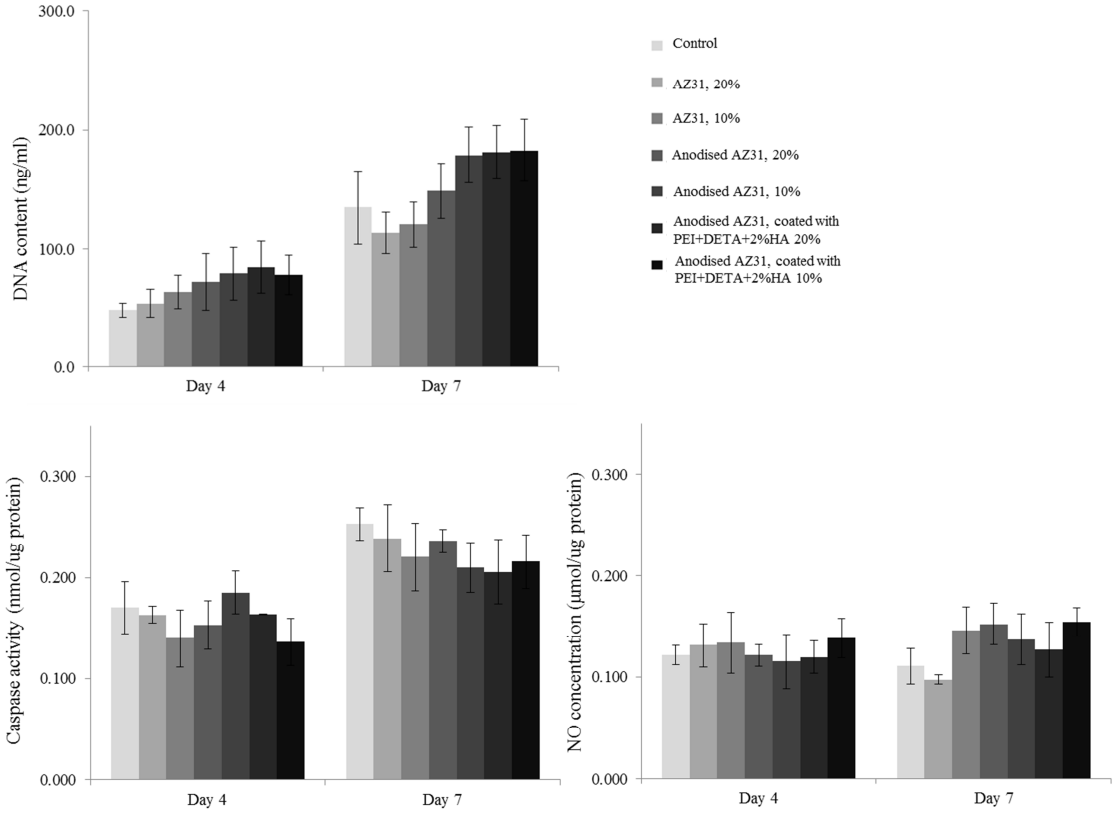

Figure 28. DNA content and Caspase-3 activity and NO concentration of HUVECs cultured in the presence of the extracts from Mg-based materials, 20% and 10%, at days 4 and 7. * Significantly different from control cultures (absence of the extracts).

DNA content of all cultures increased from day 4 to day 7, evidencing a growing cell population (Figure 28). Comparing to control cultures, there was a tendency for the extracts from anodised AZ31 and anodised AZ31 coated with PEI+DETA+2%HA to increase DNA content, although without attaining statistical significance.

In all cultures, there was a small increase in caspase-3 activity from day 4 to day 7 (Figure 28). At day 7, the cell layer was close to confluence which increases the amount of cell death by apoptosis. However, this behaviour was similar in control cultures and in the cultures exposed to the extracts from the three materials.

NO synthesis is an important marker of endothelial cells. The synthesis of NO, normalized to the protein content, was similar at days 4 and 7 (Figure 28). Additionally, no differences were found between control cultures and those exposed to the extracts.

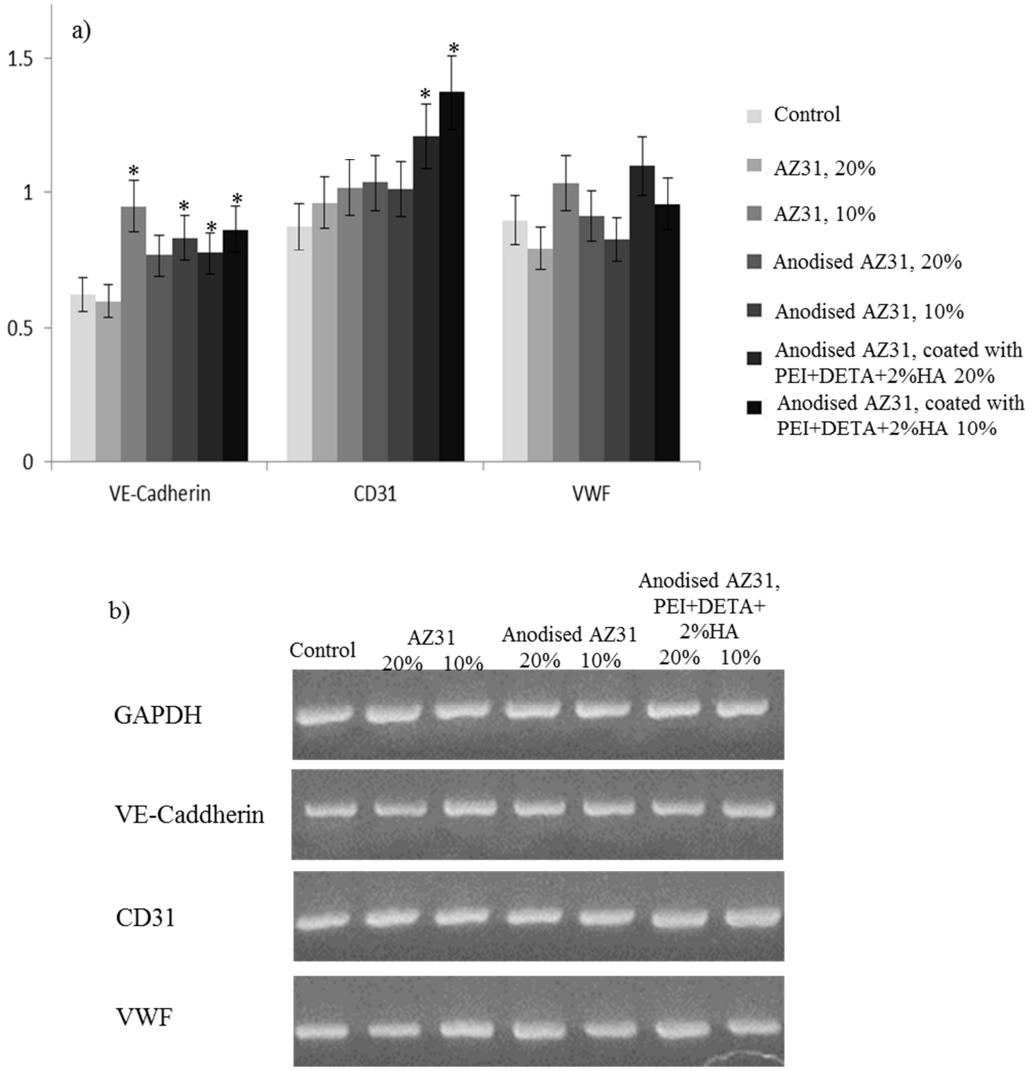

Figure 29. RT-PCR gene expression of HUVECs cultured in the presence of the extracts from the Mg-based alloys. a) RT-PCR products were subjected to a densitometric analysis and were normalized to the corresponding GAPDH value. * Significantly different from control (absence of the extracts. b) Representative gel band images.

Expression of the endothelial genes VE-Cadherin, CD31 and VWF was analysed at day 4 (Figure 29). VE-Cadherin presented an increased expression in the cells exposed to the extracts from the Mg-based alloys, except for the 20% AZ31 extract. The same tendency was observed for the expression of CD31, although statistical significance was only observed with the extracts from anodised AZ31 coated with PEI+DETA+2%HA. VWF expression was similar in all cultures.

The *in vitro* ability to organize the cell layer in a network of cord-like formations under certain conditions, i.e. upon contact with an extracellular matrix, is an important feature of endothelial cells, suggesting its functional performance in undergoing angiogenesis. For this assay, HUVECs were cultured for 4 days, in control conditions and in the presence of the extracts. The cell layer attained a confluence of about 70% in all cultures. At this stage, Matrigel (an extracellular matrix) was added to the cultures, and the organization of the cell layer was documented after 24h (details of the methodology were described in Chapter 3). Representative images are shown in Figure 30. All cultures, control and exposed to the extracts, organized the cell layer in a network of tube-like structures, and no differences were noted between the control cultures and those exposed to the extracts.

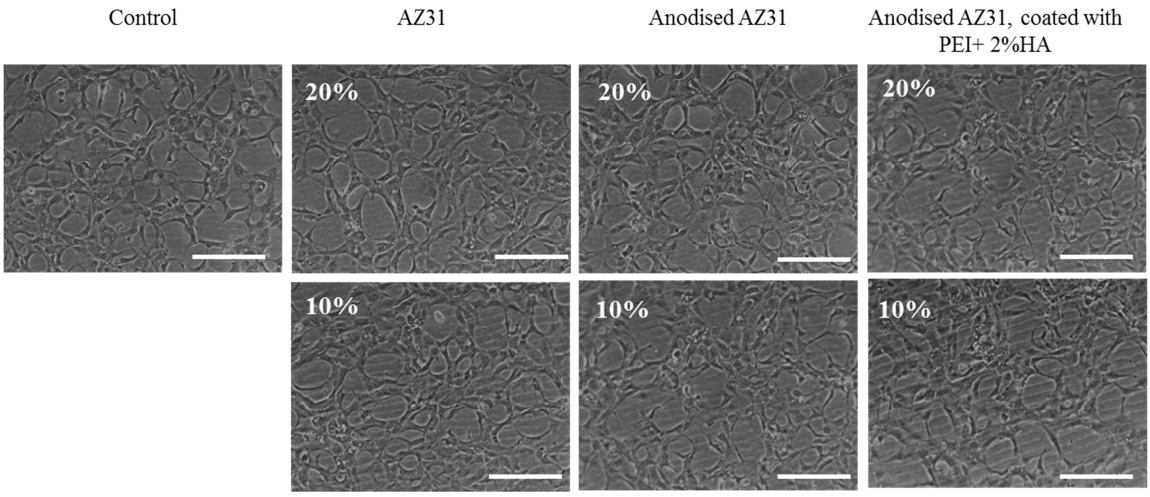

Figure 30. The Matrigel assay: representative images of HUVECs cultured in control conditions and in the presence of the extracts from the Mg-based materials (20 and 10%), showing the organization of the cell layer in a network of cord-like structures upon the addition of Matrigel. Bar: 200 μm.

The effect of the extracts from the Mg-based substrates in angiogenesis was also evaluated in *in vivo* conditions, by performing the CAM assay (Chapter 3). In this work,

a piece of filter paper, impregnated with the extracts, was placed in the surface of the chicken chorioallantoic membrane. The extracts were tested undiluted. After three days, the number of blood vessels formed around the paper filter was quantified. Angiogenesis was observed in all conditions, as observed in Figure 31. In control conditions, a slightly higher number of blood vessels was counted, compared to that found with the extracts. However, this difference did not attain statistical significance.

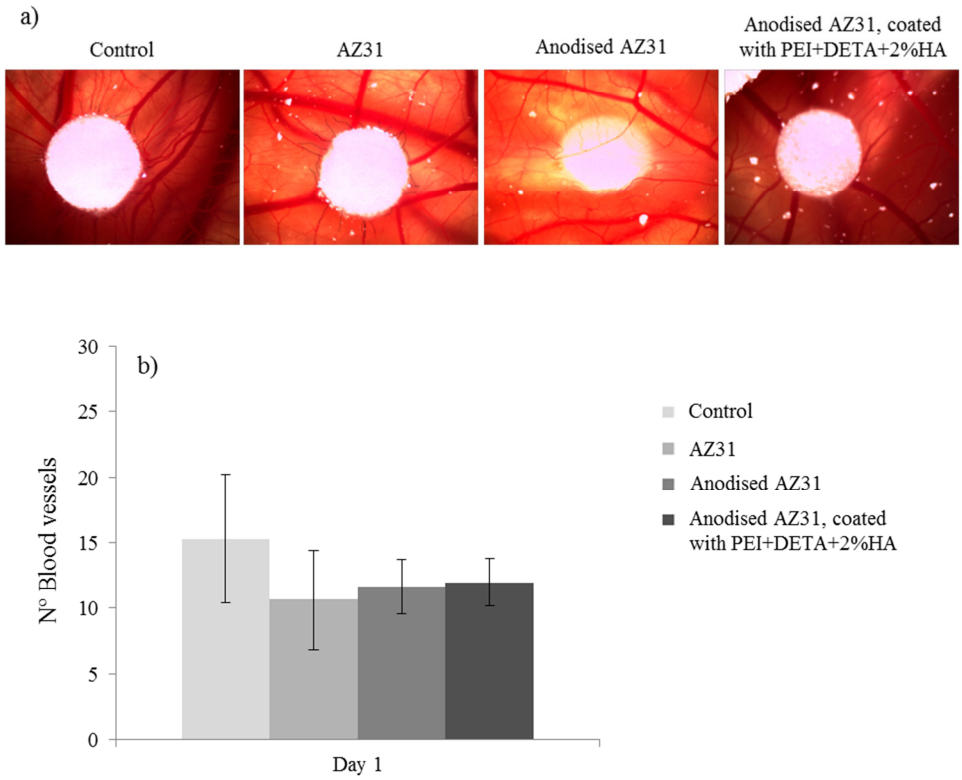

Figure 31. The CAM assay: effect of the extracts from the Mg-based alloys in the angiogenic response. a) representative images of the angiogenic response surrounding the filter samples impregnated with the extracts; b) number of blood vessels counted in the presence of the extracts.

The results presented in this section showed that the extracts from the three Mg-based alloys, at concentrations of 20 and 10% increased the cell viability/proliferation of HUVECs. Also, an increase in the expression of VE-Cadherin and CD31 was

observed with the same extract concentrations. Additionally, the *in vitro* and the *in vivo* angiogenesis assays showed similar behaviour in control conditions and in the presence of the extracts, suggesting a reduced or absence of toxicity of the extracts.

5.2 Effects of Magnesium ion on the osteoblastic, osteoclastic and endothelial cell response

The results regarding the behaviour of osteoblastic, osteoclastic and endothelial cell cultures in the presence of the extracts from the Mg-based alloys with different surface treatments showed interesting dose-dependent effects. Overall, higher extract concentrations caused cytotoxic effects, but lower concentrations had a stimulatory effect. To understand the contribution of the Mg ion in the observed results, the three types of cell cultures were performed in the presence of a concentration range of Mg (1mM to 100mM), in the form of $MgCl_2$, and the cell response was characterized for viability/proliferation and specific phenotype markers.

Figure 32 shows the results of hMCS cultured in the presence of a set of Mg concentrations, from 1mM to 100mM. Overall, levels similar and higher than 20mM Mg caused dose-dependent inhibitory effects in the viability/proliferation (Figure 32.a) DNA content (Figure 32.b) and ALP activity (Figure 32c). However, at a concentration of 1 mM, Mg increased ALP activity by ~30%, Figure 32c.

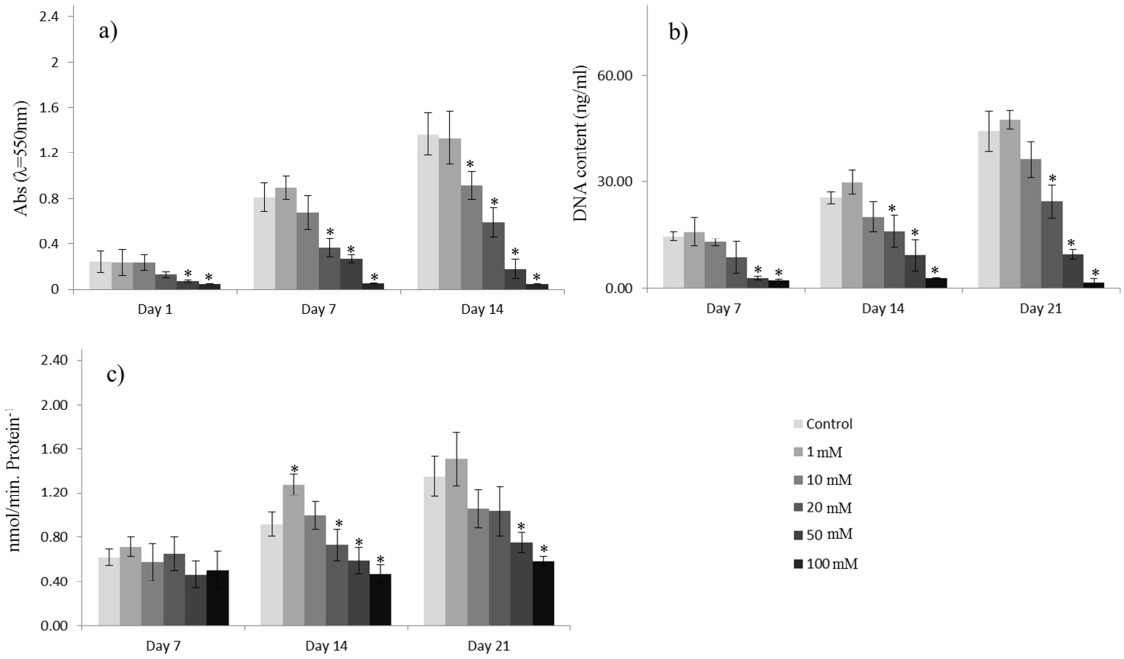

Figure 32. Osteoblastic behaviour of hMSC exposed to Mg, 1 to 100 mM, at days 7, 14 and 21. a) Viability/proliferation (MTT assay), b) DNA content and c) ALP activity. * Significantly different from control cultures.

Cultures of hMSC, exposed to 1 mM and 10mM Mg, were performed in the presence of several signalling pathways inhibitors and characterized for ALP activity (Figure 33). In control cultures, all inhibitors decreased ALP activity, as previously observed. Cultures exposed to 1 and 10mM of Mg showed a decrease in ALP activity when exposed to the inhibitors (Figure 33.b). When compared to control cultures, cultures exposed to 1 and 10mM of Mg showed an up-regulation of MEK and NF-KB signalling pathways, i.e. the decrease of ALP activity was more pronounced. Both, JNK and p38 MAPK signal pathways showed similar results to those observed in control.

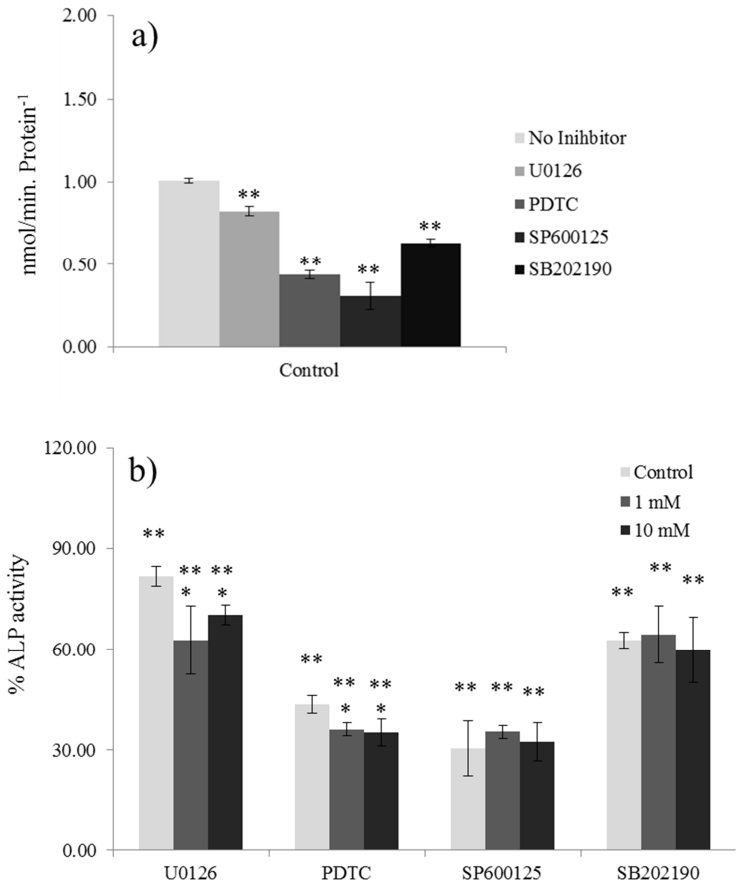

Figure 33. ALP activity of hMSC exposed to Mg, 1mM and 10 mM, in the presence of signalling pathway inhibitors, at day 14. a) Effect of signalling pathways inhibitors in control cultures, b) % of variation of ALP activity in cultures performed in the presence of 1mM and 10mM of Mg. U0126: MEK signalling pathway inhibitor; PDTC: NF-kB signalling pathway inhibitor; SP600125: JNK signalling pathway inhibitor; SB202190: p38 MAPK signalling pathway. ** significantly different from the cultures performed in the absence of inhibitor. * significantly different from the control cultures.

The influence of Mg ion was also analysed in osteoclastic cell cultures. Figure 34 presents the results for DNA content, TRAP activity and Caspase-3 activity (apoptosis). Mg ion increased DNA content in the range 10 to 50 mM. Regarding caspase-3 activity, decreased values were observed with 10 to 50 mM, and increased values with 100 mM. Mg ion also increased TRAP activity at 10 to 20 mM and had an inhibitory effect at 100 mM (day 14) and 50 and 100 mM (days 14 and 21).

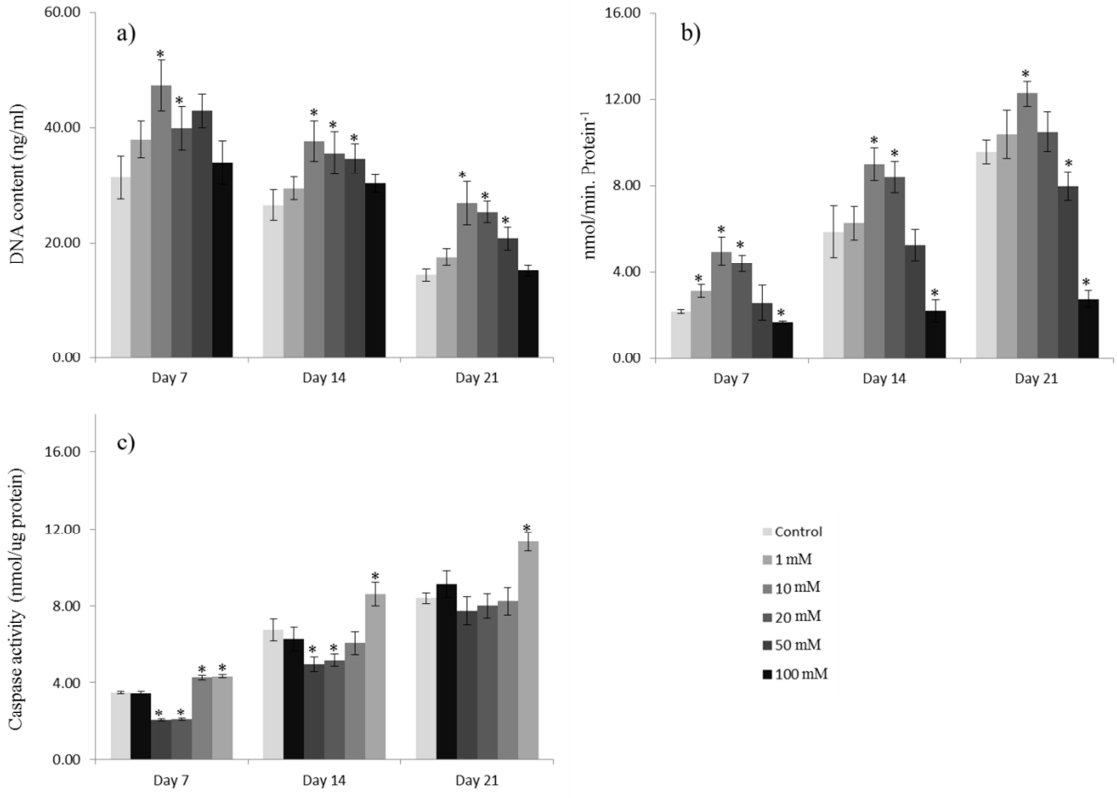

Figure 34. Osteoclastic cell behaviour of cultures exposed to Mg, 1 to 100 mM, at days 7, 14 and 21. a) DNA content, b) TRAP activity and c) Caspase-3 activity. * Significantly different from control cultures.

Mg concentrations of 10 and 20 mM showed a stimulatory effect in osteoclastic cell cultures, so they were further analysed for the effects in several signalling pathways involved in osteoclastogenesis. Figure 35 presents the results for TRAP activity of the cultures performed in the presence of specific signalling pathways inhibitors. All inhibitors decreased TRAP activity in control cultures (Figure 35.a) Cell cultures exposed to 10 and 20 mM showed a decrease in TRAP activity compared to the same conditions without the inhibitors. MEK, NF-KB and p38 MAPK signal pathways showed a down-regulation after the addition of 10 and 20 mM of Mg. The opposite effect was observed for the JNK signal pathway, i.e. it was observed a decreased in TRAP activity compared to the results in control cultures.

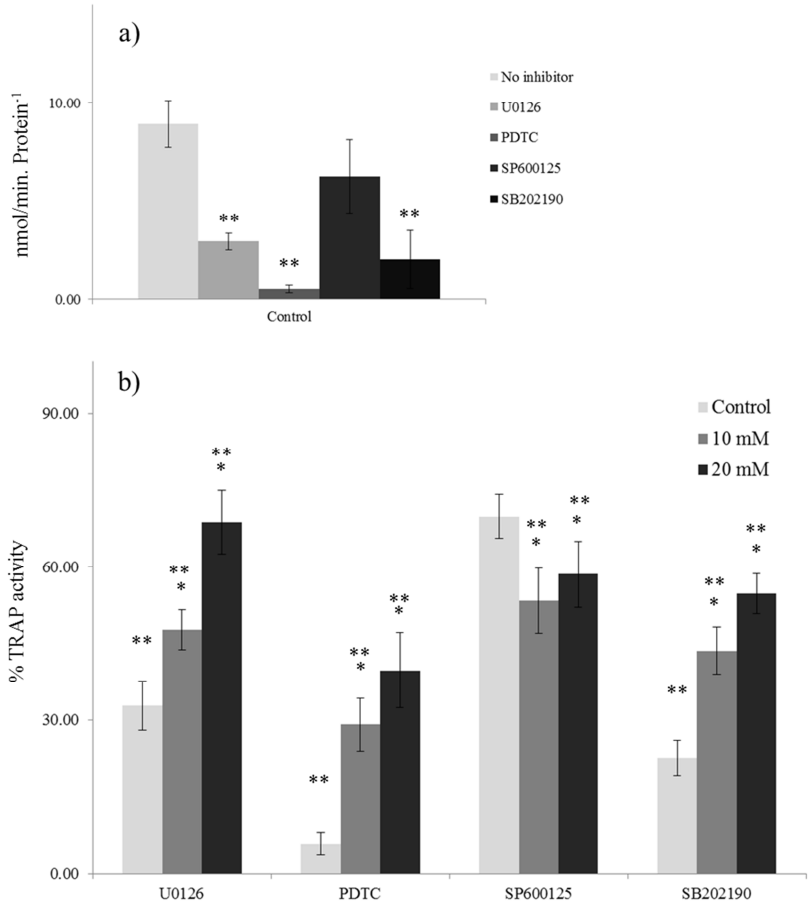

Figure 35. TRAP activity of osteoclastic cells exposed to Mg, 10 mM and 20 mM, in the presence of signalling pathway inhibitors, at day 14. a) Effect of signalling pathways inhibitors in control cultures, b) % of variation of TRAP activity in cultures performed in the presence of 10 mM and 20 mM of Mg. U0126: MEK signalling pathway inhibitor; PDTC: NF-kB signalling pathway inhibitor; SP600125: JNK signalling pathway inhibitor; SB202190: p38 MAPK signalling pathway. ** significantly different from the cultures performed in the absence of inhibitor. * significantly different from the control cultures.

The effect of Mg ion on the behaviour of endothelial cell cultures was also analysed, and the results are summarised in Figure 36. Cell cultures exposed to high concentrations of Mg ions, 20 to 100 mM, showed a decrease in viability/proliferation accompanied by an increase in caspase-3 activity (apoptosis). Cell cultures exposed to

Mg concentrations between 1 and 10 mM showed results similar to control cultures. The presence of Mg ion did not affect the synthesis of NO by endothelial cells.

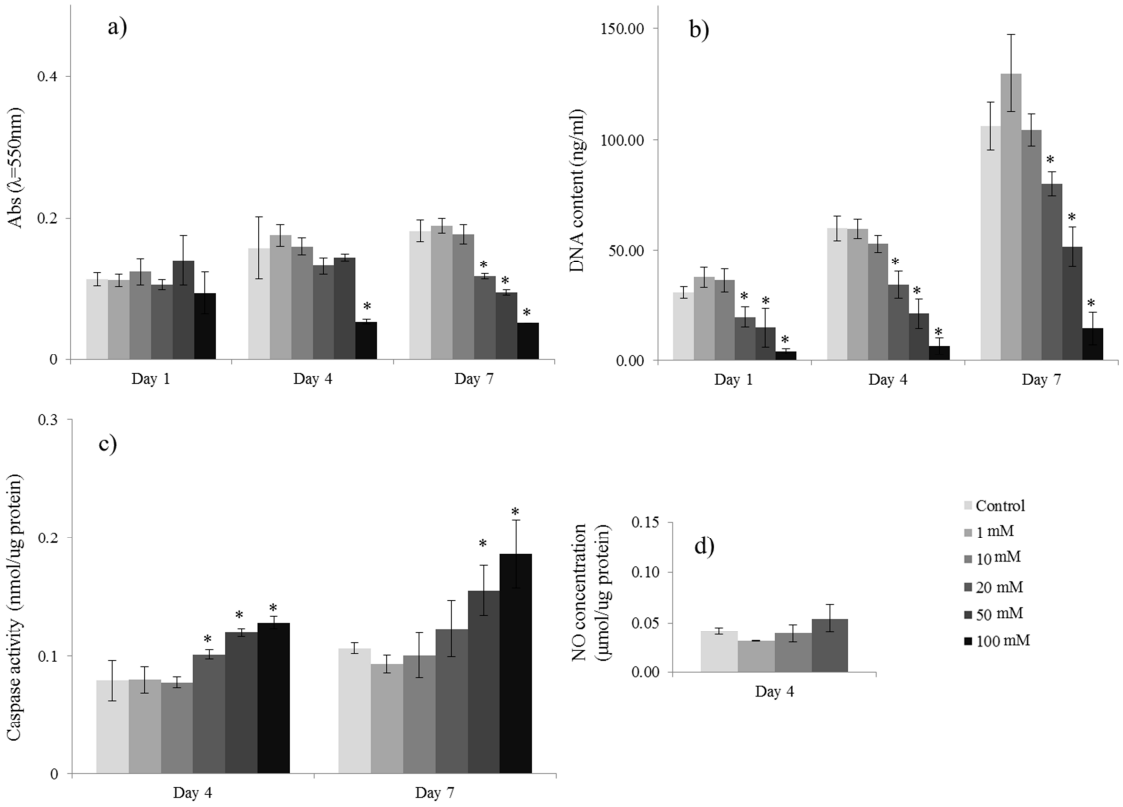

Figure 36. Endothelial behaviour of HUVECs cultures exposed to Mg concentrations, 1 to 100 mM, at days 1, 4 and 7 . a) Viability/proliferation (MTT assay), b) DNA content, c) capase-3 activity and d) NO concentration. * Significantly different from control cultures.

Figure 37 shows the results observed in the Matrigel assay for endothelial cell cultures exposed to Mg ion, 1, 10 and 20 mM. Control cultures were able to organize the cell layer in a network of tube-like formations, upon the contact with Matrigel. Mg ion caused a dose-dependent inhibitory effect, which began to be apparent with 1 mM and was significant with 20 mM.

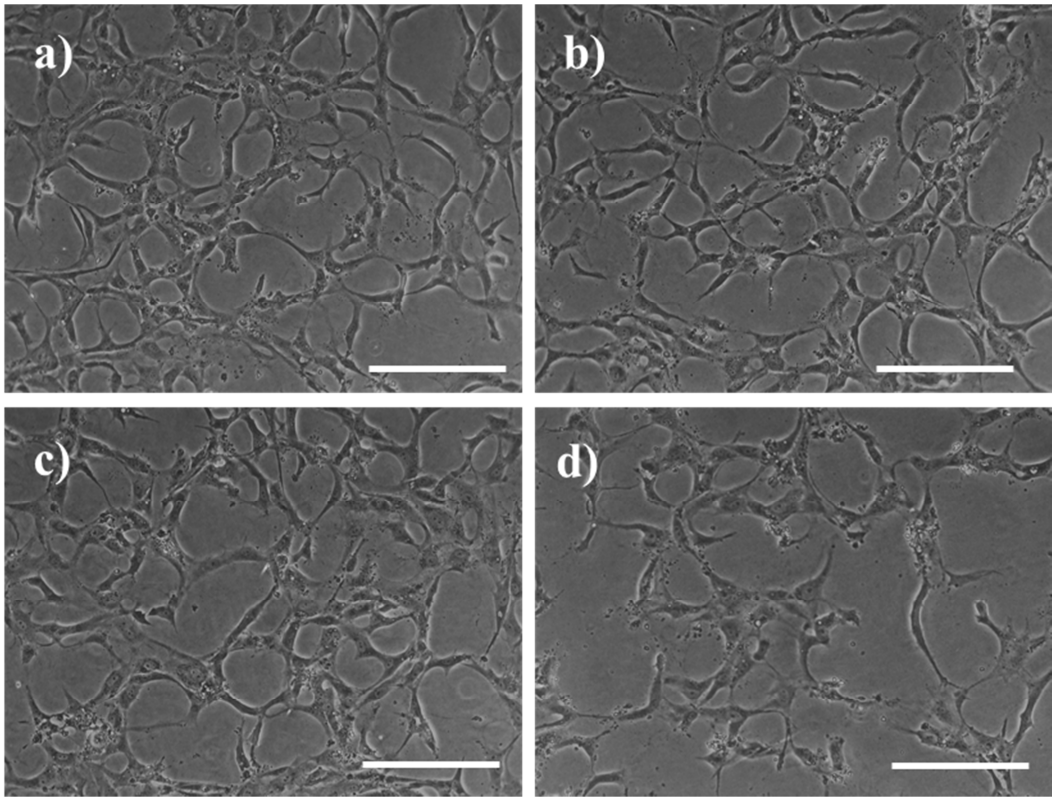

Figure 37. The Matrigel assay: representative images of HUVECs cultured in control conditions and in the presence of Mg ion, showing the organization of the cell layer in a network of cord-like structures, upon the addition of Matrigel . Control cultures (a) and cultures exposed to 1 mM (b), 10mM (c) and 20 mM (d) of Mg. bar: 200μm.

Mg ion showed dose-dependent effects in osteoblastic, osteoclastic and endothelial cell cultures, although with noticeable differences among the three cell populations. At high concentrations, 50 and 100 mM, Mg ion caused a common inhibitory effect in the cell response. hMSC and endothelial cells were not significantly affected by lower concentrations of Mg ion (1 and 10 mM). However, osteoclastic cell cultures showed an increase in the DNA content and TRAP activity at concentrations of 10 and 20 mM.

5.3 Discussion

The results obtained in the previous chapter showed a better biocompatible performance in coated alloys, especially for polymeric coatings such as PEI and PCL. It is difficult to compare with other reports since the composition and methods, used to create the various coating, vary greatly. Also, it has being described that the effects can show a discrepancy depending on the type of cytocompatibility tests [100]. Two types of test can be used to analyse citocompatibility of degradable materials, direct test such as performed in the previous chapter of this work and indirect test. The results of the direct assays are influenced by the corrosion of the alloy itself, hence it has been difficult to isolate the effect of increased corrosion rate and the toxicity of the Mg or other alloying components [146]. In indirect tests, cells are cultured in the presence of different concentrations of extracts, avoiding the effects from the dynamic surface present in Mg alloys in a physiologic environment [7].

In this work, the indirect cytocompatibility of magnesium alloy AZ31, anodised AZ31 and anodised AZ31 coated with PEI +DETA+ 2% HA was evaluated in three cell types: human mesenchymal stem cells (osteogenic induced), human precursor osteoclastic cells (osteoclastogenic induced) and human endothelial cells. Cell cultures were evaluated for viability/proliferation and also specific characteristics of the cells. The extracts were prepared by incubation of the Mg alloys in culture medium for 24h, and tested in the cells at different concentrations (50, 20, 10, 5 and 2%).

Osteogenic-induced hMSC were used to evaluate the effect of Mg-based extract and Mg ion in osteoblastic cells. It was observed a high cytotoxicity of hMSC exposed to high levels of extracts from AZ31 and anodised AZ31. Also, it was observed an opposite effect when cells were exposed to 10% extracts. At this concentration, hMSC increased viability/proliferation, functional activity and gene expression of ALP, Runx-2 and OPG. The results indicate an increase in differentiation of hMSC to osteogenic lineage, corresponding to an increase in ALP activity [125], and expression of important osteoblastic-related genes such as ALP, Runx-2 and OPG [147]. A similar result has been described previously, i.e. an increase in proliferation and differentiation of hMSC, including increased expression of BMP-2, with extracts from Mg, Mg-1Y and Mg-5Al alloys [110]. Also, using MG-63 cells, Pichler *et al.* (2014) showed an increase in gene

expression of ALP and osteocalcin in cultures incubated with extracts from Mg-based materials [111].

Osteoclastic-induce PMBC were used to analyse the effect of Mg- based extracts and Mg ion concentration in osteoclastic lineage. As previously observed in hMSC, high concentrations of extracts from AZ31 and anodised AZ31 (50 and 20%) inhibited the functional activity of these cells and decreased the number of cells. At concentrations 10% a stimulatory effect was observed with the increase in functional activity (TRAP) and gene expression of Ca_2 and TRAP. Such features are an indication of the increase in differentiation of PMBC cells towards a osteoclastic lineage [126].

The exposure of these two cell types to the extracts also influenced different cellular signalling pathways important in osteoblastogenesis and osteoclastogenesis. Both, AZ31 and anodised AZ31 induced an up-regulation of MEK signal pathway in osteoblasts, and a down-regulation of NF-KB and JNK. In osteoclastic cells, it was observed a down-regulation of all signalling pathways, with the exception of JNK.

It has been described a better performance of Mg alloys when an indirect assay was used, as observed in this work. An Mg-Ca alloy showed high cytotoxicity when MG-63 cells were cultured directly on the biomaterial, but in the indirect testing, the same material showed promising results [117]. Another work performed by Park *et al.* (2012) have described similar effects, with no deleterious effects of the conditioned medium, from MG-35Zn-3Ca alloys, in cell cultures [100]. Zhao *et al.* (2014) compared the results of both cytocompatibility studies obtaining similar results [115].

In the present work, a similar result was observed in AZ31 and anodised sample extracts. Anodisation is reported to increase corrosion resistance of Mg alloys, with different degrees of results [119]. In a study using MC3T3 cells, cultured in the presence of extracts from AZ31, AZ91 and ZK60A and anodised samples, it was reported an alteration in viability depending on the base alloy. ZK60A showed a decreased viability in both samples, base and anodised. AZ31 and AZ91 showed an increase in viability of MC3T3 cell, especially the anodised samples [119].

The effects of the extracts in these cells can be influenced by various factors such as pH, osmolality of the culture medium, concentration of Mg ion and other alloying elements, etc. [43]. Both, osteoblasts and osteoclasts are influenced by pH in an

opposite manner. It has been described a steady increase in the activity of osteoblast cells in contact with a medium with a pH in the range 7.0 to 7.8 [148]. pH level of the culture medium has been found to influence osteoclast differentiation and function. Osteoclasts reabsorption activity was found to be activated by acidic levels in physiologic environment [149]. At a pH higher than 7.4, the reabsorption activity of the osteoclasts decreases. The inhibitory effect found at higher levels of extract (50% and 20%) could be a direct result of pH increase of the medium. Besides pH alterations, it has been reported an increase in Mg^{2+} and a decrease in Ca^{2+} and PO_4^{3-} in Mg materials incubated in Hank's solution [139].

Mg ion concentration in the extracts is also an important factor contributing to the final results. The pure extract used in osteoblastic and osteoclastic cell cultures showed an increase in Mg ion compared to control cultures. In control cultures and polymeric-coated sample de concentration of Mg was approximately 1 mM, while in the AZ31 extract was 21 mM and in anodised AZ31was 14 mM. To evaluate the contribution this ion, a set of Mg concentration (1, 10, 20, 50, 100 mM) were analysed in this work.

hMSC cells exposed to high concentration of $MgCl_2$ (10 to 100 mM) showed a high toxicity, with a decrease in viability/proliferation and a decrease in ALP activity. These results are in accordance with the previous results observed in the extracts, since the concentration of Mg in the extracts at 50% would be close to 10 mM. A similar stimulation observed in extracts was also observed in the cells exposed to 1 mM of Mg, with an increase in viability/proliferation and ALP activity. It is possible that the effect observed in the extracts at 10% were related to the concentration of Mg ions present in the extracts. Yoshizawa *et al.* (2014) described a similar effect when testing bone marrow stromal cells in the presence of $MgSO_4$ at concentrations between 1 to 10mM [150]. This observation suggested that the enhancement of bone tissue regeneration around Mg-based implants might be due to the presence of Mg ions. It has been described that materials supplemented with Mg^{2+} can lead to an improved osteoblastic cell adhesion, due to its influence in integrin receptors [116]. Integrins modulate cellular migration, proliferation, differentiation and apoptosis of different cell types such as osteoblasts. Mg^{2+} has an important role in the ion transport by pumps, carriers and channels, and possibly modulating signal transduction and the cytosolic concentration of electrolytes such as K^+, Na^+ and Ca^{2+} [39]. The depletion of Mg has also been

described to create impairment in bone growth, decrease osteoblast number and increase osteoclast number in young mice [2].

Osteoclastic cells exposed to Mg ion concentrations between 100 to 50 mM also show a reduction in functional activity. Also, the same cells exposed to 10 mM of Mg show an increase in functional activity. The results are in accordance to previously reports showing that a concentration of 25 mM of Mg could enhance osteoclasts function [151]. On the other side, the cells exposed to the extracts from Mg alloys were shown to be more affected by the concentrations of Mg ions, needing less amount of Mg to have a beneficial effect [151].

The influence of Mg ion in the cellular signalling pathways important in osteoblastogenesis and osteoclastogenesis was also analysed. In osteoblastic cells, it was observed an up-regulation of MEK signal pathway, which is in accordance to the results observed in the Mg-based extracts. MEK signal pathway appears to have an important role in the effect of Mg extracts and Mg ion in osteoblastic cultures. The inhibition of this pathway, by U0126, is known to inhibit the ECM-dependent induction of the osteocalcin and BMP action in osteoblasts [152] and, as observed in this work, decreases the activity of ALP. MEK signal pathway (MEK/ERK) is also one of the primary transducers of integrin signals to the cell nucleus [152]. Mg ion is also known to be a co-regulator and activator of integrins [4], which could explain the importance of the MEK signal pathway in the effects observed this work.

In osteoclastic cell cultures, a down-regulation of all signal pathways was observed, with the exception of JNK. These results are also in accordance to observe in the extracts tested. JNK signal pathway is important in osteoclastogenesis [153] and has been showed to have a role in the regulation of apoptosis of osteoclasts [154]. It is possible that the influence of Mg ion in osteoclastogenesis is regulated by other signal pathways besides the ones studied in this work. Osteoclastogenesis is a complex process regulated by various proteins, such as RANKL, and signal pathways [153].

Endothelial cells were also analysed for the citocompatibility in the presence of Mg extracts and Mg ions. It was observed a lower influence of Mg extracts from AZ31 and anodised AZ31 in these cells. Only at the highest concentration analysed, 50%, a deleterious effect of Mg extracts was observed. By measuring the concentrations of Mg ion in the extracts used in these cells it was found a lower concentration compared to

that observed in the previous medium (osteoblastic and osteoclastic cells). While in the control medium the concentration of Mg was the similar (1 mM), the concentration of pure extract from AZ31 was 17 mM and in the anodised sample was 14 mM. At a concentration of 20 to 10%, the extracts caused a stimulatory effect in cell viability/proliferation and increased the expression of ve-cadherin. In the other important characteristics, such as NO production, apoptosis and production of lumen-like structure in the presence of an extracellular matrix there were no significant effects. Also, the results from the *in vivo* analyses, CAM assay, showed almost no effect from the concentrated extracts of AZ31 and anodised AZ31. Endothelial cells exposed to high level of Mg ion, between 20 to 100mM, showed a decrease in viability/proliferation especially at day 7. Also, in the presence of an extracellular matrix, the capability of producing a lumen-like structure was found to be impaired at concentrations higher than 20 mM. It has been reported that concentration around 10 mM of extracellular Mg ion could stimulate the proliferation of endothelial cells, such as human coronary artery endothelial cells [155]. Also, Mg ion concentrations up to 10 mM have been described to increase migration rate of endothelial cells, angiogenesis and cell adhesion [156,157].

The results described for the extracts from AZ31 and anodised AZ31 indicated to be dependent on the concentration but also on the cell type. The same was found in the cultures incubated with different concentrations of Mg ion. Although the effect at high levels of extracts was similar for the different types of cells, the concentration that could be beneficial for the cells was different.

The extracts produced from anodised AZ31 coated with PEI+DETA+2%HA were found to have no significant effect in all cell cultures used in this work. These results are in accordance with the results in the direct assay, in previous chapter. The coating with PEI has shown to enhance cells attachment and proliferation. Also it is reported that this coating increase the corrosion resistance of the Mg material [55], hence decreasing the amount of corrosion products being released to the culture medium. This is also evident in the concentration of Mg ion in the polymeric coating extract, which is similar to that observed in the control culture medium.

So, using the polymeric coating would increase cells attachment in a first period, but as the coating would degrade the cells would be in contact with Mg ions at concentrations that could increase cell proliferation and activity.

Chapter 6

General discussion

In this work, a series of surface treatments were used with the aim of controlling the corrosion rate and increasing the cytocompatibility of Mg-based materials. Three methods were used to control the corrosion rate: alloying composition, anodisation and polymeric coatings. Chapter 4, of this work, presented the results from *in vitro* direct assays used to evaluate the cytocompatibility of different compositions of Mg alloys, anodisation and polymeric-based coatings. Chapter 5 described the results from the indirect assay in a series of Mg-based materials previously analysed in Chapter 4.

Naked Mg alloys, with different alloying compositions, showed a decreased cytocompatibility, observed in the viability/proliferation assay (MTT) and morphology. Mg alloys show a high corrosion rate when in contact with aqueous medium, such as culture medium [40]. This corrosion is accompanied with the release of hydrogen bubbles, increased pH and release of Mg alloy particles which have been found to decrease the biocompatibility of these materials [26,43]. Also, it was observed that the 3 alloys tested (AZ61, AZ31 and RZ5) showed different degrees of cytocompatibility AZ61 showed the lowest cytocompatibility which could be a result from the higher corrosion rate observed in alloys with high concentration of Al [66,67]. It has been described that the composition of the Mg alloys can influence the corrosion rate and therefore affecting the compatibility of these materials [44,58].

Besides the corrosion rate on the surface of Mg alloys, other alterations in the surrounding environment have been described. These effects include an increase in pH and alteration in the concentration of important ions (Mg, Ca and PO_4^{3-}) [139]. In this work, the incubation of AZ31 alloy in culture medium up to 24h showed an increase in Mg ion, from 1 mM in control medium to 21 mM in the respective extract, in the medium. In order to access the effect of these alterations, an indirect assay was performed and the results were analysed in Chapter 5.

In the indirect assay, high concentrations of the extracts from AZ31 alloy caused a toxic effect in osteoblastic, osteoclastic and endothelial cells. These effects were characterized by a decrease in viability/proliferation and functional activity of these cells. These results could be linked to an alteration in the concentration of Mg ion in the culture medium. Cells cultured in the presence of high concentrations of Mg ions showed a decrease in viability proliferation (Chapter 5). This observation has been also

described by other authors for osteoblastic, osteoclastic and endothelial cells [150,151,155].

The results from the direct and indirect assays, in AZ31 alloy, showed that the cytocompatibility of the alloy is influenced by the corrosion rate [26,43], pH of the medium [43], concentration of ions [150,151,155] and debris. In fact, the direct assay might show a lower cytocompatibility due to the fact that it has a combination of the effects of corrosion on the surface of the materials plus the effects in the culture medium.

Two of the alloys previously tested, AZ31 and RZ5, were coated by anodisation. This method created a coat of magnesium, oxygen, phosphorous and fluoride which has been described to decrease corrosion rate of Mg alloys [124]. The direct assays in both alloys showed an increase in viability/proliferation compared to the results in naked samples. The controlled corrosion rate increased the attachment of the osteoblastic cells to the surface of the alloys. This coating method has been described to reduce the hydrogen evolution hence increasing the attachment of cells to the surface [11]. Although anodisation leads to the reduction of hydrogen evolution, it has been described that it might not be able to delay the beginning of degradation [11]. An indication of this effect is the fact that, in this work (Chapter 3), it was observed an increase of Mg ion concentration in culture medium when anodised AZ31 was incubated for 24h; a result similar to the one observed for the naked alloy.

The indirect tests of anodised AZ31 showed a similar result to the one observed in naked samples, i.e., at high concentrations a toxic effect is observed. As described in Chapter 5, the high concentrations of anodised extract decreased the viability/proliferation and the functional activity of osteoblastic, osteoclastic and endothelial cells. These results could be affected by the concentration of Mg ions, as observed in the quantification of Mg ion in these extracts showing a significant increase of this ion compared to control culture medium. As previously discussed, high concentrations of Mg ion can lead to toxic effects such has the ones observed in this work. Anodisation created a protection coating that limits the effects of corrosion on the surface but it allowed the dissolution of a high quantity of Mg ions and other debris that could seriously affect cells.

In both materials, naked and anodised AZ31 it was observed a beneficial effect at lower concentrations of extracts, in the indirect assays. This was possibly correlated to the increase of Mg ion in the culture, which was showed to have a beneficial effect such as increasing the viability/proliferation, functional activity and gene expression (Chapter 5). The same effects have been described in the literature for osteoblastic cells [110,111], osteoclastic cells [151] and endothelial cells [155]. These results show the importance that controlling the corrosion rate could have in the success of Mg-based implants. The release of tolerated or beneficial concentrations of Mg ions to the surrounding environment could lead to an increase in osteocompatibility of Mg alloys and further increase in bone formation.

To achieve a better control in corrosion rate, a third method based in polymeric coatings was used. As described by Zomorodian *et al.*, both polymeric coatings showed a decrease in corrosion rate [55,56]. In both polymeric coatings, cells were able to attach to the surface of the materials and further proliferate. Compared to naked and anodised samples, these polymeric coatings presented a better performance with a high proliferation rate and the morphology of the cells was closer to control cultures. In literature similar results were described for these coatings [89,122]. The polymeric coatings have been described to decrease the corrosion effects, such as release of hydrogen bubbles, creating a better surface for cells to attach and proliferate [11,55,56]. Furthermore, the use of HA particles showed an increase in viability/proliferation and even functional activity (Chapter 4). HA particles have been described to increase the functional activity and further increase the osteocompatibility of osteoblastic cells [136].

A combination of treatments, anodisation and polymeric coating, was evaluated by an indirect assay. Firstly, incubation of the coated alloy in culture medium, for 24h, showed a limited release of Mg ions to the medium, evidencing the corrosion protection of this coating. In the indirect tests, the coated alloy showed a similar result to control cultures, for all the cells tested (Chapter 5).

The results of this work showed that the decrease in corrosion rate by surface treatments, such as anodisation and polymeric coatings, can lead to a better cell attachment and proliferation. Furthermore, the controlled release of Mg ions to the surrounding environment could lead to a better osteocompatibility. Specific

concentrations of Mg ion can lead to increased viability/proliferation of osteoblastic, osteoclastic and endothelial cells, as observed in this work.

In conclusion, the surface treatments analysed in this work showed promising results, increasing the cytocompatibility of Mg alloys. The combination of the surface treatments could be an interesting alternative for using Mg alloys as biodegradable implants in orthopaedic applications.

Chapter 7

Conclusions and Future Perspectives

7.1 Conclusions

In this work, a series of Mg alloys and surface treatments used to control corrosion rate were analysed. The surface treatments performed on the Mg alloys, anodisation and polymeric-based coatings, resulted in enhanced biological performance.

Firstly, three Mg alloy with different alloying compositions were tested for their biocompatibility: AZ31, AZ61 and RZ5 in a direct assay. From the tested alloys, AZ31 and RZ5 showed a better biological performance, i.e. cells were able to attach to the substrate and proliferate. Although, for longer culture periods cells would began to exhibit cytotoxic effects. AZ31 alloy was also tested in an indirect assay, in which the extracts from the alloy were added to osteoblastic, osteoclastic and endothelial cell cultures. The extracts showed a cytotoxic effect common to all tested cultures at higher concentrations, in accordance to the direct tests. At lower concentrations, it was observed an enhanced differentiation of osteoblastic and osteoclastic cells, with increased viability/proliferation, functional activity (ALP or TRAP) and gene expression. It was observed an influence of the Mg ion in the results observed in the indirect assay. At specific concentrations, 1 mM (osteoblasts), 10 mM (osteoclasts), Mg ion was also able to increase viability/proliferation, functional activity and gene expression in these cells.

A second approach to control corrosion rate used in this work was anodisation by PEO. Compared to bare alloys, anodisation was able to create a less dynamic environment for cell attachment and survival. In both anodised tested alloys, AZ31 and RZ5, cells were able to attached and proliferate. It was observed an increase in viability/proliferation and a normal cell morphology in both alloys. However, for longer periods, the anodised coating also showed evident signs of cytotoxicity. Anodised AZ31 was also tested in an indirect assay for its biocompatibility. At higher concentrations, it was also observed a cytotoxic effect in all tested cells. At low concentrations, a similar effect to the one observed in the extract from AZ31 alloy was observed. At 10%, the extracts were able to increase vialibity/proliferation, functional activity (ALP or TRAP) and gene expression, as observed for AZ31.

The polymeric coatings, PEI- and PCL-based coatings, were found to be the most efficient surface treatment to control corrosion rate, allowing cell attachment,

proliferation and function. Cells were able to attach and showed higher proliferation rates compared to bare and anodised alloys, especially at longer periods of culture. In the PEI coatings, it was observed a better performance in the coatings with DETA+HA+ nanoparticles. The coating with DETA+2%HA presented a higher viability/proliferation and the morphology of the cells was closer to observed in control conditions. The alloy coated with this composition and also anodisation was also tested in an indirect assay. In this assay, the various concentrations of the extract tested showed a similar effect to the one observed in control conditions. Both assays, showed similar results, with a better performance of these coatings compared to the other options tested in this work.

PCL-based coatings showed results similar to those observed in PEI-based coatings. The coatings with HA nanoparticles showed an increase in viability/proliferation and functional activity (ALP).

Using a combination of anodisation and polymeric coating, as with PEI+DETA+2%HA, a significant increase in the cytocompatibility of Mg alloys is expected. In a first phase, cells would attach to the polymeric coating. With the progressive degradation of the coating, cells would be in contact with the anodised layer, therefore benefiting to the presence of the released Mg ions that would enhance cell growth and activity. Also, with the anodisation, the base alloy would be protected for a longer period of time, supporting the surrounding bone and the newly formed bone for a longer period before being reabsorbed.

In conclusion, the multifunctionalization approach of the Mg alloys proposed in this study appears to be a promising strategy to obtain biologically safe and active biodegradable Mg-based materials for bone tissue applications.

7.2 Future Perspectives

Further studies are necessary to understand the results presented in this work.

The base alloys used in this work are not made for biomedical applications, so some of the alloying materials and the quantity of impurities might not be recommended to biomedical applications. There should be a focus in creating biomaterials with similar

characteristics to the ones used in this work but with more suitable characteristics for biomedical applications.

Polymeric-based coatings showed a potential as Mg coatings, and the long-term response of cells in direct contact with the substrate, such as gene expression and functional activity, needs to be further explored.

In indirect tests a few questions remain unanswered, such has the effect of pH, osmolality and concentration of the various corrosion materials in the effect of the extracts. Also, a further analyse of the various components of corrosion present in the extracts should be performed.

From the results of indirect tests, the coatings used in this work also presented good results in endothelial cells and could be suitable candidates for other applications, such as in stents.

In vivo tests should also be performed to better understand the biocompatibility of using the polymeric coatings and the effectiveness in controlling the rate corrosion.

References

1. Rude RK, Singer FR, Gruber HE (2009) Skeletal and hormonal effects of magnesium deficiency. Journal of the American College of Nutrition 28 (2): 131-141.
2. Rude RK, Gruber HE, Wei LY, Frausto A, Mills BG (2003) Magnesium deficiency: effect on bone and mineral metabolism in the mouse. Calcified tissue international 72 (1): 32-41.
3. Hartwig A (2001) Role of magnesium in genomic stability. Mutation research 475 (1-2): 113-121.
4. Witte F, Hort N, Vogt C, Cohen S, Kainer KU, et al. (2008) Degradable biomaterials based on magnesium corrosion. Current Opinion in Solid State and Materials Science 12 (5-6): 63-72.
5. Gu X, Zheng Y, Cheng Y, Zhong S, Xi T (2009) In vitro corrosion and biocompatibility of binary magnesium alloys. Biomaterials 30 (4): 484-498.
6. Kirkland NT, Birbilis N, Walker J, Woodfield T, Dias GJ, et al. (2010) In-vitro dissolution of magnesium-calcium binary alloys: clarifying the unique role of calcium additions in bioresorbable magnesium implant alloys. Journal of biomedical materials research Part B, Applied biomaterials 95 (1): 91-100.
7. Tan LL, Wang Q, Geng F, Xi XS, Qiu JH, et al. (2010) Preparation and characterization of Ca-P coating on AZ31 magnesium alloy. Transactions of Nonferrous Metals Society of China 20 S648-S654.
8. Witte F, Feyerabend F, Maier P, Fischer J, Stormer M, et al. (2007) Biodegradable magnesium-hydroxyapatite metal matrix composites. Biomaterials 28 (13): 2163-2174.
9. Jang Y, Tan Z, Jurey C, Collins B, Badve A, et al. (2014) Systematic understanding of corrosion behavior of plasma electrolytic oxidation treated AZ31 magnesium alloy using a mouse model of subcutaneous implant. Materials Science and Engineering: C 45 (0): 45-55.
10. Xu L, Yamamoto A (2012) Characteristics and cytocompatibility of biodegradable polymer film on magnesium by spin coating. Colloids and surfaces B, Biointerfaces 93 67-74.
11. Rosemann P, Schmidt J, Heyn A (2013) Short and long term degradation behaviour of Mg–1Ca magnesium alloys and protective coatings based on plasma-chemical oxidation and biodegradable polymer coating in synthetic body fluid. Materials and Corrosion 64 (8): 714-722.
12. Clarke B (2008) Normal bone anatomy and physiology. Clinical journal of the American Society of Nephrology : CJASN 3 Suppl 3 S131-139.
13. Proff P, Romer P (2009) The molecular mechanism behind bone remodelling: a review. Clinical oral investigations 13 (4): 355-362.
14. Rho JY, Kuhn-Spearing L, Zioupos P (1998) Mechanical properties and the hierarchical structure of bone. Medical engineering & physics 20 (2): 92-102.
15. Cohen MM (2006) The new bone biology: Pathologic, molecular, and clinical correlates. American Journal of Medical Genetics Part A 140A (23): 2646-2706.
16. Sodek J, McKee MD (2000) Molecular and cellular biology of alveolar bone. Periodontology 2000 24 99-126.
17. Weiner S, Wagner HD (1998) The material bone: Structure-Mechanical Function Relations. Ann Rev Mater Sci 28 271–298.
18. Olszta MJ, Cheng XG, Jee SS, Kumar R, Kim YY, et al. (2007) Bone structure and formation: A new perspective. Materials Science & Engineering R-Reports 58 (3-5): 77-116.
19. Bao CLB, Teo EY, Chong MSK, Liu Y, Choolani M, et al. (2013) Advances in Bone Tissue Engineering. In: Andrades JA, editor. Regenerative Medicine and Tissue Engineering.
20. Chau JF, Leong WF, Li B (2009) Signaling pathways governing osteoblast proliferation, differentiation and function. Histology and histopathology 24 (12): 1593-1606.
21. Sommerfeldt DW, Rubin CT (2001) Biology of bone and how it orchestrates the form and function of the skeleton. European Spine Journal 10 S86-S95.
22. Aubin JE, Bonnelye E (2000) Osteoprotegerin and its ligand: A new paradigm for regulation of osteoclastogenesis and bone resorption. Medscape women's health 5 (2): 5.

23. Athanasiou KA, Zhu CF, Lanctot DR, Agrawal CM, Wang X (2000) Fundamentals of biomechanics in tissue engineering of bone. Tissue Engineering 6 (4): 361-381.
24. Witte F (2010) The history of biodegradable magnesium implants: a review. Acta biomaterialia 6 (5): 1680-1692.
25. Salahshoor M, Guo Y (2012) Biodegradable Orthopedic Magnesium-Calcium (MgCa) Alloys, Processing, and Corrosion Performance Materials(5): 135-155.
26. Chen Y, Xu Z, Smith C, Sankar J (2014) Recent advances on the development of magnesium alloys for biodegradable implants. Acta biomaterialia 10 (11): 4561-4573.
27. Yaszemski MJ, Payne RG, Hayes WC, Langer R, Mikos AG (1996) In vitro degradation of a poly(propylene fumarate)-based composite material. Biomaterials 17 (22): 2127-2130.
28. Johnson EO, Troupis T, Soucacos PN (2011) Tissue-engineered vascularized bone grafts: basic science and clinical relevance to trauma and reconstructive microsurgery. Microsurgery 31 (3): 176-182.
29. Staiger MP, Pietak AM, Huadmai J, Dias G (2006) Magnesium and its alloys as orthopedic biomaterials: a review. Biomaterials 27 (9): 1728-1734.
30. Alvarez-Lopez M, Pereda MD, del Valle JA, Fernandez-Lorenzo M, Garcia-Alonso MC, et al. (2010) Corrosion behaviour of AZ31 magnesium alloy with different grain sizes in simulated biological fluids. Acta biomaterialia 6 (5): 1763-1771.
31. Chou D-T, Hong D, Saha P, Ferrero J, Lee B, et al. (2013) In vitro and in vivo corrosion, cytocompatibility and mechanical properties of biodegradable Mg–Y–Ca–Zr alloys as implant materials. Acta biomaterialia 9 (10): 8518-8533.
32. Cordewener FW, Schmitz JP (2000) The future of biodegradable osteosyntheses. Tissue engineering 6 (4): 413-424.
33. Witte F, Kaese V, Haferkamp H, Switzer E, Meyer-Lindenberg A, et al. (2005) In vivo corrosion of four magnesium alloys and the associated bone response. Biomaterials 26 (17): 3557-3563.
34. Gu X-N, Zheng Y-F (2010) A review on magnesium alloys as biodegradable materials. Frontiers of Materials Science in China 4 (2): 111-115.
35. Noronha JL, Matuschak GM (2002) Magnesium in critical illness: metabolism, assessment, and treatment. Intensive care medicine 28 (6): 667-679.
36. Alfrey AC, Miller NL (1973) Bone magnesium pools in uremia. The Journal of clinical investigation 52 (12): 3019-3027.
37. Kupetsky-Rincon EA, Uitto J (2012) Magnesium: Novel Applications in Cardiovascular Disease – A Review of the Literature. Annals of Nutrition and Metabolism 61 (2): 102-110.
38. Mazur A, Maier JAM, Rock E, Gueux E, Nowacki W, et al. (2007) Magnesium and the inflammatory response: Potential physiopathological implications. Archives of Biochemistry and Biophysics 458 (1): 48-56.
39. Chakraborti S, Chakraborti T, Mandal M, Mandal A, Das S, et al. (2002) Protective role of magnesium in cardiovascular diseases: A review. Molecular and cellular biochemistry 238 (1-2): 163-179.
40. Mueller WD, Lucia Nascimento M, Lorenzo de Mele MF (2010) Critical discussion of the results from different corrosion studies of Mg and Mg alloys for biomaterial applications. Acta biomaterialia 6 (5): 1749-1755.
41. Seitz JM, Eifler R, Bach FW, Maier HJ (2014) Magnesium degradation products: Effects on tissue and human metabolism. Journal of Biomedical Materials Research Part A 102 (10): 3744-3753.
42. Gray-Munro JE, Strong M (2013) A study on the interfacial chemistry of magnesium hydroxide surfaces in aqueous phosphate solutions: Influence of Ca2+, Cl− and protein. Journal of colloid and interface science 393 421-428.

43. Persaud-Sharma D, McGoron A (2012) Biodegradable Magnesium Alloys: A Review of Material Development and Applications. Journal of biomimetics, biomaterials, and tissue engineering 12 25-39.
44. Walker J, Shadanbaz S, Woodfield TBF, Staiger MP, Dias GJ (2014) Magnesium biomaterials for orthopedic application: A review from a biological perspective. Journal of Biomedical Materials Research Part B: Applied Biomaterials 102 (6): 1316-1331.
45. Song GL, Atrens A (1999) Corrosion Mechanisms of Magnesium Alloys. Advanced Engineering Materials 1 (1): 11-33.
46. Ding Y, Wen C, Hodgson P, Li Y (2014) Effects of alloying elements on the corrosion behavior and biocompatibility of biodegradable magnesium alloys: a review. Journal of Materials Chemistry B 2 (14): 1912-1933.
47. Manivasagam G, Dhinasekaran D, Rajamanickam A (2010) Biomedical implants: Corrosion and its prevention-a review. Recent Patents on Corrosion Science 2 (1): 40-54.
48. Williams D (1987) Tissue-biomaterial interactions. Journal of Materials science 22 (10): 3421-3445.
49. Xin Y, Huo K, Tao H, Tang G, Chu PK (2008) Influence of aggressive ions on the degradation behavior of biomedical magnesium alloy in physiological environment. Acta biomaterialia 4 (6): 2008-2015.
50. Jang Y, Collins B, Sankar J, Yun Y (2013) Effect of biologically relevant ions on the corrosion products formed on alloy AZ31B: An improved understanding of magnesium corrosion. Acta biomaterialia 9 (10): 8761-8770.
51. Keim S, Brunner JG, Fabry B, Virtanen S (2011) Control of magnesium corrosion and biocompatibility with biomimetic coatings. Journal of biomedical materials research Part B, Applied biomaterials 96 (1): 84-90.
52. Yang JX, Cui FZ, Lee IS, Zhang Y, Yin QS, et al. (2011) In vivo biocompatibility and degradation behavior of Mg alloy coated by calcium phosphate in a rabbit model. Journal of biomaterials applications 0(0) 1–13.
53. Scharnagl N, Blawert C, Dietzel W (2009) Corrosion protection of magnesium alloy AZ31 by coating with poly(ether imides) (PEI). Surface and Coatings Technology 203 (10–11): 1423-1428.
54. Zhao N, Workman B, Zhu D (2014) Endothelialization of novel magnesium-rare earth alloys with fluoride and collagen coating. International journal of molecular sciences 15 (4): 5263-5276.
55. Zomorodian A, Garcia MP, Moura e Silva T, Fernandes JCS, Fernandes MH, et al. (2013) Corrosion resistance of a composite polymeric coating applied on biodegradable AZ31 magnesium alloy. Acta biomaterialia 9 (10): 8660-8670.
56. Zomorodian A, Garcia MP, Moura e Silva T, Fernandes JCS, Fernandes MH, et al. (2015) Biofunctional composite coating architectures based on polycaprolactone and nanohydroxyapatite for controlled corrosion activity and enhanced biocompatibility of magnesium AZ31 alloy. Materials Science and Engineering: C 48 (0): 434-443.
57. Nassif N, Ghayad I (2013) Corrosion Protection and Surface Treatment of Magnesium Alloys Used for Orthopedic Applications. Advances in Materials Science and Engineering 2013.
58. Hort N, Huang Y, Fechner D, Stormer M, Blawert C, et al. (2010) Magnesium alloys as implant materials - Principles of property design for Mg-RE alloys. Acta biomaterialia 6 (5): 1714-1725.
59. Bondy SC (2010) The neurotoxicity of environmental aluminum is still an issue. Neurotoxicology 31 (5): 575-581.
60. Hirano S, Suzuki KT (1996) Exposure, metabolism, and toxicity of rare earths and related compounds. Environmental health perspectives 104 Suppl 1 85-95.
61. Bitanihirwe BK, Cunningham MG (2009) Zinc: the brain's dark horse. Synapse 63 (11): 1029-1049.

62. Yamaguchi M (2010) Role of nutritional zinc in the prevention of osteoporosis. Molecular and cellular biochemistry 338 (1-2): 241-254.
63. Kelleher SL, McCormick NH, Velasquez V, Lopez V (2011) Zinc in specialized secretory tissues: roles in the pancreas, prostate, and mammary gland. Advances in nutrition 2 (2): 101-111.
64. Ilich JZ, Kerstetter JE (2000) Nutrition in bone health revisited: a story beyond calcium. Journal of the American College of Nutrition 19 (6): 715-737.
65. Leontis TE, Rhines FN (1946) Rates of High-Temperature Oxidation of Magnesium and Magnesium Alloys. Transactions of the American Institute of Mining and Metallurgical Engineers 166 265-294.
66. Pardo A, Merino MC, Coy AE, Viejo F, Arrabal R, et al. (2008) Influence of microstructure and composition on the corrosion behaviour of Mg/Al alloys in chloride media. Electrochimica Acta 53 (27): 7890-7902.
67. Ghoneim AA, Fekry AM, Ameer MA (2010) Electrochemical behavior of magnesium alloys as biodegradable materials in Hank's solution. Electrochimica Acta 55 (20): 6028-6035.
68. Birbilis N, Easton MA, Sudholz AD, Zhu SM, Gibson MA (2009) On the corrosion of binary magnesium-rare earth alloys. Corrosion Science 51 (3): 683-689.
69. Pinto R, Ferreira MGS, Carmezim MJ, Montemor MF (2011) The corrosion behaviour of rare-earth containing magnesium alloys in borate buffer solution. Electrochimica Acta 56 (3): 1535-1545.
70. Johnson I, Perchy D, Liu H (2012) In vitro evaluation of the surface effects on magnesium-yttrium alloy degradation and mesenchymal stem cell adhesion. Journal of Biomedical Materials Research Part A 100A (2): 477-485.
71. Liu CL, Wang YJ, Zeng RC, Zhang XM, Huang WJ, et al. (2010) In vitro corrosion degradation behaviour of Mg–Ca alloy in the presence of albumin. Corrosion Science 52 (10): 3341-3347.
72. Nguyen TL, Blanquet A, Staiger MP, Dias GJ, Woodfield TBF (2012) On the role of surface roughness in the corrosion of pure magnesium in vitro. Journal of Biomedical Materials Research Part B-Applied Biomaterials 100B (5): 1310-1318.
73. Kannan MB, Dietzel W, Zettler R (2011) In vitro degradation behaviour of a friction stir processed magnesium alloy. Journal of Materials Science-Materials in Medicine 22 (11): 2397-2401.
74. Zhang XB, Yuan GY, Niu JL, Fu PH, Ding WJ (2012) Microstructure, mechanical properties, biocorrosion behavior, and cytotoxicity of as-extruded Mg-Nd-Zn-Zr alloy with different extrusion ratios. Journal of the Mechanical Behavior of Biomedical Materials 9 153-162.
75. Gray JE, Luan B (2002) Protective coatings on magnesium and its alloys — a critical review. Journal of Alloys and Compounds 336 (1–2): 88-113.
76. Poinern GEJ, Brundavanam S, Fawcett D (2012) Biomedical Magnesium Alloys: A Review of Material Properties, Surface Modifications and Potential as a Biodegradable Orthopaedic Implant. American Journal of Biomedical Engineering 2 (6): 218-240.
77. Blawert C, Dietzel W, Ghali E, Song G (2006) Anodizing Treatments for Magnesium Alloys and Their Effect on Corrosion Resistance in Various Environments. Advanced Engineering Materials 8 (6): 511-533.
78. Quach N-C, Uggowitzer PJ, Schmutz P (2008) Corrosion behaviour of an Mg–Y–RE alloy used in biomedical applications studied by electrochemical techniques. Comptes Rendus Chimie 11 (9): 1043-1054.
79. Zainal Abidin NI, Da Forno A, Bestetti M, Martin D, Beer A, et al. (2015) Evaluation of Coatings for Mg Alloys for Biomedical Applications. Advanced Engineering Materials 17 (1): 58-67.
80. de Oliveira MCL, Pereira VSM, Correa OV, Antunes RA (2014) Corrosion Performance of Anodized AZ91D Magnesium Alloy: Effect of the Anodizing Potential on the Film

Structure and Corrosion Behavior. Journal of Materials Engineering and Performance 23 (2): 593-603.
81. Chu C-l, Han X, Bai J, Xue F, Chu P-k (2014) Surface modification of biomedical magnesium alloy wires by micro-arc oxidation. Transactions of Nonferrous Metals Society of China 24 (4): 1058-1064.
82. Shi Z, Song G, Atrens A (2006) The corrosion performance of anodised magnesium alloys. Corrosion Science 48 (11): 3531-3546.
83. Ramakrishna S, Mayer J, Wintermantel E, Leong KW (2001) Biomedical applications of polymer-composite materials: a review. Composites Science and Technology 61 (9): 1189-1224.
84. Kim S-B, Jo J-H, Lee S-M, Kim H-E, Shin K-H, et al. (2013) Use of a poly(ether imide) coating to improve corrosion resistance and biocompatibility of magnesium (Mg) implant for orthopedic applications. Journal of Biomedical Materials Research Part A 101A (6): 1708-1715.
85. da Conceicao TF, Scharnagl N, Dietzel W, Kainer KU (2011) Corrosion protection of magnesium AZ31 alloy using poly(ether imide) [PEI] coatings prepared by the dip coating method: Influence of solvent and substrate pre-treatment. Corrosion Science 53 (1): 338-346.
86. Abdal-hay A, Dewidar M, Lim JK (2012) Biocorrosion behavior and cell viability of adhesive polymer coated magnesium based alloys for medical implants. Applied Surface Science 261 (0): 536-546.
87. Cai K, Sui X, Hu Y, Zhao L, Lai M, et al. (2011) Fabrication of anticorrosive multilayer onto magnesium alloy substrates via spin-assisted layer-by-layer technique. Materials Science and Engineering: C 31 (8): 1800-1808.
88. Wong HM, Yeung KW, Lam KO, Tam V, Chu PK, et al. (2010) A biodegradable polymer-based coating to control the performance of magnesium alloy orthopaedic implants. Biomaterials 31 (8): 2084-2096.
89. Ostrowski N, Lee B, Enick N, Carlson B, Kunjukunju S, et al. (2013) Corrosion protection and improved cytocompatibility of biodegradable polymeric layer-by-layer coatings on AZ31 magnesium alloys. Acta biomaterialia 9 (10): 8704-8713.
90. Hanzi AC, Gerber I, Schinhammer M, Loffler JF, Uggowitzer PJ (2010) On the in vitro and in vivo degradation performance and biological response of new biodegradable Mg-Y-Zn alloys. Acta biomaterialia 6 (5): 1824-1833.
91. Pietak A, Mahoney P, Dias GJ, Staiger MP (2008) Bone-like matrix formation on magnesium and magnesium alloys. Journal of materials science Materials in medicine 19 (1): 407-415.
92. Gu XN, Li N, Zheng YF, Ruan L (2011) In vitro degradation performance and biological response of a Mg–Zn–Zr alloy. Materials Science and Engineering: B 176 (20): 1778-1784.
93. Xu L, Yu G, Zhang E, Pan F, Yang K (2007) In vivo corrosion behavior of Mg-Mn-Zn alloy for bone implant application. Journal of biomedical materials research Part A 83 (3): 703-711.
94. Castellani C, Lindtner RA, Hausbrandt P, Tschegg E, Stanzl-Tschegg SE, et al. (2011) Bone–implant interface strength and osseointegration: Biodegradable magnesium alloy versus standard titanium control. Acta biomaterialia 7 (1): 432-440.
95. Erdmann N, Angrisani N, Reifenrath J, Lucas A, Thorey F, et al. (2011) Biomechanical testing and degradation analysis of MgCa0.8 alloy screws: A comparative in vivo study in rabbits. Acta biomaterialia 7 (3): 1421-1428.
96. Kraus T, Fischerauer SF, Hänzi AC, Uggowitzer PJ, Löffler JF, et al. (2012) Magnesium alloys for temporary implants in osteosynthesis: In vivo studies of their degradation and interaction with bone. Acta biomaterialia 8 (3): 1230-1238.

97. Bondarenko A, Angrisani N, Meyer-Lindenberg A, Seitz JM, Waizy H, et al. (2014) Magnesium-based bone implants: Immunohistochemical analysis of peri-implant osteogenesis by evaluation of osteopontin and osteocalcin expression. Journal of Biomedical Materials Research Part A 102 (5): 1449-1457.
98. Henderson SE, Verdelis K, Maiti S, Pal S, Chung WL, et al. (2014) Magnesium alloys as a biomaterial for degradable craniofacial screws. Acta biomaterialia 10 (5): 2323-2332.
99. Mushahary D, Sravanthi R, Li Y, Kumar MJ, Harishankar N, et al. (2013) Zirconium, calcium, and strontium contents in magnesium based biodegradable alloys modulate the efficiency of implant-induced osseointegration. International journal of nanomedicine 8 2887-2902.
100. Park RS, Kim YK, Lee SJ, Jang YS, Park IS, et al. (2012) Corrosion behavior and cytotoxicity of Mg-35Zn-3Ca alloy for surface modified biodegradable implant material. Journal of biomedical materials research Part B, Applied biomaterials 100 (4): 911-923.
101. Zberg B, Uggowitzer PJ, Loffler JF (2009) MgZnCa glasses without clinically observable hydrogen evolution for biodegradable implants. Nat Mater 8 (11): 887-891.
102. Lalk M, Reifenrath J, Angrisani N, Bondarenko A, Seitz J-M, et al. (2013) Fluoride and calcium-phosphate coated sponges of the magnesium alloy AX30 as bone grafts: a comparative study in rabbits. Journal of Materials Science: Materials in Medicine 24 (2): 417-436.
103. Smith MR, Atkinson P, White D, Piersma T, Gutierrez G, et al. (2012) Design and assessment of a wrapped cylindrical Ca-P AZ31 Mg alloy for critical-size ulna defect repair. Journal of Biomedical Materials Research Part B: Applied Biomaterials 100B (1): 206-216.
104. Razavi M, Fathi M, Savabi O, Vashaee D, Tayebi L (2015) In vivo biocompatibility of Mg implants surface modified by nanostructured merwinite/PEO. Journal of Materials Science: Materials in Medicine 26 (5): 1-7.
105. ISO 10993-5 (1999) Biological Evaluation of Medical Devices Part 5: Tests for In Vitro Cytotoxicity. Switzerland: International Organization for Standardization.
106. ISO 10993-12 (2007) Biological Evaluation of Medical Devices Part 12: Sample preparation and reference materials. Switzerland: International Organization for Standardization.
107. Jung O, Smeets R, Porchetta D, Kopp A, Ptock C, et al. (2015) Optimized in vitro procedure for assessing the cytocompatibility of magnesium-based biomaterials. Acta biomaterialia 23 354-363.
108. Harrison R, Maradze D, Lyons S, Zheng Y, Liu Y (2014) Corrosion of magnesium and magnesium–calcium alloy in biologically-simulated environment. Progress in Natural Science: Materials International 24 (5): 539-546.
109. Cao JD, Martens P, Laws KJ, Boughton P, Ferry M (2013) Quantitative in vitro assessment of Mg65Zn30Ca5 degradation and its effect on cell viability. Journal of Biomedical Materials Research Part B: Applied Biomaterials 101B (1): 43-49.
110. Li RW, Kirkland NT, Truong J, Wang J, Smith PN, et al. (2014) The influence of biodegradable magnesium alloys on the osteogenic differentiation of human mesenchymal stem cells. Journal of Biomedical Materials Research Part A 102 (12): 4346-4357.
111. Pichler K, Kraus T, Martinelli E, Sadoghi P, Musumeci G, et al. (2014) Cellular reactions to biodegradable magnesium alloys on human growth plate chondrocytes and osteoblasts. International orthopaedics 38 (4): 881-889.
112. Yun Y, Dong Z, Yang D, Schulz MJ, Shanov VN, et al. (2009) Biodegradable Mg corrosion and osteoblast cell culture studies. Materials Science and Engineering: C 29 (6): 1814-1821.
113. Willbold E, Gu X, Albert D, Kalla K, Bobe K, et al. (2015) Effect of the addition of low rare earth elements (lanthanum, neodymium, cerium) on the biodegradation and biocompatibility of magnesium. Acta biomaterialia 11 554-562.

114. Niederlaender J, Walter M, Krajewski S, Schweizer E, Post M, et al. (2014) Cytocompatibility evaluation of different biodegradable magnesium alloys with human mesenchymal stem cells. Journal of Materials Science: Materials in Medicine 25 (3): 835-843.
115. Zhao N, Watson N, Xu Z, Chen Y, Waterman J, et al. (2014) In vitro biocompatibility and endothelialization of novel magnesium-rare Earth alloys for improved stent applications. PloS one 9 (6): e98674.
116. Zreiqat H, Howlett CR, Zannettino A, Evans P, Schulze-Tanzil G, et al. (2002) Mechanisms of magnesium-stimulated adhesion of osteoblastic cells to commonly used orthopaedic implants. Journal of Biomedical Materials Research 62 (2): 175-184.
117. Gu XN, Li N, Zhou WR, Zheng YF, Zhao X, et al. (2011) Corrosion resistance and surface biocompatibility of a microarc oxidation coating on a Mg-Ca alloy. Acta biomaterialia 7 (4): 1880-1889.
118. Lorenz C, Brunner JG, Kollmannsberger P, Jaafar L, Fabry B, et al. (2009) Effect of surface pre-treatments on biocompatibility of magnesium. Acta biomaterialia 5 (7): 2783-2789.
119. Pompa L, Rahman ZU, Munoz E, Haider W (2015) Surface characterization and cytotoxicity response of biodegradable magnesium alloys. Materials Science and Engineering: C 49 761-768.
120. Amaravathy P, Sathyanarayanan S, Sowndarya S, Rajendran N (2014) Bioactive HA/TiO2 coating on magnesium alloy for biomedical applications. Ceramics International 40 (5): 6617-6630.
121. Iskandar ME, Aslani A, Liu H (2013) The effects of nanostructured hydroxyapatite coating on the biodegradation and cytocompatibility of magnesium implants. Journal of Biomedical Materials Research Part A 101A (8): 2340-2354.
122. Ostrowski N, Lee B, Roy A, Ramanathan M, Kumta P (2013) Biodegradable poly(lactide-co-glycolide) coatings on magnesium alloys for orthopedic applications. Journal of Materials Science: Materials in Medicine 24 (1): 85-96.
123. Abdal-hay A, Barakat NAM, Lim JK (2013) Hydroxyapatite-doped poly(lactic acid) porous film coating for enhanced bioactivity and corrosion behavior of AZ31 Mg alloy for orthopedic applications. Ceramics International 39 (1): 183-195.
124. Kwiatkowski L, Kapuścińska A, Bałkowiec A, Lutze R. Increasing the Surface Functionality of Mg Alloys by Means of Plasma Electrolytic Oxidation; 2015. Trans Tech Publ. pp. 495-498.
125. Coelho MJ, Fernandes MH (2000) Human bone cell cultures in biocompatibility testing. Part II: effect of ascorbic acid, β-glycerophosphate and dexamethasone on osteoblastic differentiation. Biomaterials 21 (11): 1095-1102.
126. Costa-Rodrigues J, Fernandes A, Fernandes MH (2011) Spontaneous and induced osteoclastogenic behaviour of human peripheral blood mononuclear cells and their CD14+ and CD14− cell fractions. Cell Proliferation 44 (5): 410-419.
127. Villa P, Kaufmann SH, Earnshaw WC (1997) Caspases and caspase inhibitors. Trends in Biochemical Sciences 22 (10): 388-393.
128. Tao C-T, Young T-H (2006) Polyetherimide membrane formation by the cononsolvent system and its biocompatibility of MG63 cell line. Journal of Membrane Science 269 (1–2): 66-74.
129. Albrecht W, Seifert B, Weigel T, Schossig M, Holländer A, et al. (2003) Amination of Poly(ether imide) Membranes Using Di- and Multivalent Amines. Macromolecular Chemistry and Physics 204 (3): 510-521.
130. Albrecht W, Santoso F, Lützow K, Weigel T, Schomäcker R, et al. (2007) Preparation of aminated microfiltration membranes by degradable functionalization using plain PEI membranes with various morphologies. Journal of Membrane Science 292 (1–2): 145-157.

131. Tzoneva R, Seifert B, Albrecht W, Richau K, Lendlein A, et al. (2008) Poly(ether imide) membranes: studies on the effect of surface modification and protein pre-adsorption on endothelial cell adhesion, growth and function. Journal of Biomaterials Science, Polymer Edition 19 (7): 837-852.
132. Rüder C, Sauter T, Becker T, Kratz K, Hiebl B, et al. (2012) Viability, proliferation and adhesion of smooth muscle cells and human umbilical vein endothelial cells on electrospun polymer scaffolds. Clinical Hemorheology and Microcirculation 50 (1): 101-112.
133. Conceicao TF, Scharnagl N, Blawert C, Dietzel W, Kainer KU (2010) Corrosion protection of magnesium alloy AZ31 sheets by spin coating process with poly(ether imide) [PEI]. Corrosion Science 52 (6): 2066-2079.
134. da Conceicao TF, Scharnagl N, Dietzel W, Kainer KU (2010) On the degradation mechanism of corrosion protective poly(ether imide) coatings on magnesium AZ31 alloy. Corrosion Science 52 (10): 3155-3157.
135. Kittel J, Celati N, Keddam M, Takenouti H (2003) Influence of the coating–substrate interactions on the corrosion protection: characterisation by impedance spectroscopy of the inner and outer parts of a coating. Progress in Organic Coatings 46 (2): 135-147.
136. Lee JM, Lee JI, Lim YJ (2010) In vitro investigation of anodization and CaP deposited titanium surface using MG63 osteoblast-like cells. Applied Surface Science 256 (10): 3086-3092.
137. Snihirova D, Lamaka SV, Taryba M, Salak AN, Kallip S, et al. (2010) Hydroxyapatite Microparticles as Feedback-Active Reservoirs of Corrosion Inhibitors. ACS Applied Materials & Interfaces 2 (11): 3011-3022.
138. Ulery BD, Nair LS, Laurencin CT (2011) Biomedical Applications of Biodegradable Polymers. Journal of polymer science Part B, Polymer physics 49 (12): 832-864.
139. Huan ZG, Leeflang MA, Zhou J, Fratila-Apachitei LE, Duszczyk J (2010) In vitro degradation behavior and cytocompatibility of Mg–Zn–Zr alloys. Journal of materials science Materials in medicine 21 (9): 2623-2635.
140. Vu T-N, Veys-Renaux D, Rocca E (2012) Potential bioactivity of coatings formed on AZ91D magnesium alloy by plasma electrolytic anodizing. Journal of Biomedical Materials Research Part B: Applied Biomaterials 100B (7): 1846-1853.
141. Witte F, Fischer J, Nellesen J, Crostack HA, Kaese V, et al. (2006) In vitro and in vivo corrosion measurements of magnesium alloys. Biomaterials 27 (7): 1013-1018.
142. Bilezikian JP, Raisz LG, Martin TJ (2008) Principles of Bone Biology: Two-Volume Set. London: Academic Press.
143. Shi Z, Huang X, Cai Y, Tang R, Yang D (2009) Size effect of hydroxyapatite nanoparticles on proliferation and apoptosis of osteoblast-like cells. Acta biomaterialia 5 (1): 338-345.
144. Fox K, Tran PA, Tran N (2012) Recent Advances in Research Applications of Nanophase Hydroxyapatite. ChemPhysChem 13 (10): 2495-2506.
145. Deligianni DD, Katsala ND, Koutsoukos PG, Missirlis YF (2000) Effect of surface roughness of hydroxyapatite on human bone marrow cell adhesion, proliferation, differentiation and detachment strength. Biomaterials 22 (1): 87-96.
146. Kirkland NT (2012) Magnesium biomaterials: past, present and future. Corrosion Engineering, Science and Technology 47 (5): 322-328.
147. Datta HK, Ng WF, Walker JA, Tuck SP, Varanasi SS (2008) The cell biology of bone metabolism. Journal of Clinical Pathology 61 (5): 577-587.
148. Kaysinger KK, Ramp WK (1998) Extracellular pH modulates the activity of cultured human osteoblasts. Journal of cellular biochemistry 68 (1): 83-89.
149. Arnett TR (2008) Extracellular pH regulates bone cell function. The Journal of nutrition 138 (2): 415S-418S.

150. Yoshizawa S, Brown A, Barchowsky A, Sfeir C (2014) Magnesium ion stimulation of bone marrow stromal cells enhances osteogenic activity, simulating the effect of magnesium alloy degradation. Acta biomaterialia 10 (6): 2834-2842.
151. Wu L, Luthringer BJ, Feyerabend F, Schilling AF, Willumeit R (2014) Effects of extracellular magnesium on the differentiation and function of human osteoclasts. Acta biomaterialia 10 (6): 2843-2854.
152. Franceschi RT, Xiao G (2003) Regulation of the osteoblast-specific transcription factor, Runx2: Responsiveness to multiple signal transduction pathways. Journal of cellular biochemistry 88 (3): 446-454.
153. Blair HC, Robinson LJ, Zaidi M (2005) Osteoclast signalling pathways. Biochemical and Biophysical Research Communications 328 (3): 728-738.
154. Ikeda F, Matsubara T, Tsurukai T, Hata K, Nishimura R, et al. (2008) JNK/c-Jun Signaling Mediates an Anti-Apoptotic Effect of RANKL in Osteoclasts. Journal of Bone and Mineral Research 23 (6): 907-914.
155. Sternberg K, Gratz M, Koeck K, Mostertz J, Begunk R, et al. (2012) Magnesium used in bioabsorbable stents controls smooth muscle cell proliferation and stimulates endothelial cells in vitro. Journal of Biomedical Materials Research Part B: Applied Biomaterials 100B (1): 41-50.
156. Zhao N, Zhu D (2015) Endothelial responses of magnesium and other alloying elements in magnesium-based stent materials. Metallomics : integrated biometal science 7 (1): 118-128.
157. Maier JAM, Bernardini D, Rayssiguier Y, Mazur A (2004) High concentrations of magnesium modulate vascular endothelial cell behaviour in vitro. Biochimica et Biophysica Acta (BBA) - Molecular Basis of Disease 1689 (1): 6-12.